UNIVERSITY OF LIVERPOOL

Control of Molecular Motor Motility in Electrical Devices

Thesis submitted in accordance with the requirements of The University of Liverpool for the degree of Doctor in Philosophy

By

Laurence Charles Ramsey

Department of Electrical Engineering & Electronics

April 2014

Abstract

In the last decade there has been increased interest in the study of molecular motors. Motor proteins in particular have gained a large following due to their high efficiency of force generation and the ability to incorporate the motors into linear device designs. Much of the recent research centres on using these protein systems to transport cargo around the surface of a device.

The studies carried out in this thesis aim to investigate the use of molecular motors in lab-on-a-chip devices. Two distinct motor protein systems are used to show the viability of utilising these nanoscale machines as a highly specific and controllable method of transporting molecules around the surface of a lab-on-a-chip device. Improved reaction kinetics and increased detection sensitivity are just two advantages that could be achieved if a motor protein system could be incorporated and appropriately controlled within a device such as an immunoassay or microarray technologies.

The first study focuses on the motor protein system Kinesin. This highly processive motor is able to propel microtubules across a surface and has shown promise as an *in vitro* nanoscale transport system. A novel device design is presented where the motility of microtubules is controlled using the combination of a structured surface and a thermoresponsive polymer. Both topographic confinement of the motility and the creation of localised 'gates' are used to show a method for the control and guidance of microtubules.

Two further studies use the actin myosin motor protein system. Both concentrate on the manipulation of actin filaments, gliding on immobilised myosin, by DC electrical fields. Motor protein is adsorbed onto several surface chemistries with varying protein adsorption properties. A range of electrical fields are applied to the motility assay and the performance is analysed in terms of the directionality and any changes in the average velocity of filaments on each surface. This enables us to attribute surface properties to particular motility characteristics and hypothesise as to the nature of protein adsorption. The same electrical motility device is used with an alternative method to allow a more detailed study of the effect of surface chemistry on the motility function and the response of the motility after exposure to an electrical field. The movement of actin filaments on myosin motors is accelerated by a DC electrical field. Upon termination of the field the motility is allowed to return to pre-field function and this section of the procedure is analysed together with the data from the previous study to draw conclusions on the protein adsorption properties of each surface. Both chapters are used to draw conclusions on the response of the motor protein system when it is adsorbed on different surface chemistries.

The investigations carried out in this thesis are used to show both novel ways of controlling motor protein motility and also to highlight aspects of design that need to be taken into consideration when incorporating motor proteins into lab-on-a-chip devices. The electrical motility device in particular has proved to be a dynamic and inexpensive tool in investigating motor protein motility.

Acknowledgements

I would first like to thank Prof. Dan Nicolau for giving me the opportunity to begin this project. Massive thanks goes to Dr. Harm van Zalinge for taking me on as one of his first PhD students at a particularly stressful time in the group's history. Without the guidance and support offered my continuation in the program would not have been possible. I would like to extend a very special thank you to Dr. Jenny Aveyard (aka the hammer hanson, aka jerry vulva, aka the fun police, aka captain buzzkill, aka chunk, aka full English), your support and expertise have been a constant help along the way but it is your friendship in particular that has helped me get through some pretty tricky times over the course of my time at Liverpool. To Aleks (aka the Russian), I thank you for the constant entertainment in the office and for helping me out when I was being particularly special, if I ever need a fake passport you'll be the first person I call.

Finally I'd like to thank my family who through thick and thin have always been there to offer whatever support they could at the drop of a hat, it honestly would not of been possible to be where I am today without them.

Table of Contents

Glossary of Terms

Actin – Monomer units of actin filaments

Amphiphilic – comprising of both hydrophilic and lipophilic constituents

Anhydrous – The absence of water as a constituent

Assay – An investigative laboratory procedure used in biology to investigate the existence of a target analyte

ATP – Adenosine triphosphate, a nucleotide and the energy source for motor proteins

Coiled coil – A structure comprising of two coiled structures, such as helices, coiled around each other

Denature – The loss of the quaternary structure of a protein usually coupled with a loss of the proteins function

Dynein – Motor protein involved in a number of biological functions including the transport of cellular cargo

F-actin – Filamentous actin, the cystoskeletal filament on which myosin moves

HMM – Heavy meromyosin, a large fragment of the motor protein myosin II containing the sites for both actin binding and ATP hydrolysis

Hydrophilic – 'Water loving', a constituent that favours attachment to water

Hydrophobic – A constituent the disfavours attachment to water

Hydrous - Containing water as a constituent

Incubation – In laboratory procedures this is a set amount of time in which a species is applied to an experiment or device

In vivo - Study of biological species within their usual environment

In vitro – Study of biological species outside of their usual environment

Kinesin – Motor protein involved in a number of biological functions including the transport of cellular cargo

Microtubules – Filament structure created by polymerisation of tubulin monomers. The cystoskeletal filament on which kinesin moves

Motility – Movement initiated by the consumption of energy. In the case of protein motors this is the movement exhibited due to the hydrolysis of ATP

Motor protein – Force generating proteins that convert chemical energy into movement

Myosin – Motor protein involved in a number of biological functions including muscle contraction

NC - Nitrocellulose

PBMA – Poly (butyl methacrylate)

Poly (N-isopropylacrylamide) (PNIPAM) – A thermoresponsive polymer which expels water molecules from its structure between 33^{o}C and 35^{o}C

PMMA – Poly (methyl methacrylate)

PtBMA – Poly (t-butyl methacrylate)

QCM – Quartz crystal microbalance, an instrument that measures mass per unit area by measuring the frequency change in a quartz crystal resonator

TECS - Triethylchlorosilane

TMCS - Trimethylchlorosilane

Tubulin – Monomer units of microtubule filaments

Chapter I: Introduction

1.1 Introduction

This thesis explores several methods with which to control the motility function of two motor protein systems, microtubule-kinesin and actin-myosin. In addition to investigating the general viability of motor proteins in lab-on-a-chip technologies, the experiments using the actin-myosin system yielded important information regarding the adsorption properties of the motor proteins on several different surface chemistries. The thesis is split in two parts, the first dealing with the microtubule-kinesin system while second part deals with the actin-myosin system.

The theory of the molecular motor protein systems used throughout this thesis will be discussed in chapter 2. Along with the cyclic reaction that the motor proteins use to convert chemical energy into mechanic work, previous work carried out on the two proteins will be outlined together with an explanation of the potential applications of motor proteins. Chapter 3 will outline the materials and methods for the investigations that follow in the remaining sections of this thesis. An explanation of the fabrication techniques used and the individual device set-ups for the gliding assays will be detailed.

The first investigation in chapter 4 utilises the motility of microtubules gliding over kinesin coated surfaces. A design combining topographical confinement and a thermoresponsive polymer is used to control the movement and positioning of microtubules. Channels are created on the surface of the gliding assay in which microtubules are guided towards ‘gates’ created at specific areas on the chip. Via localised heating, these areas allow the motility of microtubules to be controlled through the thermoresponsive polymer PNIPAM. This chapter will be used to show an example of a novel method for controlling the movement of cytoskeleton.

Chapter 5 focuses on the actin-myosin system. A device has been designed with which to guide the motility of actin filaments using DC electrical fields. This has then been used to

investigate several surface chemistries for the immobilisation of myosin. Several surfaces were chosen with a variety of properties and the movement of the actin filaments while in the presence of an electrical field was recorded and tracked. By careful analysis of the velocity and directionality of the motility on each surface, conclusions have been drawn as to the effect of hydrophobicity and rigidity on the protein adsorption properties of the surface chemistries used. Detailed explanation is given of the orientation of the motors and the impact this would have on the resulting motility in order to more appropriately asses the motility function exhibited on the surface chemistries shown in this study.

In order to further elucidate the adsorption mechanisms of three surface chemistries an alternative procedure was used in chapter 6 with respect to the electrical motility device. Actin filaments were accelerated by a DC electrical field. Upon termination of the field the motility function was allowed to 'relax' back to function seen pre exposure to a field. The response of the motility to the field is analysed in terms of the average velocity of filaments and the time taken for the motility to return to normal function. By comparing the different surface chemistries, along with the results from chapter 5, conclusions are put forward as to the protein adsorption properties of the polymers used.

In addition to this 'deceleration' study, the effect of blocking actin on the motility function is investigated, again using the electrical motility device to probe the response of the motor protein on several different surface chemistries. Discussed in both chapters 5 and 6, the effect of 'crowding' on the motility function is examined by this study. In addition, the effect of inactive motor heads is investigated.

Chapter II: Theory. Molecular Motors and their Engineering Potential

This chapter will provide an insight into protein motors. Concentrating on myosin II and kinesin 1, a brief discussion of their role *in vivo* and the processes that allows them to convert chemical energy into mechanical work will be described. Furthermore the tools used to study the proteins and the potential for their use in lab-on-a-chip devices will be examined in context of the studies that are to follow in chapters 4 – 6 of this thesis. The aims of the two individual studies on the myosin and kinesin systems are presented at the end of this chapter.

2.1 Motor proteins

Molecular motor protein is a term used to describe a wide range of proteins found in all eukaryotic cells. They are force generating enzymes that hydrolyse nucleotides, converting chemical energy into mechanical work. The discovery of the myosin crossbridge by Huxley in 1957 gave insight into the mechanism of muscle contraction.[1] Since this initial finding many more protein motors have been discovered. Their roles, including transport of cellular cargo, phagocesis, the beating of bacterial flagella as well as the aforementioned muscle contraction, have been widely studied.[1, 2] The three major types of protein motors, myosin, kinesin and dyneins, span many roles utilising two distinctive systems. Myosin uses actin filaments, a globular protein that polymerises into long filaments, to attach to the head domain of the motor, in muscle it is the sliding of myosin bundles against actin filaments that creates contraction. Kinesin and dyneins, however, utilise microtubules as the framework of attachment to the working head domains of the motors. Tubulin, another globular protein, exists as a dimer of subunits that have similar atomic structure. Tubulin, like actin, also polymerises to form long filaments though these are much larger in diameter than actin filaments. In both systems the motors move along the cytoskeletal scaffold in a step wise motion as a result of the reaction with the nucleotide adenosine triphosphate (ATP).

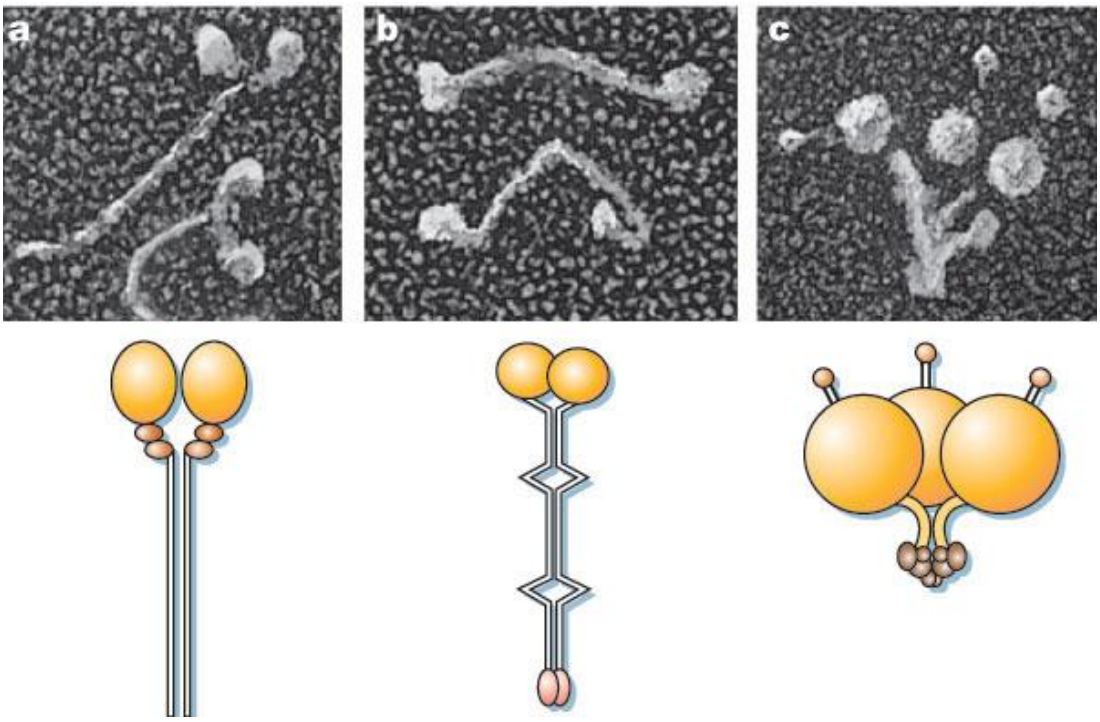

Figure.2.1. The structures of three different types of motor protein, myosin, kinesin and dynein. All contain one or more head domains (the large yellow globules on the diagram above) responsible for attachment to actin and hydrolysis of ATP. a, myosin II, b, kinesin and c, dynein.[3]

The structures of these proteins generally take the form of a tail or structure attached to one or more working head domains (see Figure 2.1). It is these that attach to their respective filament scaffolds. A conformational change within the motor protein as a consequence of ATP hydrolysis results in the movement attributed to these proteins. The function of many motor proteins are still unknown and the mechanism of force generation through ATP hydrolysis is still not fully understood, even for the most studied of the motor proteins, myosin.[1, 2] Each of the three categories of motor proteins are split into multiple sub categories and families; there are 14 families of kinesin alone. In addition to the different cytoskeleton used by the protein, their function can also be differentiated by the method of movement and in some case the direction of movement along a given filament. Dyneins, for example, are a motor protein found to move in the opposite direction along the microtubule

than kinesin. Within the myosin family there are those that walk both from the positive end to the negative end of the filament and vice versa.

The following sections will discuss the conventional kinesin and Myosin II systems that are used throughout this thesis.

2.2 Kinesin – microtubule system

Kinesin is an important motor protein which shares many similarities to myosin. Both utilise the nucleotide ATP as a means of converting chemical energy into mechanical work, but in the case of kinesin, it is the cytoskeleton filaments called microtubules that it uses as tracks for transporting cargo.

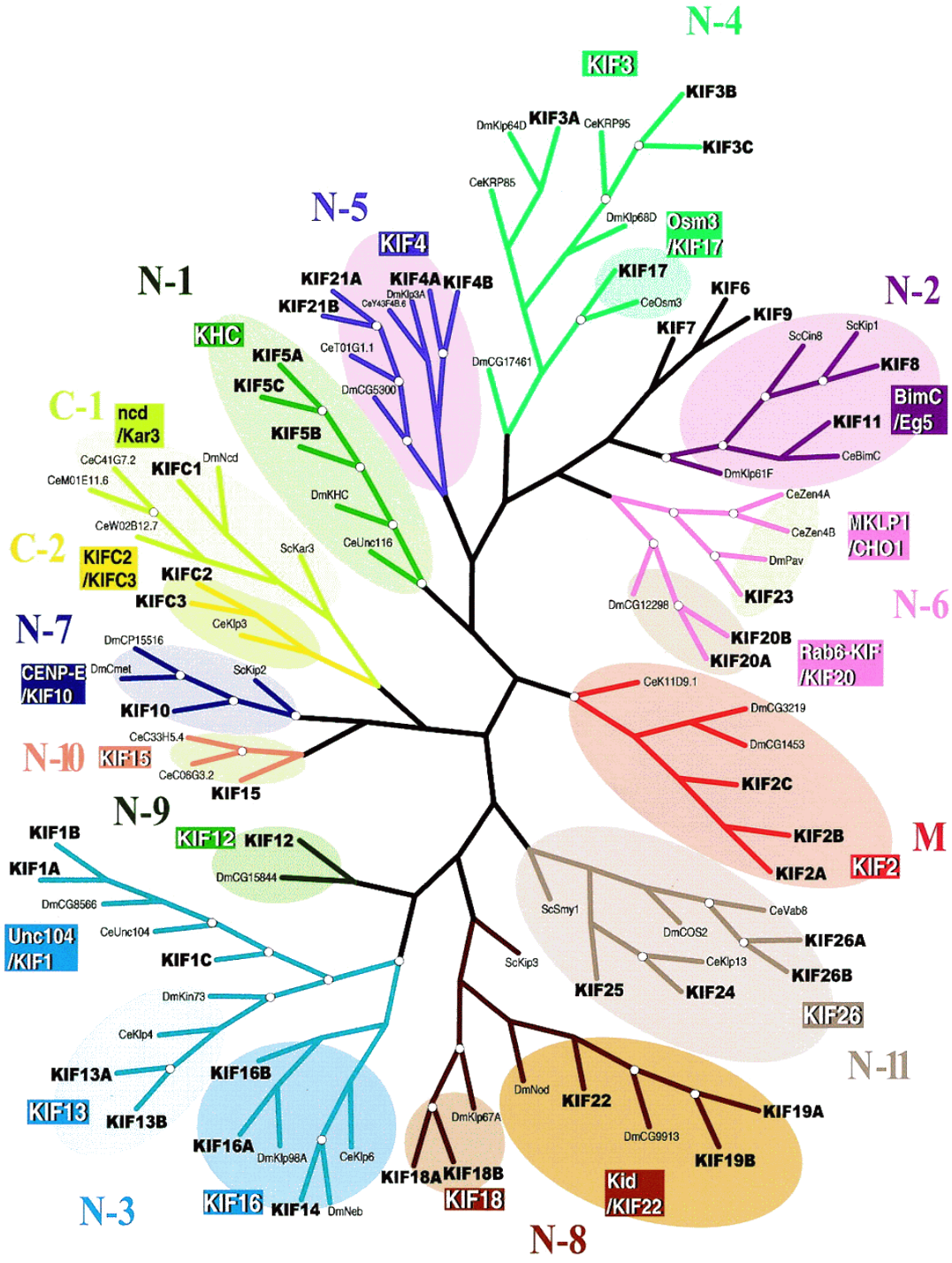

Figure.2.2. The diagram shows all of the kinesin superfamilies expressed in humans and mice.[4]

Kinesin comes in a wide variety of forms, split into several different classes with each class containing a number of families (see Figure 2.2). Each different type of kinesin holds

slightly different variations of structure and role. Some have as many as three head domains, some only one. There are 45 different genomes corresponding to kinesin in both humans and mice.[2] The sheer number of variations of the same protein shows the importance and wide variety of roles this motor protein has to play in cells.

2.2.1 Kinesin protein

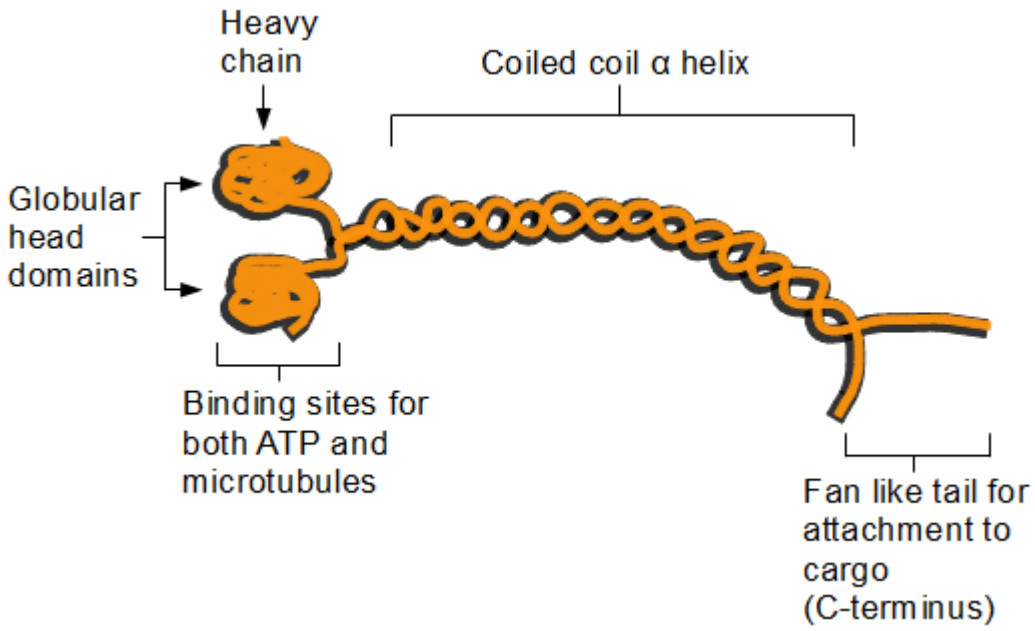

Figure.2.3. The diagram shows the basic structure of the conventional kinesin motor protein. The globular head domains responsible for the hydrolysis of ATP and binding to microtubules are connected to the tail domain via a coiled coil. The entire motor spans around 80 nm.

Conventional kinesin, kinesin-1, as used in this study, has a number of structural similarities to myosin II described in section 2.3. The protein consists of two heavy chains located in the head domain of the motor (see Figure 2.3). These contain the binding sites for microtubules and also the sites responsible for the catalysation of ATP. There are also two light chains contained within the proteins structure which connects to the fan like C-terminus via a coiled coil alpha helix. The entire structure is rod like in nature spanning approximately 80 nm. The C-terminus is responsible for attaching the motor to its cargo e.g. vesicles.[2]

While both myosin II and conventional kinesin have similar properties, both have slightly varied applications of their movement. Kinesin is a high duty ratio motor protein and is highly processive, spending a large amount of time attached to the microtubule. This explains the main role of kinesin in the transport of intracellular cargo as the motor can travel great distances without dissociating from the microtubule scaffold.[2] This type of movement favours singular motors transporting cargo from one area to another as opposed to the highly cooperative nature of myosin II.

Kinesin not only uses microtubules as a scaffold for movement but also as a means of direction. Within the families of kinesin there are those which will move to the positive end of the microtubules and those which work in the opposite direction. The conventional kinesin used in this study will move from the minus end towards the positive end of the filament (see section 2.2.2 for full description of microtubules). Like in the actin myosin system this is an extremely important characteristic of the movement of these motors as it is key in creating a highly directive cellular transport network where different proteins, even within the same motor protein family, perform highly specific roles.

2.2.2 Microtubules

The structure of microtubules is more complex than that of actin. This cytoskeletal filament is used by a number of motor proteins, including kinesin, as a scaffold for their individual roles. The units that polymerise to form the microtubules exist as a dimer of globular proteins, α-tubulin and β-tubulin. The resulting structure of the microtubule is also much larger than actin filaments, polymerising as long as 50 μm with a diameter of 25 nm.[1, 5]

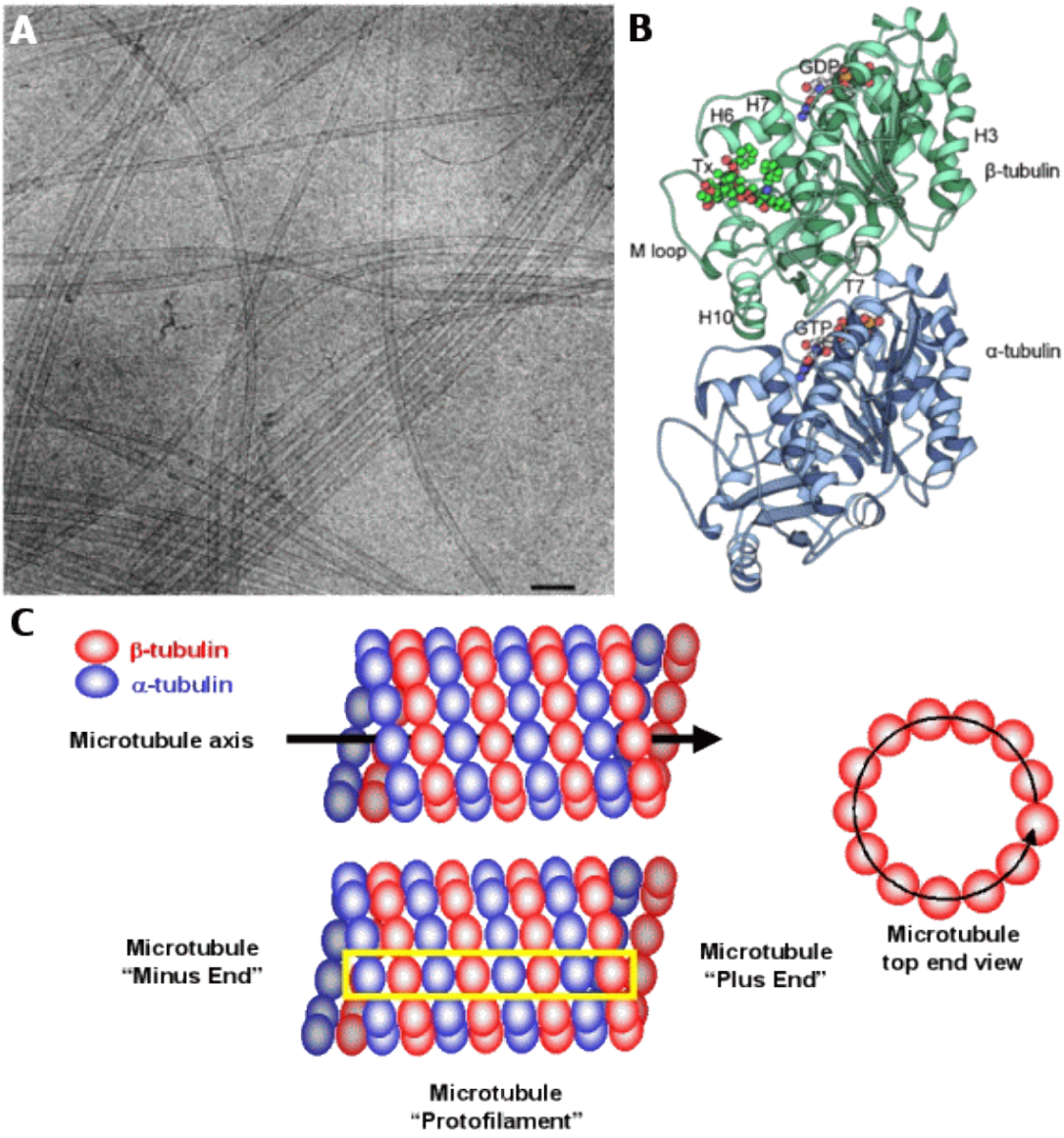

Figure.2.4. Scheme showing the structure of microtubules. A, an electron micrograph of microtubules. B, the protein structures of the two monomer units that polymerise to create a microtubule, α-tubulin and β-tubulin. C, diagram shows how the two monomers form the microtubule with the yellow box defining the protofilament on which the motor walks.[6, 7]

The dimers of tubulin first form a protofilament, polymerising head to tail as a very stable structure. The protofilaments then form a sheet which eventually closes to form the hollow tube structure of the microtubule. The asymmetry of the dimers, coupled with the head to tail binding of these and parallel binding of the resulting protofilaments, is the reason behind the

polarity of the microtubule structure. The number of protofilaments that bind together before the final closing of the tube can vary. The microtubule pictured in Figure 2.4 C is made of 13 protofilaments. In this structure there is a slight offset of ~0.92 nm between the dimers which after 13 protofilaments accounts for 3 monomer units and so forms a 3-start helical structure with each protofilament running parallel to one another.[5] As with actin the two ends of the microtubule grow at different speeds with the positive growing faster than the negative end. While most cellular microtubules have this structure there are others that form by closing at different numbers of associated protofilaments. There are for example, 12, 14 and 15 protofilament microtubules that have been characterised.[8, 9] These form the tube by making a slight twist in the structure in order to allow the dimers to bind. The structure resulting from these slight pitches are called supertwists.

The large structure of the microtubule is very strong due to the symmetry of the helices. Even in microtubules with supertwists, where the helices are not symmetric, the difference in α-tubulin and β-tubulin are so small that the different binding points of these structures does not disrupt the strength of the entire structure. In fact the size of the microtubule itself means that it is less susceptible to structural weakness due to defects when compared to actin. As a result, microtubules can form large rigid structures, spanning large distances within a cell.

2.3 Myosin – actin system

Myosin is a collective name for a family of force generating protein motors which uses actin filaments as tracks and ATP as fuel to move. The discovery of the myosin crossbridge and its function in muscle contraction sparked new research into these naturally occurring nanomachines.[10] There are many classes of myosin, each denoted by a roman numeral, and in each class there are multiple sub-categories each with its own specific role (Figure 2.5).

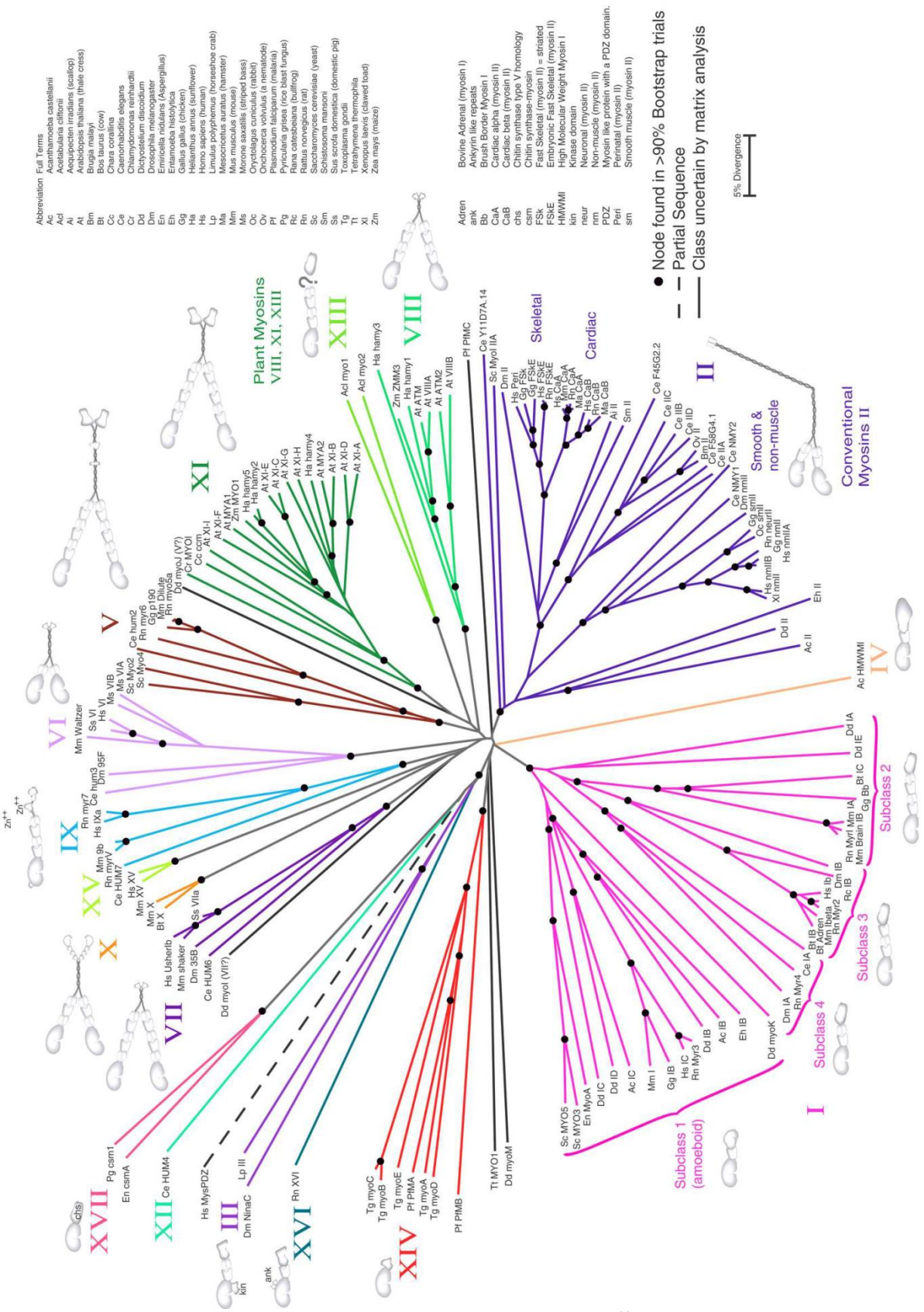

Figure.2.5. An unrooted phylogenetic tree of the myosin superfamily.[11]

There are over forty different myosin genes in humans alone spanning twelve different classes. Previous studies have found single cells with as many as 12 different classes of myosin. The sheer number of different variations of the same motor protein shows the huge range of roles it has to play in eukaryotic cells.[12]

2.3.1 Myosin protein

Myosin is made up of one or two heavy chains and one or more light chains. The heavy chains consist of several motor domains. The N-terminal domain or 'head domain' contains the binding sites for both ATP and F-actin. In rabbit muscle myosin II as used in this study, the two head domains are connected to a neck domains consisting of multiple light chain binding regions which are repeats of approximately 23-30 residues.[1, 13] It is this neck region, and more specifically the angle at which it holds the head domains to the tail of the motor, that is responsible for force generation. The C-terminal tail region, which takes the form of a coiled coil, is responsible for anchoring the motor to a specific position or cargo. Myosin II finds its role in muscle contraction. *In vivo* the protein forms bundles with using the tail regions as anchoring points. These are lined in parallel to bundles of actin filaments. It is the sliding of these two structures, upon reaction with ATP, that results in muscle contraction.[14, 15]

The duty ratio a motor protein is a term used to describe the time spent attach to actin in the 'strong bound' state (see section 2.5 for a description of the various binding states of myosin to actin). High duty ratio motor are described as being processive, each can travel a great distance without being released from the filaments, and their roles are mainly found in the transport of cargo around cells.[1] Myosin II is a low duty ratio motor meaning it spends a short amount of time bound to the filaments.[16] A key step in the ATP cycle of Myosin is the

dissociation of the motor from the filament. This characteristic, where the motor spends less time bound to the filaments, is deemed advantageous when multiple motors are working together, as is the case in muscles tissue.

Myosin uses actin filaments as tracks and can move from one end to another. The speed of this movement ranges from 100 nm/s to 60000 nm/s with myosin II having an average speed of 8000 nm/s *in vitro*.[1] Some move from the positive to the negative end of the filament and some visa versa. This is an important specificity as each carries a separate role, e.g. one motor may take cargo from the centre of a cell to the cell wall and a separate motor that works in the opposite direction would take cargo from the cell wall to the centre. In muscle contraction, as with myosin II, it is important that the motors work in collaboration and so must all move from a single end to the other; in the case of the myosin II in this study, from positive to negative.

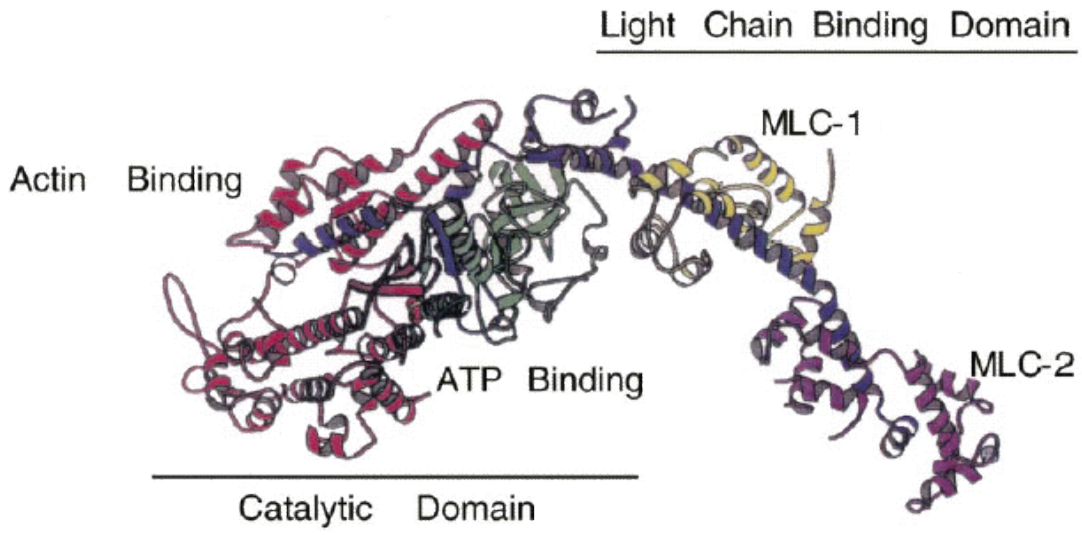

Figure.2.6. The structure of a head and neck domain of myosin II which makes up the S1 fragment of HMM. The head domain contains the heavy chains responsible for both actin binding and ATP catalysis. The neck, comprising of light chains, holds the head domain at the specific angle needed for force generation upon the conformal changes which happens as ATP is hydrolysed.[13]

When treated with the enzyme trypsin fragmentation occurs at the centre of the tail of myosin to give heavy meromyosin (HMM) and light meromyosin (LMM).[17] The structure of HMM is made up of three sub regions split over two sub fragments. The head domains, situated in the S1 fragment (see Figure 2.6), are the actin binding sections of the motor. It is also in this region that the hydrolysis of ATP takes place.

The second sub region, situated again in the S1 sub fragment, is the neck domain. The neck links the actin binding head domains to the S2 region, acting as a lever arm for the transduction of force. The neck domain is then connected to the final major section of the HMM, a short tail. The link between the two is what creates the angle needed for the step wise motion of the motor as the conformal change occurs upon hydrolysis of ATP at the head. The tail section of myosin is made up of a coiled coil structure that aids in the holding of the two heads together. In muscle it is this part of the structure that bundles with other myosin molecules to create the thick filament. LMM consists of the remaining section of tail. It is a coiled coil structure with no binding sites for either ATP or actin.

2.3.2 Actin

Actin is the cytoskeletal filament used in the myosin system. A single filament is made up of globule actin monomers (Figure 2.7 B) that polymerise to form a two stranded, right handed helical structure.[1] A full repeat of this structure is 72 nm in length with a filament diameter of ~6 nm.[18] Polymerisation of the actin filament occurs much faster at one end. This is due to the asymmetrical structure of the actin monomers, leading to a polar filament.[19, 20] The positive end of the filament grows much faster and it is this highly ordered polymerisation mechanism that *in vivo*, along with specific nucleation sites, aids in creating the highly specific structures needed for muscle tissue.

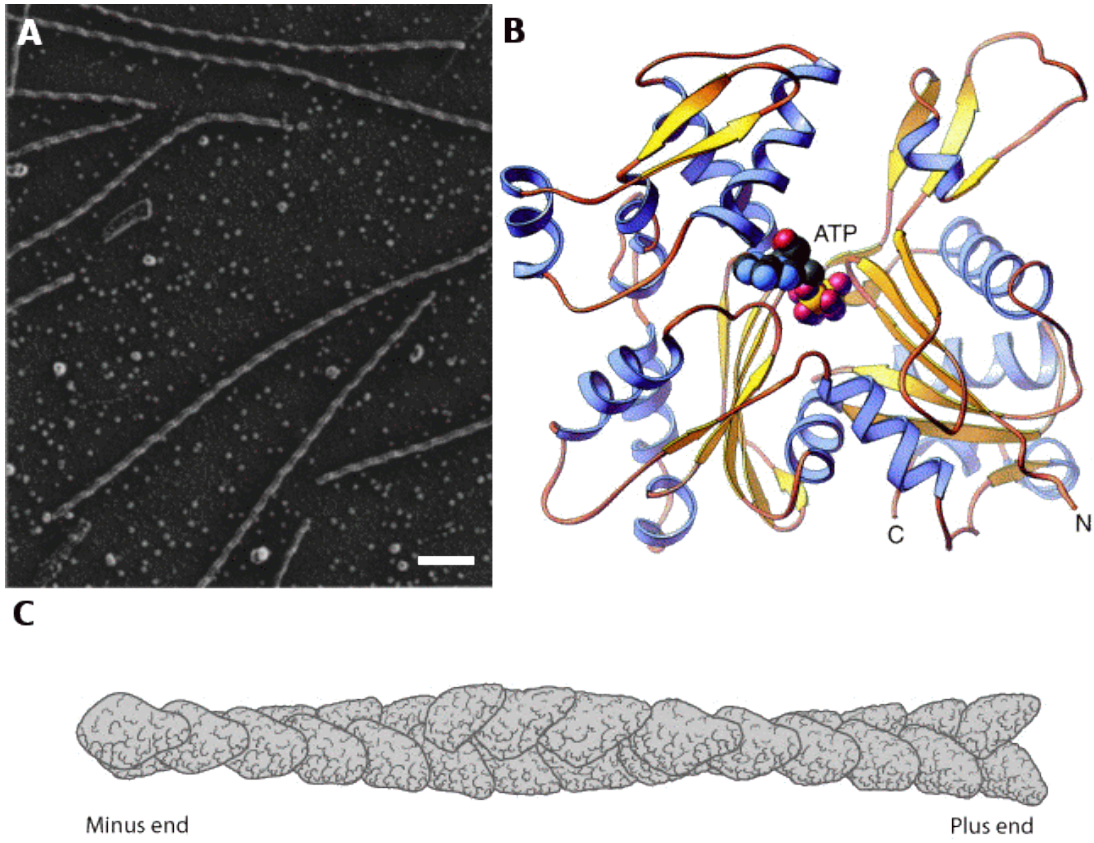

Figure.2.7. Structure of F-actin. A, electron microscopy image of actin filaments. B, protein structure of a monomer unit of actin showing the deep cleft in which ATP is bound. C, Image showing how the monomer unit polymerise to form the helical structure of the filament. Scale bar indicates 100 nm.[21, 22]

Each of the 72 nm period of the actin structure contains 26 sub units which accounts for 2.77 nm per sub unit.[23] There is a significant level of contact between each of the monomer units, as is required to polymerise into the long structures seen *in vivo*. The polarity of these filaments not only affects the speed of polymerisation at each end but also the direction in which a particular myosin motor moves along the scaffold. Actin filaments polymerised *in vitro* can reach many micrometers in length. Shown in Figure 2.7 A is an electron microscopy image of individual actin filaments. The helical structure that can be seen in this image is presented in Figure 2.7 C where the monomer sub units polymerise together to create the right handed helix upon which the myosin walks. The strength and straightness of

these filaments is due to the helical structure. The surface of the actin filament is asymmetrical, as is shown in Figure 2.7 C where the plus end seems barbed and the negative end forms an arrow. This characteristic is key in coordinating the direction of movement of the motor protein.

2.4 The ATPase cycle

The ATPase cycle itself has been a source of wide study, with the kinetics of each protein and the rate limiting steps of each cycle varying slightly. For a number of motor proteins it is still not fully understood. In this cyclic reaction ATP is hydrolysed to adenosine diphosphate (ADP) and a phosphate group is released. The reaction is in equilibrium and *in vivo* moves strongly to the right.

$$ATP \rightleftharpoons ADP + P_i \qquad \text{Eq 1.}$$

In the actin myosin system the hydrolysis of ATP is catalysed by the binding of actin. In turn the release of the myosin motor from the actin filament is catalysed by the binding of ATP. ATP activity of myosin in the absence of actin is dramatically reduced.[24, 25] This correlation between ATP activity and actin binding is shared with kinesin in that the ATP activity in the absence of microtubules is much reduced. There are key differences in the two ATPase cycles, the two head domains of myosin work independently while the head domains of kinesin work in coordination with each other, hence kinesin being highly processive and myosin II having a low duty ratio. As such each of the ATPase cyclic reactions, the mechanical forces and step sizes for both kinesin and myosin will be discussed below.

2.4.1 Kinesin ATPase cycle, step sizes and forces

Unlike the myosin, kinesin is highly processive, meaning at each stage of the cyclic reaction with ATP there is one head domain attached to the filament. The movement of kinesin along

a microtubule is best viewed as a hand over hand action and due to this characteristic the ATPase cycle of kinesin must be studied in terms of both motor heads. Similarly to myosin the ATPase cycle reaction kinetics of kinesin are linked with the association and dissociation of the microtubule. In the absence of microtubules the rate of product release is extremely slow and is the rate limiting step of the entire process. The rate is as low as 0.01 s^{-1} per head at high concentration of ATP.[1]

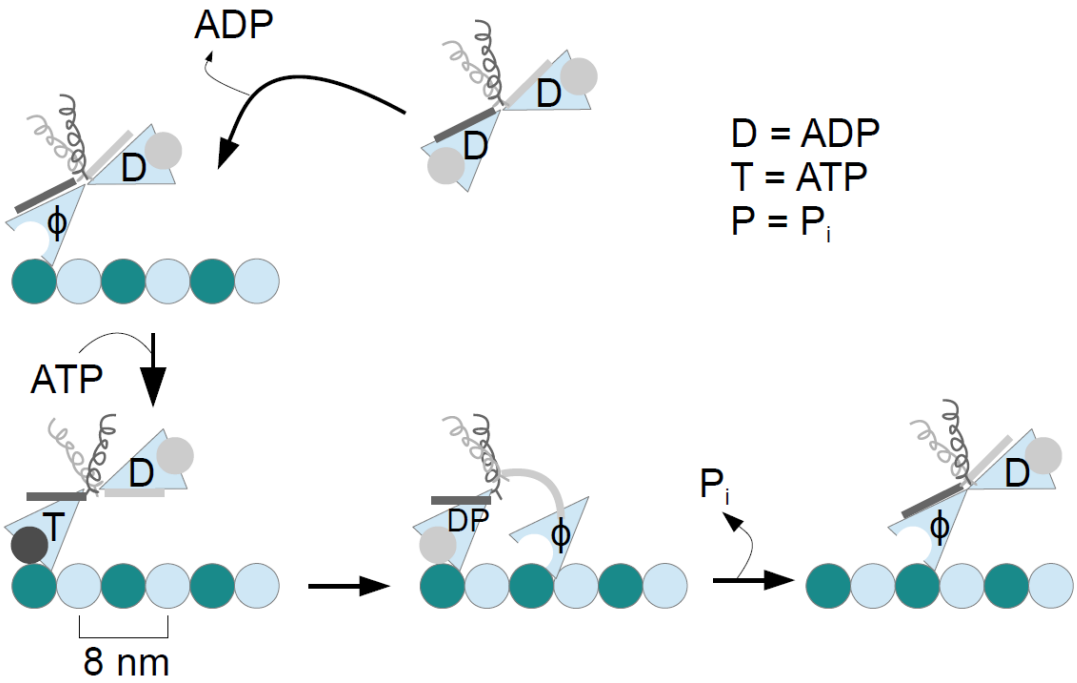

Figure.2.8. Scheme showing the ATPase cycle of the conventional kinesin motor. The motor is processive with a hand over hand movement along the filament. The attachment to the filaments occurs with the dissociation of ADP. ATP then binds and hydrolyses while the other head domain binds to the filament. The head domain will dissociate with the microtubule upon release of the phosphate. ϕ represents an unoccupied site ready for the nucleotide (ATP) to bind.

The increase in the ATPase rate in the presence of microtubules is around 5000 fold at ~50 s^{-1} per head. This is due to a number of factors, not just the increase rate of ADP release, the rate limiting step of the cycle. As well as product release, the rate of hydrolysis of ATP is also increased when the motor is attached to a microtubule. As shown in Figure 2.8 the

motor first attaches to the microtubules via one head with the release of ADP from the head domain. The other head domain cannot attach to the microtubule until the bound head associates with ATP.[26-28] ATP binding of the first head domain attached to the filament initiates a conformal change in the protein and produces the movement. The second head can now bind to the microtubule and release ADP while hydrolysis occurs at the first head domain. The binding of the second head accelerates the release of the first. This is the key difference of the kinesin ATPase cycle to that of myosin. The chemical binding of ATP accelerates the mechanical step of the second head binding to the microtubules, this in turn catalyses the release of ADP from the first second head. The release of ADP, a chemical step, then catalyses another mechanical step with detachment of the first head domain from the microtubule. Within one second conventional kinesin and take one hundred steps along a microtubule without dissociating from the filament.[29]

2.4.2 Myosin ATPase cycle, step sizes and forces

In the absence of actin the ATPase cycle of myosin is slow, roughly 0.1 s^{-1}.[1, 24] The rate limiting step of this cycle is the release of phosphate meaning that the main species is with the motor, ADP and phosphate bound together. The difference in ATP activity in the presence of filaments is substantial with actin increasing the rate of ADP release around 200 fold to ~25 s^{-1}.[1, 25] As this is a cyclic reaction with several steps in equilibrium (see Figure 2.9) there is no formal start point, however for simplicity the following explanation will use the state of myosin bound only ATP in the prepowerstroke state as the starting point. The powerstroke step of the cycle is where the conformal change in structure to the protein due to ATP hydrolysis creates the stepping movement required for force generation. For ease of explanation the following acronyms will be used, **M** = motor, **T** = ATP, **D** = ADP, **P** = P_i, **A** = actin and so for example **MDP** represents the motor bound to both a molecule of ADP and the phosphate. Myosin II is a low duty ratio motor, as opposed to processive motors where

when one head domain is not bound to the filament the other must be. As this is not the case we need only look at the cycle in terms of one myosin head as they work independently.

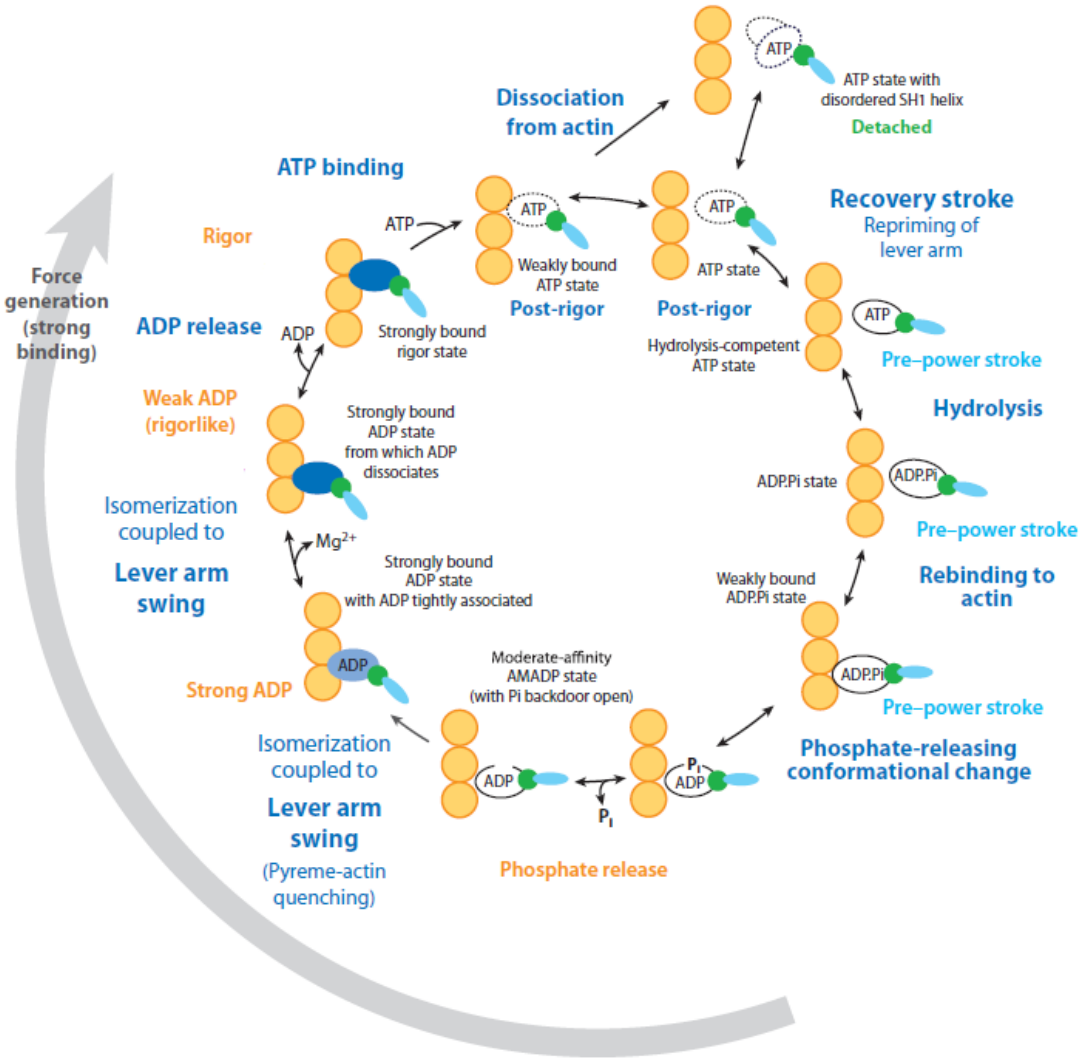

Figure.2.9. Schematic shows the ATPase cycle for a single head of myosin. The motor goes through a number of strongly and weakly bound states. This is due to the difference in affinity that myosin has for actin filaments as it cycles through the hydrolysis of ATP.[30]

After binding with **T**, hydrolysis of the nucleotide takes places giving the next step of the cycle as **MDP** where all products are bound to the motor. After this has taken place the motor will bind to actin giving **AMDP** which leads to phosphate release. Upon this

phosphate release the motor begins the powerstroke phase of the cycle and is now the strong bound state with **D** and actin. This strong bound state is coupled with the lever arm swing of the motor which is the force generating step. The motor remains strongly bound to actin while **D** is released to leave **AM**. It is only when the motor binds to another molecule of ATP that the affinity for actin drops and the motor eventually dissociates from the filament entirely to start the prepowerstroke phase again.

The force generation occurs due to a conformational change within the protein and the angle at which the head domain is attached to the neck of the motor. Studies have shown that there is a cleft in the head of the motor that closes upon phosphate release when the motor binds to actin.[31, 32] The step size of each powerstroke is around 5 nm meaning that an entire ATPase cycle with two headed myosin II will result in a step size in the range of 10 nm with the cycle taking just a few milliseconds.[1, 24] The forces applied to the filament during the powerstroke have been measured by using bead assays (see section 2.6) and the maximum force exerted by a myosin motor is ≥10 pN.[24, 30, 33]

2.5 The in vitro motility assay

The *in vitro* motility assay (IVMA) is a key instrument in the elucidation of the motility function of motor proteins as it is not yet possible to assign attributes by amino acid comparison alone. The discovery of kinesin was a direct result of the creation of this technique.[34-36] The initial breakthrough was the visualisation of myosin coated beads moving on actin filaments in the cytoplasm of the alga *Nitella*.[37] Following on from this came the first fully *in vitro* bead assay which consisted of myosin coated beads moving on actin filaments spread over a microscope slide.[38] Advances in microscopy meant it was possible to view single fluorescently labelled filaments and microtubules, and later even single fluorescently labelled motors.[39-43] The study of protein motors and their mechanisms of force generation have been greatly advanced by these techniques and the speed of movement and

forces projected *in vitro* are in agreement with the action in the cell.[1, 38, 40, 44, 45] Many of these forces have been measured by utilising optical traps. For instance the force with which myosin holds on to a filaments along with its step size and level of proccesivity have all been measured via this method.[33]

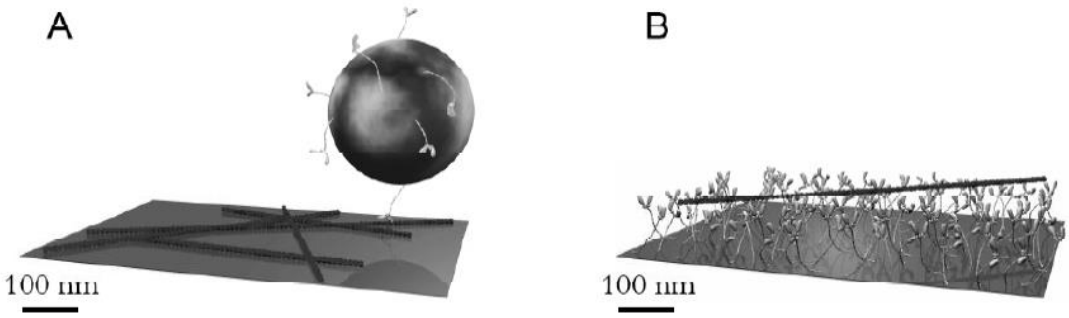

Figure.2.10. The two geometries of the in vitro motility assay. A, the bead assay takes the form of a glass or plastic bead coating with motor protein. Filaments attached to flat surface allow the visualisation the bead as it moves. B, the gliding assay is a reversal of the bead assay. The motor protein is immobilised across a planar surface and fluorescently labelled filaments allowed to attach and their movement recorded via fluorescence microscopy.[2]

The IVMA exists in two major forms, shown in Figure 2.10. The gliding assay consists of a flow cell in which one surface is coated with purified motor protein. Fluorescently labelled filaments are then allowed to attach to the motors and their movement is observed via fluorescence microscopy. The bead assay, or stepping assay, is the reverse of this. Filaments are spread across a planar surface and the movement of motor coated beads is visualised. This can be seen as being close to the *in vivo* transport of cellular cargo where the bead would represent the payload that the motor protein transports. Throughout this thesis, both with kinesin and myosin, the gliding assay will be utilised.

In both gliding assay the filaments are viewed via fluorescence microscopy. To allow this visualisation the actin filaments are labelled with rhodamine phalloidin which is a high

affinity F-actin probe conjugated to the red-orange fluorescent dye tetramethylrhodamine. This phalloidin is highly selective to actin binding, water soluble and isolated from the deadly *Amanita phalloides* mushroom.[46] In the kinesin gliding assay the microtubules are polymerized from rhodamine-labeled porcine brain tubulin where a mixture of 1:3 labelled with unlabelled units was used. The labelled units have been modified to contain covalently attached rhodamine at 1-2 dyes per heterodimer. The rhodamine is a red-orange fluorescent dye emitting at around 580 – 600 nm.

2.6 Future prospects of molecular motors

The creation and implementation of the IVMA's outlined in section 2.6 show two separate outcomes for molecular motors and motor proteins. On the one hand they have created powerful tools with which to study these proteins and further elucidate their complex workings. On the other hand the IVMA can be viewed as an initial proof of concept for the ability to extract these nanomachines and retain their function within an environment entirely different to that which they have evolved to exist. Once these developments had been made it was a small step to envisage the potential applications of these specialised proteins in a variety of purposes mainly concerning the movement of objects around a surface. Many technological advances have taken inspiration from nature and so it is not surprising that many are optimistic about the future uses of motor proteins in lab-on-chip devices. Our rapidly increasing understanding of the *in vivo* function of motor proteins only adds to the number of potential applications that are suggested. The huge range of motor proteins in existence and the specificity of each to its particular role in cells shows us that while the number of applications may be large, the implementation of these nanomachines will need to be highly specialised in order for any system created to work close to the efficiency seen *in vivo*. This efficiency of force generation is perhaps the most attractive property of molecular motors. The kinesin motor can take 100 steps along a microtubule in one second, 8 nm steps at a time, and can pull against a force of 6 pN. The motor takes one

step for each molecule of ATP it hydrolyses at an energy efficiency of around 50 %, which is remarkable when compared that to a modern combustion engine found in the average car which has an energy efficiency of up to 40 %.[47-49] Other motor proteins such as the rotary motor F1-ATPase has had a reported efficiency of between 80 % and 100 %.[50] The size and structure of purified motor proteins also lends itself for use in parallel nanotechnological applications. Alongside the ease of purification, thanks to developments in this sector, and their low cost, it would seem that these motor systems could be very powerful tools.

Many of the applications envisioned begin by looking at the role of the particular motor protein being studied. For example, the main role of kinesin is to transport cellular cargo, and it does this by using microtubule tracks. However, after the implementation of the gliding assay many have come to the conclusion that this system could be used for molecular transport within a device but instead utilising the microtubules as 'shuttles' that could carry species from one area of a chip to another.[51-55] The same can also be said of the actin-myosin system where the transport of cargo could be carried out via decorated actin filaments and, due to the speed advantage over kinesin, could be a fast delivery system.[56-58] The movement of these filaments over a surface coated in motors is a theme that can be used for a large variety of device designs. As well as transport of cargo this dynamic translocation has shown promise in both self assembly and molecular sorting with the majority of the device designs being angled at miniaturised analytical systems such as diagnostic, drug discovery and biosensing systems.[47, 48, 59-64]

Utilising molecular proteins in lab-on-a-chip devices, no matter what the desired system is, does not come without several issues and limitations such as the following:

- Purification of the protein while retaining functionality
- Occurrence of non-functioning motors on a given surface
- Motor proteins must be kept in a hydrous environment at all times

- Cystoskeletal filaments must be successfully polymerised and stabilised along with the appropriate fluorescent labelling if they are to be visualise by fluorescence microscopy
- Flow cell design must allow for rapid replacement of solutions for each step of the motility assay
- Blocking species such as BSA must be used to reduce the chance of denaturing the motor protein through unwanted surface interactions
- Each device may require a specialised motility assay procedure to ensure that a healthy motor protein layer exists on the surface of the device
- Must control temperature, salt concentrations and pH of assay solutions

Firstly the purification of the protein must be done in such a way that allows the retention of the active sites of the motor, the head domains, while also leaving the tail domains largely undamaged for successful adsorption to the surface of a gliding assay.[17, 29, 65, 66] A second issue of utilising motor proteins is presence of non-functioning motors attached to a surface of a gliding assay. This population of motors needs to be kept to an absolute minimum if a device of high quality and reproducibility is to be created. Any device that utilises motor proteins need also be a 'wet device' so the motor are kept in a hydrous environment throughout. From purification to surface adsorption, every step of the motility assay is done in aqueous solution. While studies have shown that an entire assay can be frozen, stored and motility re-initiated, if the assay dries at any point the motility is permanently terminated.[67, 68] Apart from the purification of the protein it is also essential that the filaments are polymerised successfully, be they actin or microtubules. In the case of microtubules this becomes particularly important if one is trying to create microtubules that contain the standard 13 protofilaments that are all horizontal to each other, as explained in section 2.2.2. Production of microtubules with other numbers of protofilaments will lead to the

microtubule encountering a slight spin as it is propelled across the surface, which may impact on its ability to transport cargo. There are steps that need to be taken to ensure the stability of the filaments, it is common for the microtubule stabilising drug taxol to be included in the process to ensure that there is little depolymerisation.[1, 2, 69] Actin filaments are polymerised using phalloidin (see section 2.3.2) which aids in the polymerisation and helps to stabilise the resulting ph-actin.[1, 2, 65, 70] IVMA's provide a good tool to check if the individual components of the assay are performing correctly; however, the motility assay itself can be problematic. The gliding assay must be sealed on at least two sides in order for the solutions to be kept within the flow cell. The cell design must also allow for the rapid replacement of the different solutions required during the process. For example, in the actin-myosin motility assay a solution of given motor protein concentration is allowed to incubate in the flow cell for a set amount of time in an attempt to create repeatable protein layers on multiple devices. If the device design does not allow for rapid 'flushing' of the flow cell, there is likely to be disparity between incubation times. It is important that blocking species be used in the flow cell, such as BSA or casein, as these help prevent the denaturing of the motor protein and unwanted binding of the cytoskeleton to the surface of the gliding assay. For assays that contain fluorescently labelled filaments, an anti-bleaching system must be used as this prevents free radical creation, which will not only cause the filaments to bleach but also destroy the motility. Finally the motility assay solutions need to be tuned, in terms of concentration and incubation time, for each device design to ensure that the appropriate concentration of protein, both motor and blocking, are present on the surface. This will become much more complicated as the device designs increase in their complexities, especially if combined with micro/nano fluidics. As a side note to protein, ATP and salt concentrations, another physical component that must be controlled within the device is temperature. There is a direct correlation between temperature and the velocity of filaments.[71, 72] High temperature will also denature the proteins within the assay.

While all of these limitations of the motor protein system need to be taken into account, the need for appropriate control of the motility on a given surface is of paramount importance. Without this the movement of cytoskeleton on the surface of a gliding assay is highly random. Currently there is no way of placing the motors on a surface in an ordered manner, meaning that when the protein is adsorbed to the surface the orientation of the motor and its direction of propulsion is disordered. This means that alternative means of guiding or directing the movement of filaments is required and can be achieved in a number of different ways. This is an area of research that is being extensively studied by a number of groups and is the main focus of this thesis.[48, 73]

2.7 Methods for control and analysis of kinesin and myosin systems

There are a number of obvious methods to control the movement of filaments in a gliding assay, many of which have been shown, and like the issue of the choice of motors, all have their advantages and disadvantages.[64, 69, 74-84] The method of control can be attempted in a variety of ways. This can include guidance of the filaments via structures on a surface or chemical patterning of a surface in the hope of provided regions of preferential protein binding leaving other areas free of motors. In the following sections several key methods for the control of motility will be discussed.

2.7.1 Topographical confinement

The first and perhaps the most obvious is the topographical confinement of the motility (Figure 2.11 A and B). By patterning the surface of the gliding assay with structures or channels that prohibit the movement of the filaments to certain areas of the surface, it is possible to confine the motility to set regions.

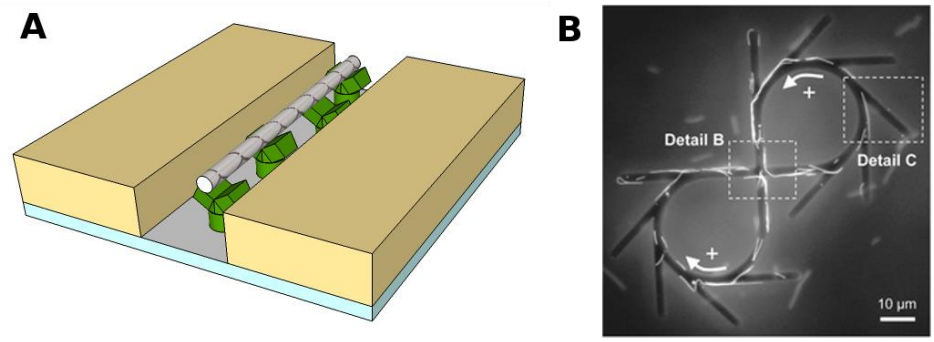

Figure.2.11. A, topographical confinement of motor protein motility. Microfabrication of surfaces creates trenches or channels in which the floors are functionalised with motors. The walls of these channels prevent the filaments from moving outside of the structure. B, kinesin motility is confined within the microfabricated structure of a glass substrate. The walls of the channels are designed in such a way to prohibit the microtubules from 'climbing' out of the structure.[84]

Success has been shown in creating devices where actin filaments or microtubules are placed within channels where either only the floor of the channel is functionalised with the motor protein, or the walls of the channel are designed in such a way to prevent the filaments from 'climbing' out of the structure.[78, 84-87] These two methods of topographical confinement approach the same issue in alternative manners, how to keep the filament within the set boundaries of the channel. If one is to coat the entire surface, including channels, with motor protein, it is vital that a barrier is put in place to stop the filaments from simply attaching and climbing out of the channel via the motors immobilised on the sides of the structure. One method which has been used to great effect is to create a channel of which the cross section resembles an upside down Ω.[88] With this method, as the filaments climb the wall of the channel they reach a roof that is of sufficient distance to the bottom surface of the channel to allow motor attachment to the filament. Thus preventing the cytoskeleton from leaving the structure. Alternatively, the second method requires that only the floor of the channel is able to immobilise the motor protein.[84, 85] With no motor protein attached to the walls of the channels there it is impossible for the filament to climb out and is therefore restricted to

wherever the channel flows. Topographical confinement has been used as a proof of concept in devices that could be used to collect and aggregate filaments, and potentially the cargo they could carry.[59, 82] By specifically designing the flow of the channels it is possible to direct the filaments to specific areas. One example of this is the inclusion of 'rectifiers' where filaments moving in the wrong direction along a channel are taken out, moved around a specially designed loop, and then returned to the original channel now moving in the correct direction.[82] This solves an important issue with the topographical control of motor protein motility, that of directionality. While it is obvious that the movement of the filaments can be confined within a structure, the direction of these filaments is still independent of the structure, i.e. the filaments may move either up or down the channel. The directionality of the filaments within these structures are therefore still defined in one dimension by Brownian motion and, probably more importantly, the lateral positioning of the motor. Due to the method of immobilisation of the protein this positioning is very random, meaning without significant alterations to the channel design, the direction of filament movement is still relatively random. Although these rectifiers and 'roundabouts' (Figure 2.11 B) seem to solve this issue they also add significant surface area and complexity to the overall device design, especially if the surface of the gliding assay is large (>100 μm^2) and requires multiple rectifier structures to keep the filament moving in the correct direction.

2.7.2 Chemical confinement

A second method of controlling the movement of filaments across the gliding assay is the use of chemical tracks, which preferentially bind the protein thus creating a highway of motors (Figure 2.12 A and B). Like topographical control, many have used this method with a high degree of success not only to create tracks but also to alter the overall motility function seen on the surface in terms of velocity, directionality and 'quality' of motility.[75, 77, 79, 81, 89-92]

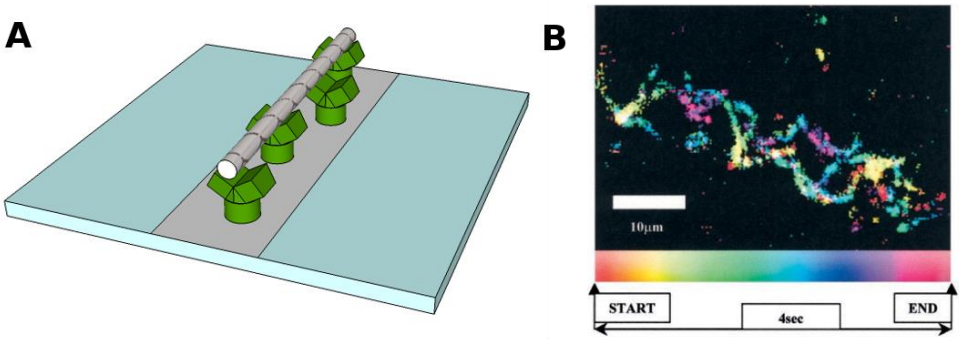

Figure.2.12. A, Chemical patterning of a surface can create areas where the motor protein will preferentially adsorb. B, E-beam patterning of a poly[(*tert*-butyl-methacrylate)-*co*-(methyl methacrylate)](PMMA) coated substrate gives rise to a change in hydrophobicity of the exposed areas. The coloured tracks show the movement of filaments in hydrophobic areas of the surface where the motility of actin filaments is being confined due to the preferential binding of the protein to these regions.[77]

Due to the processive nature of kinesin, and its ability to attach to a variety of chemical surfaces these studies into altering the motility function mainly concentrate on the myosin system. This is down to the fact that only a small number of kinesin motors are required on the surface for motility to takes place as the filament is constantly held by the motor during motility. Myosin, however, works via a cooperative mechanism in which the motor spends very little time attached to the filament, and so requires a number of motors on the surface working in cooperation, but not necessarily in tandem, for filament translocation.[1, 2, 49, 73] This means that the motility function seen on the gliding assays of actin myosin can be readily altered by small changes in the concentration of motor proteins and the orientation of motor proteins.[91] The subject of motor protein adsorption to different surface chemistries is one that is of high interest within the field and one that will be covered in chapters 5 and 6 of this thesis. The disadvantages of this method for confinement are obvious. Similar to topographical confinement there is no way of directing the filaments, they are free to move up or down any given track. On top of this, chemical tracks have a limit to the amount of

confinement they can create. It has been reported that filaments need to be moving within a certain angle of the edges of the tracks. If the filament approaches at an angle of incidence greater than ~20^{o} it will tend to come off the track and float into the assay solution.[77, 93] This is obviously a serious weakness of chemical confinement unless one can tune these to be so narrow that an angle of incidence that would lead to filament loss is impossible once the filament has begun moving along the track. This issue, however, means that it would be impossible to build small rectifiers, seen in some examples of topographical confinement. This is due to being unable to make the filaments make sharp turns on chemical tracks as the filament is more likely to dissociate from the motors as there is no obstacle stopping it from doing this.[82, 84] Altering the surface chemistry alone may not be an accurate method of confinement, but it does open up options for tuning the motility function either over an entire surface or just in set regions.[81, 85, 92, 94]

2.7.3 Guidance by electrical fields

The polarity of both microtubules and actin filaments opens up the possibility of directing and guiding the motility using electrical fields (Figure 2.13). This has been shown in both myosin and kinesin systems and also in the absence of motor proteins.[59, 76, 81, 95-97]

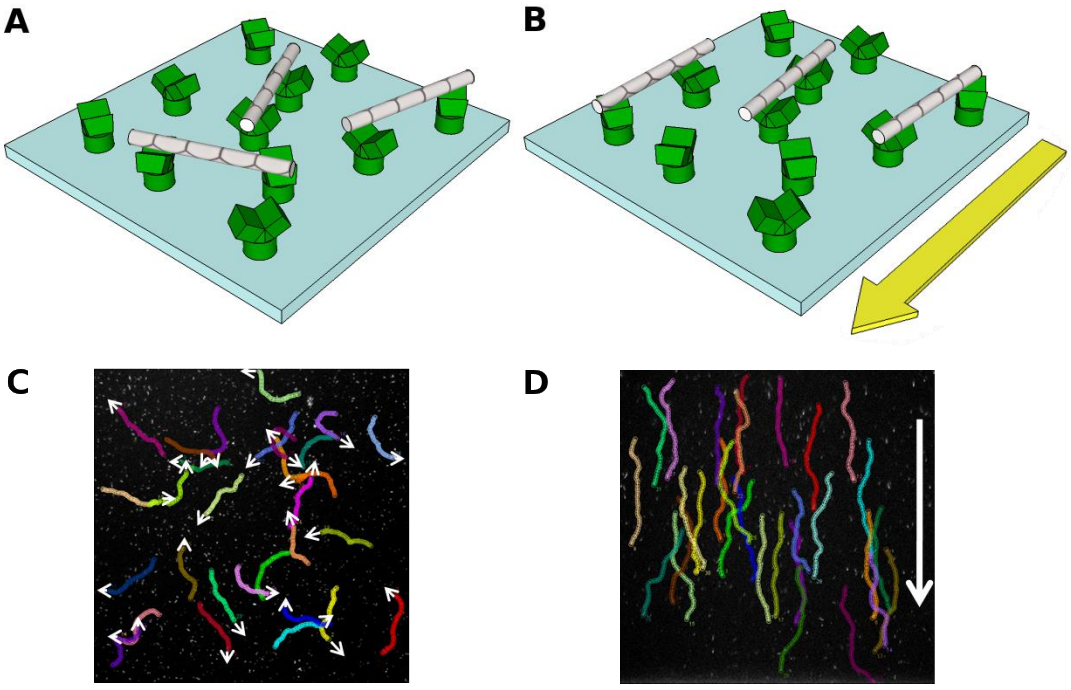

Figure .2.13. Electrical guidance of filaments in a gliding assay. A, In the absence of an electrical field the directionality of the filaments movement will be dominated by Brownian motion and the lateral orientation of the protein motors. B, The yellow arrow shows the direction of the field with the point representing the position of the positive electrode. In this instance the polarity of the filaments will result in an overall propensity for the leading, negatively charged, head of the filament to move towards the positive electrode. C, Image shows the tracks of individual actin filaments with arrows showing their direction of movement. D, The image shows the directing of actin filament movement by an electrical field. The white arrow represents the direction of the field and general direction of filament motion. The images shown in C and D are produce from work in this thesis.

The distinct advantage that this method has over both chemical and topographic confinement is the ability to control the direction of filament movement. Most designs utilise a set-up where the flow cell incorporates an electrophoritic cell, where the negatively charged, leading tips, of the filaments can be guided towards the positive electrode. The electrode set-up can either be included within the flow cell, or incorporated outside the flow cell within a container containing an ionic solution.[59, 76, 98] It has been shown that reasonably low

electrical fields can influence the motility and in combination with topographic confinement, it can even be used to measure the lateral forces exhibited by the motor.[76] A drawback of this method is the creation of gas and species e.g. radicals, at the electrodes that are harmful to the motor proteins. Lab-on-chip designs utilising this method of control will need to circumvent this issue if there is to be no damage done to the protein layer. This may be achieved by either having the electrodes far away from any surface area containing motor protein, although the large potentials required could present a safety risk, or by the careful placement of electrodes inside the structures on the gliding assay.[76, 81, 98] A design may be implemented that only requires the electrical field to be activated for a fraction of a second, for example at a junction between channels.[59] This would rapidly decrease the chance of destroying the proteins in that area.

These separate methods of motility control can, and in some cases have, been used in conjunction with each other to create a highly specific guidance system where filaments are directed, collected or sorted to predefined positions in a gliding assay.[85] Other novel control methods have also been successfully demonstrated to affect the motility of both actin and microtubules.[49, 99] Microtubules have been decorated with cargo that has shown to control the speed of microtubule motility.[62, 100] Thermoresponsive polymers which block the attachment of the cytoskeleton to the motor have been shown to create gates and motility prohibiting areas.[80, 83] Many of these control method have been implemented in functional devices for, sensing, sorting and cargo transport.[62, 64, 100, 101] In the following chapters of this thesis two separate systems, microtubules kinesin and actin myosin motility, are utilised in two separate devices that implement several of the control methods for the confinement and guidance of motor protein motility.

2.8 References

1. Howard, J., *Mechanics of motor proteins and the cytoskeleton*, Sinauer Associates, Inc., sunderland Massachusetts (2001).
2. Manfred, S., *Molecular Motors*, Wiley-VCH, Weinheim (2003).
3. Schliwa, M. and Woehlke, G., "Molecular motors," *Nature* 422(6933), 759-765 (2003)
4. Miki, H., Setou, M., Kaneshiro, K. and Hirokawa, N., "All kinesin superfamily protein, KIF, genes in mouse and human," *Proceedings of the National Academy of Sciences* 98(13), 7004-7011 (2001)
5. Amos, L. A. and Klug, A., "Arrangement of subunit in flagellar microtubules," *Journal of Cell Science* 14(3), 523-549 (1974)
6. McGrogan, B. T., Gilmartin, B., Carney, D. N. and McCann, A., "Taxanes, microtubules and chemoresistant breast cancer," *Biochimica et Biophysica Acta (BBA) - Reviews on Cancer* 1785(2), 96-132 (2008)
7. Wade, R. H. and Chrétien, D., "Cryoelectron Microscopy of Microtubules," *Journal of Structural Biology* 110(1), 1-27 (1993)
8. Ray, S., Meyhöfer, E., Milligan, R. A. and Howard, J., "Kinesin follows the microtubule's protofilament axis," *The Journal of Cell Biology* 121(5), 1083-1093 (1993)
9. Chretien, D. and Wade, R. H., "New data on the microtubule surface lattice," *Biology of the cell / under the auspices of the European Cell Biology Organization* 71(1-2), 161-174 (1991)
10. Kris, T., R, Vale, "Cytoskeletal and Motor Proteins," 1st), (1993)
11. Hodge, T. and Cope, M., "A myosin family tree," *Journal of Cell Science* 113(19), 3353-3354 (2000)
12. Baker, J. P. and Titus, M. A., "Myosins: matching functions with motors," *Current Opinion in Cell Biology* 10(1), 80-86 (1998)
13. Rayment, I., Rypniewski, W. R., Schmidt-Base, K., Smith, R., Tomchick, D. R., Benning, M. M., Winkelmann, D. A., Wesenberg, G. and Holden, H. M., "Three-dimensional structure of myosin subfragment-1: a molecular motor," *Science* 261(5117), 50-58 (1993)
14. Huxley, H. and Hanson, J., "Changes in the cross-striations of muscle during contraction and stretch and their structural interpretation," *Nature* 173(4412), 973-976 (1954)
15. Huxley, A. F. and Niedergerke, R., "Structural changes in muscle during contraction – interference microscopy of living muscle fibres," *Nature* 173(4412), 971-973 (1954)
16. Ishijima, A., Kojima, H., Higuchi, H., Harada, Y., Funatsu, T. and Yanagida, T., "Multiple- and single-molecule analysis of the actomyosin motor by nanometer piconewton manipulation with a microneedle: Unitary steps and forces," *Biophysical Journal* 70(1), 383-400 (1996)
17. Margossian, S. S. and Lowey, S., "Preparation of myosin and its subfragments from rabbit skeletal-muscle," *Methods Enzymol.* 85(55-71 (1982)
18. Moore, P. B., Huxley, H. E. and DeRosier, D. J., "Three-dimensional reconstruction of F-actin, thin filaments and decorated thin filaments," *J. Mol. Biol.* 50(2), 279-292 (1970)
19. Hase, M. and Yoshikawa, K., "Structural transition of actin filament in a cell-sized water droplet with a phospholipid membrane," *J. Chem. Phys.* 124(10), (2006)
20. Hosek, M. and Tang, J. X., "Polymer-induced bundling of F actin and the depletion force," *Physical Review E* 69(5), (2004)
21. Katayama, E., "Quick-freeze deep-etch electron microscopy of the actin-heavy meromyosin complex during the in vitro motility assay," *J. Mol. Biol.* 278(2), 349-367 (1998)

22. Pollard, T. D., "Reflections on a quarter century of research on contractile systems," *Trends in Biochemical Sciences* 25(12), 607-611 (2000)
23. Squire, J., "The structural basis of muscular contraction," (1981)
24. Spudich, J. A., "How Molecular Motors Work," *Nature* 372(6506), 515-518 (1994)
25. Lymn, R. W. and Taylor, E. W., "Mechanism of Adenosine Triphosphate Hydrolysis by Actomyosin," *Biochemistry* 10(25), 4617-& (1971)
26. Ma, Y. Z. and Taylor, E. W., "Mechanism of microtubule kinesin ATPase," *Biochemistry* 34(40), 13242-13251 (1995)
27. Ma, Y. Z. and Taylor, E. W., "Interacting head mechanism of microtubule-kinesin ATPase," *The Journal of biological chemistry* 272(2), 724-730 (1997)
28. Wriggers, W. and Schulten, K., "Nucleotide-dependent movements of the kinesin motor domain predicted by simulated annealing," *Biophys J* 75(2), 646-661 (1998)
29. Coy, D. L., Wagenbach, M. and Howard, J., "Kinesin takes one 8-nm step for each ATP that it hydrolyzes," *J. Biol. Chem.* 274(6), 3667-3671 (1999)
30. Sweeney, H. L. and Houdusse, A., "Structural and functional insights into the Myosin motor mechanism," *Annual review of biophysics* 39(539-557 (2010)
31. Volkmann, N., Hanein, D., Ouyang, G., Trybus, K. M., DeRosier, D. J. and Lowey, S., "Evidence for cleft closure in actomyosin upon ADP release," *Nature structural biology* 7(12), 1147-1155 (2000)
32. Yengo, C. M., Chrin, L., Rovner, A. S. and Berger, C. L., "Intrinsic Tryptophan Fluorescence Identifies Specific Conformational Changes at the Actomyosin Interface upon Actin Binding and ADP Release†," *Biochemistry* 38(44), 14515-14523 (1999)
33. Spudich, J. A., Rice, S. E., Rock, R. S., Purcell, T. J. and Warrick, H. M., "Optical Traps to Study Properties of Molecular Motors," *Cold Spring Harbor Protocols* 2011(11), pdb.top066662 (2011)
34. Nicolau, D. V. and Muller, U. V., *Microarray Technology and Its Applications*, Springer-Verlag Berlin Heidelberg Germany (2005).
35. Vale, R. D., Reese, T. S. and Sheetz, M. P., "Identification of a novel force-generating protein, kinesin, involved in microtubule-based motility," *Cell* 42(1), 39-50 (1985)
36. Brady, S. T., "A novel brain ATPase with properties expected for the fast axonal-transport motor," *Nature* 317(6032), 73-75 (1985)
37. Sheetz, M. P. and Spudich, J. A., "Movement of myosin-coated fluorescent beads on actin cables in vitro," *Nature* 303(5912), 31-35 (1983)
38. Spudich, J. A., Kron, S. J. and Sheetz, M. P., "Movement of myosin-coated beads on oriented filaments reconstituted from purified actin," *Nature* 315(6020), 584-586 (1985)
39. Harada, Y., Noguchi, A., Kishino, A. and Yanagida, T., "Sliding movement of single actin-filaments on one-headed myosin-filaments," *Nature* 326(6115), 805-808 (1987)
40. Kron, S. J. and Spudich, J. A., "Fluorescent actin filaments move on myosin fixed to a glass surface," *Proceedings of the National Academy of Sciences* 83(17), 6272-6276 (1986)
41. Sellers, J. R., "In Vitro Motility Assay to Study Translocation of Actin by Myosin," in *Current Protocols in Cell Biology*, John Wiley & Sons, Inc. (2001).
42. Funatsu, T., Harada, Y., Tokunaga, M., Saito, K. and Yanagida, T., "Imaging of single fluorescent molecules and individual ATP turnovers by single myosin molecules in aqueous solution," *Nature* 374(6522), 555-559 (1995)
43. Ishijima, A., Harada, Y., Kojima, H., Funatsu, T., Higuchi, H. and Yanagida, T., "Single-molecule analysis of the actomyosin motor using nano-manipulation," *Biochem Biophys Res Commun* 199(2), 1057-1063 (1994)
44. Kron, S. J., Toyoshima, Y. Y., Uyeda, T. Q. P. and Spudich, J. A., "Assays for actin sliding movement over myosin-coated surfaces," *Methods Enzymol.* 196(399-416 (1991)

45. Warrick, H. M., Simmons, R. M., Finer, J. T., Uyeda, T. Q. P., Chu, S. and Spudich, J. A., "In-vitro methods for measuring force and velocity of the actin-myosin interaction using purified proteins," *Methods in Cell Biology, Vol 39* 39(1-21 (1993)
46. Lengsfeld, A. M., Low, I., Wieland, T., Dancker, P. and Hasselbach, W., "Interaction of phalloidin with actin," *Proc Natl Acad Sci U S A* 71(7), 2803-2807 (1974)
47. Korten, T., Mansson, A. and Diez, S., "Towards the application of cytoskeletal motor proteins in molecular detection and diagnostic devices," *Curr. Opin. Biotechnol.* 21(4), 477-488 (2010)
48. Hess, H., Bachand, G. D. and Vogel, V., "Powering nanodevices with biomolecular motors," *Chem.-Eur. J.* 10(9), 2110-2116 (2004)
49. Stefan Diez, J. H., "Nanotechnological Applications of Biomolecular Motor Systems," *La Physique au Canada* 65(1), 7-12 (2009)
50. Kinosita, K., Yasuda, R., Noji, H., Ishiwata, S. and Yoshida, M., "F-1-ATPase: A rotary motor made of a single molecule," *Cell* 93(1), 21-24 (1998)
51. Hess, H., Clemmens, J., Qin, D., Howard, J. and Vogel, V., "Light-controlled molecular shuttles made from motor proteins carrying cargo on engineered surfaces," *Nano Lett.* 1(5), 235-239 (2001)
52. Nitta, T. and Hess, H., "Dispersion in active transport by kinesin-powered molecular shuttles," *Nano Lett* 5(7), 1337-1342 (2005)
53. Boal, A. K., Bachand, G. D., Rivera, S. B. and Bunker, B. C., "Interactions between cargo-carrying biomolecular shuttles," *Nanotechnology* 17(2), 349-354 (2006)
54. Ramachandran, S., Ernst, K. H., Bachand, G. D., Vogel, V. and Hess, H., "Selective loading of kinesin-powered molecular shuttles with protein cargo and its application to biosensing," *Small* 2(3), 330-334 (2006)
55. Doot, R. K., Hess, H. and Vogel, V., "Engineered networks of oriented microtubule filaments for directed cargo transport," *Soft Matter* 3(3), 349-356 (2007)
56. Suzuki, N., Miyata, H., Ishiwata, S. and Kinosita, K., "Preparation of bead-tailed actin filaments: Estimation of the torque produced by the sliding force in an in vitro motility assay," *Biophysical Journal* 70(1), 401-408 (1996)
57. Mansson, A., Sundberg, M., Balaz, M., Bunk, R., Nicholls, I. A., Omling, P., Tagerud, S. and Montelius, L., "In vitro sliding of actin filaments labelled with single quantum dots," *Biochemical and Biophysical Research Communications* 314(2), 529-534 (2004)
58. Patolsky, F., Weizmann, Y. and Willner, I., "Actin-based metallic nanowires as bio-nanotransporters," *Nat. Mater.* 3(10), 692-695 (2004)
59. van den Heuvel, M. G. L., De Graaff, M. P. and Dekker, C., "Molecular sorting by electrical steering of microtubules in kinesin-coated channels," *Science* 312(5775), 910-914 (2006)
60. Dennis, J. R., Howard, J. and Vogel, V., "Molecular shuttles: directed motion of microtubules slang nanoscale kinesin tracks," *Nanotechnology* 10(3), 232-236 (1999)
61. Hess, H., Clemmens, J., Brunner, C., Doot, R., Luna, S., Ernst, K. H. and Vogel, V., "Molecular self-assembly of "nanowires" and "nanospools" using active transport," *Nano Lett.* 5(4), 629-633 (2005)
62. Korten, T. and Diez, S., "Setting up roadblocks for kinesin-1: mechanism for the selective speed control of cargo carrying microtubules," *Lab Chip* 8(9), 1441-1447 (2008)
63. Fischer, T., Agarwal, A. and Hess, H., "A smart dust biosensor powered by kinesin motors," *Nat. Nanotechnol.* 4(3), 162-166 (2009)
64. Lard, M., ten Siethoff, L., Mansson, A. and Linke, H., "Tracking Actomyosin at Fluorescence Check Points," *Sci Rep* 3((2013)
65. Pardee, J. D. and Spudich, J. A., "Purification of muscle actin," *Methods in cell biology* 24(271-289 (1982)

66. Weeds, A. G. and Pope, B., "Studies on chymotryptic digestion of myosin – effects of divalent-cations on proteolytic susceptibility," *J. Mol. Biol.* 111(2), 129-157 (1977)
67. Seetharam, R., Wada, Y., Ramachandran, S., Hess, H. and Satir, P., "Long-term storage of bionanodevices by freezing and lyophilization," *Lab Chip* 6(9), 1239-1242 (2006)
68. Sundberg, M., Rosengren, J. P., Bunk, R., Lindahl, J., Nicholls, I. A., Tagerud, S., Omling, P., Montelius, L. and Mansson, A., "Silanized surfaces for in vitro studies of actomyosin function and nanotechnology applications," *Analytical Biochemistry* 323(1), 127-138 (2003)
69. Ionov, L., Stamm, M. and Diez, S., "Size sorting of protein assemblies using polymeric gradient surfaces," *Nano Lett.* 5(10), 1910-1914 (2005)
70. Lengsfel.Am, Low, I., Wieland, T., Dancker, P. and Hasselba.W, "Interaction of phalloidin with actin," *Proc. Natl. Acad. Sci. U. S. A.* 71(7), 2803-2807 (1974)
71. Kawaguchi, K. and Ishiwata, S. i., "Temperature Dependence of Force, Velocity, and Processivity of Single Kinesin Molecules," *Biochemical and Biophysical Research Communications* 272(3), 895-899 (2000)
72. Rossi, R., Maffei, M., Bottinelli, R. and Canepari, M., "Temperature dependence of speed of actin filaments propelled by slow and fast skeletal myosin isoforms," *Journal of Applied Physiology* 99(6), 2239-2245 (2005)
73. Bakewell, D. J. G. and Nicolau, D. V., "Protein linear molecular motor-powered nanodevices," *Aust. J. Chem.* 60(5), 314-332 (2007)
74. Mansson, A., Bunk, R., Sundberg, M. and Montelius, L., "Self-Organization of Motor-Propelled Cytoskeletal Filaments at Topographically Defined Borders," *J. Biomed. Biotechnol.* (2012)
75. Sundberg, M., Bunk, R., Albet-Torres, N., Kvennefors, A., Persson, F., Montelius, L., Nicholls, I. A., Ghatnekar-Nilsson, S., Omling, P., Tagerud, S. and Mansson, A., "Actin filament guidance on a chip: Toward high-throughput assays and lab-on-a-chip applications," *Langmuir* 22(17), 7286-7295 (2006)
76. Riveline, D., Ott, A., Julicher, F., Winkelmann, D. A., Cardoso, O., Lacapere, J. J., Magnusdottir, S., Viovy, J. L., Gorre-Talini, L. and Prost, J., "Acting on actin: the electric motility assay," *Eur. Biophys. J. Biophys. Lett.* 27(4), 403-408 (1998)
77. Nicolau, D. V., Suzuki, H., Mashiko, S., Taguchi, T. and Yoshikawa, S., "Actin motion on microlithographically functionalized myosin surfaces and tracks," *Biophysical Journal* 77(2), 1126-1134 (1999)
78. Bunk, R., Rosengren, J., Forlander, K., Sundberg, M., Montelius, L., Nicholls, I. A., Omling, P., Tagerud, S. and Mansson, A., "Actomyosin motility on nanostructured resist polymers and silanes," *Biophysical Journal* 84(2), 327A-327A (2003)
79. Suzuki, H., Yamada, A., Oiwa, K., Nakayama, H. and Mashiko, S., "Control of actin moving trajectory by patterned poly(methyl methacrylate) tracks," *Biophysical Journal* 72(5), 1997-2001 (1997)
80. Schroeder, V., Korten, T., Linke, H., Diez, S. and Maxirnov, I., "Dynamic Guiding of Motor-Driven Microtubules on Electrically Heated, Smart Polymer Tracks," *Nano Lett.* 13(7), 3434-3438 (2013)
81. Ramsey, L. C., Aveyard, J., van Zalinge, H., Persson, M., Månsson, A. and Nicolau, D. V., "Electric field modulation of the motility of actin filaments on myosin-functionalised surfaces," 85940R-85940R-85947 (2013).
82. Lard, M., ten Siethoff, L., Kumar, S., Persson, M., te Kronnie, G., Linke, H. and Månsson, A., "Ultrafast molecular motor driven nanoseparation and biosensing," *Biosensors and Bioelectronics* 48(0), 145-152 (2013)
83. Ionov, L., Stamm, M. and Diez, S., "Reversible switching of microtubule motility using thermoresponsive polymer surfaces," *Nano Lett.* 6(9), 1982-1987 (2006)

84. Clemmens, J., Hess, H., Doot, R., Matzke, C. M., Bachand, G. D. and Vogel, V., "Motor-protein "roundabouts": microtubules moving on kinesin-coated tracks through engineered networks," *Lab Chip* 4(2), 83-86 (2004)
85. Bunk, R., Sundberg, M., Mansson, A., Nicholls, I. A., Omling, P., Tagerud, S. and Montelius, L., "Guiding motor-propelled molecules with nanoscale precision through silanized bi-channel structures," *Nanotechnology* 16(6), 710-717 (2005)
86. Moorjani, S. G., Jia, L., Jackson, T. N. and Hancock, W. O., "Lithographically patterned channels spatially segregate kinesin motor activity and effectively guide microtubule movements," *Nano Lett.* 3(5), 633-637 (2003)
87. Mahanivong, C., Wright, J. P., Kekic, M., Pham, D. K., Remedios, C. d. and Nicolau, D. V., "Manipulation of the motility of protein molecular motors on microfabricated substrates," *Biomedical Microdevices* 4(2), 111-116 (2002)
88. Hess, H., Matzke, C. M., Doot, R. K., Clemmens, J., Bachand, G. D., Bunker, B. C. and Vogel, V., "Molecular shuttles operating undercover: A new photolithographic approach for the fabrication of structured surfaces supporting directed motility," *Nano Lett.* 3(12), 1651-1655 (2003)
89. Hanson, K. L., Solana, G. and Nicolau, D. V., "Effect of surface chemistry on in vitro actomyosin motility," in *Biomedical Applications of Micro- and Nanoengineering II* D. V. Nicolau, Ed., pp. 13-18, Spie-Int Soc Optical Engineering, Bellingham (2005).
90. Balaz, M., Sundberg, M., Persson, M., Kvassman, J. and Monsson, A., "Effects of surface adsorption on catalytic activity of heavy meromyosin studied using a fluorescent ATP analogue," *Biochemistry* 46(24), 7233-7251 (2007)
91. Persson, M., Albet-Torres, N., Ionov, L., Sundberg, M., Hook, F., Diez, S., Mansson, A. and Balaz, M., "Heavy Meromyosin Molecules Extending More Than 50 nm above Adsorbing Electronegative Surfaces," *Langmuir* 26(12), 9927-9936 (2010)
92. Sundberg, M., Rosengren, J. P., Bunk, R., Lindahl, J., Nicholls, I. A., Tågerud, S., Omling, P., Montelius, L. and Månsson, A., "Silanized surfaces for in vitro studies of actomyosin function and nanotechnology applications," *Analytical Biochemistry* 323(1), 127-138 (2003)
93. Suzuki, H., Yamada, A., Oiwa, K., Nakayama, H. and Mashiko, S., "Control of actin moving trajectory by patterned poly(methylmethacrylate) tracks," *Biophys J* 72(5), 1997-2001 (1997)
94. Nicolau, D. V., Solana, G., Kekic, M., Fulga, F., Mahanivong, C., Wright, J. and dos Remedios, C. G., "Surface Hydrophobicity Modulates the Operation of Actomyosin-Based Dynamic Nanodevices," *Langmuir* 23(21), 10846-10854 (2007)
95. Arsenault, M. E., Zhao, H., Purohit, P. K., Goldman, Y. E. and Bau, H. H., "Confinement and manipulation of actin filaments by electric fields," *Biophysical Journal* 93(8), L42-L44 (2007)
96. Chilakamarri, R., "Actin nanokinematics under the influence of DC electric fields," p. 105 p., West Virginia University, United States -- West Virginia (2005).
97. Takatsuki, H., Chilakamarri, R., Famouri, P. and Kohama, K., "Electrophoretic Mobility of Nano-sized Actin Filaments in Biomolecular Device," in *Nanotechnology, 2006. IEEE-NANO 2006. Sixth IEEE Conference on*, pp. 166-169 (2006).
98. Hanson, K. L., Solana, G. and Nicolau, D. V., "Electrophoretic control of actomyosin motility," in *Microtechnology in Medicine and Biology, 2005. 3rd IEEE/EMBS Special Topic Conference on*, pp. 205-206 (2005).
99. van den Heuvel, M. G. L. and Dekker, C., "Motor Proteins at Work for Nanotechnology," *Science* 317(5836), 333-336 (2007)
100. Schmidt, C., Kim, B., Grabner, H., Ries, J., Kulomaa, M. and Vogel, V., "Tuning the “Roadblock” Effect in Kinesin-Based Transport," *Nano Lett.* 12(7), 3466-3471 (2012)

101. Persson, M., Gullberg, M., Tolf, C., Lindberg, A. M., Mansson, A. and Kocer, A., "Transportation of Nanoscale Cargoes by Myosin Propelled Actin Filaments," *PLoS One* 8(2), (2013)

Chapter III: Materials and Methods

The following chapter contains the materials and methods used in the studies contained within this thesis. The fabrication technique used to structure the surface of a gliding assay will be detailed along with the procedure for both the myosin and kinesin motility assays. Also included are the methods used to functionalise the surface of the electrical motility assay for the study of motor protein adsorption on a variety of polymers and silanes.

All chemical were bought from Sigma Aldrich and all water used was Millipore 18.2 MΩ·cm unless stated.

3.1 Kinesin motility with thermoresponsive PINPAM gate

The thermoresponsive polymer PNIPAM was used as a means to inhibit the motility of microtubules at specific regions on a surface via localised heating. In these experiments a specialised gliding assay was created to incorporate a structured surface along with heat control 'gates' at junctions of the ablated channels. The motility gating device was created in collaboration with Dresden University and is a continuation of previous work achieved using PNIPAM to control kinesin motility.[1] The device takes the form of a kinesin gliding assay on which a set of electrodes are fabricated on the surface of the flow cell. A glass slide with a 200 nm thick gold surface, purchased from Ssens, Enschede, The Netherlands, with a chromium adhesion layer, was patterned to create a series of channels and a 'gate' area where via localised heating the structure of the thermoresponsive polymer in that region of the chip could be controlled.

3.1.1 Laser ablation

The patterning of the PNIPAM chips was performed by laser ablation, QuikLase-50ST from ESI/NewWave Research, of the gold layer. Laser ablation of the gold layer of the chip takes place due to a sharp temperature rise as the photons in the laser beam are absorbed as the laser is applied in short pulses in a predefined pattern resulting in vaporisation of the metal.[2, 3] The laser beam, with a spot size of around 2 x 10 μm^2 was pulsed at 10 Hz and moved across the surface at no more than 10 μm/s. Multiple passes were made to ensure complete ablation of the gold layer.

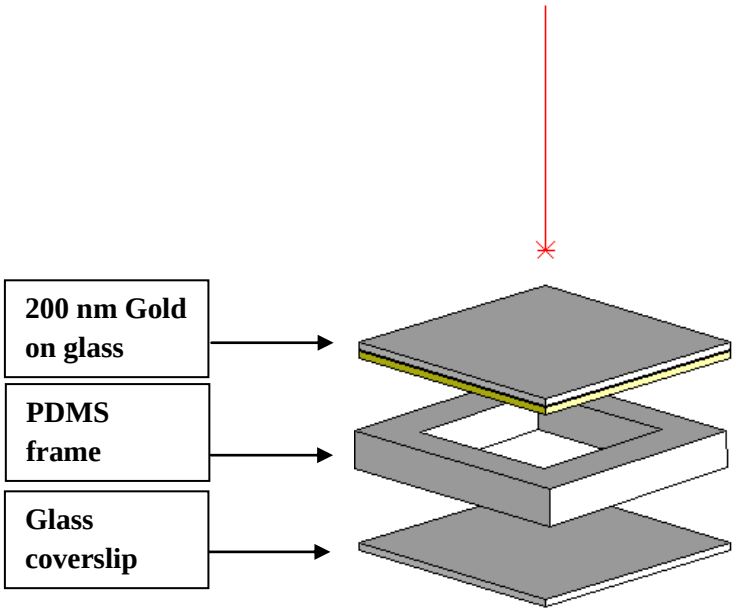

Figure.3.1 The scheme shows the laser ablation method for patterning the gold surface of the gliding assay. The ablation is performed through the back of the sample; a PDMS frame containing water is sealed to the gold and captures any debris created during ablation.

There was a significant amount of debris left on the surface after direct ablation of the gold, and upon application of the motility assay, this was found to obstruct the motility function in key areas of the design. Therefore a slightly altered ablation technique was designed. A water cell was created using frames cast from PDMS (Figure 3.1). The chips were mounted so that the ablation would take place through the glass back of the chips and any debris created during the patterning would be captured by the water cell, unable to be deposited onto the surface.

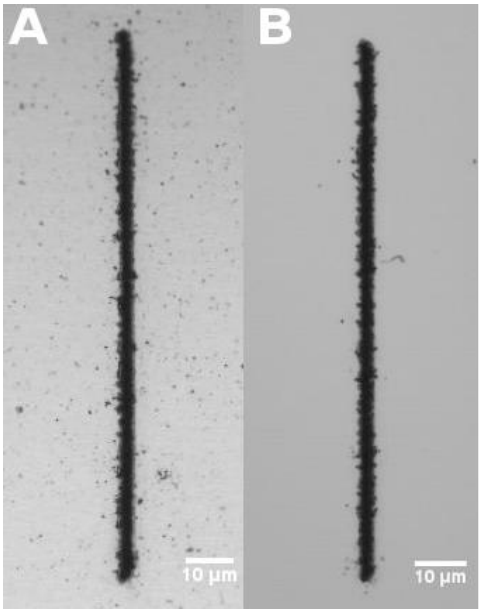

Figure.3.2 Two confocal images of channels ablated into a 200 nm gold surface. After ablation both were rinsed with ethanol and water before imaging. A, 4 µm wide channel ablated without the use of the flow cell detailed in Figure 3.1, extensive debris is visible around the ablated area. B, Channel ablated with the use of the water cell, shows a dramatic decrease in the amount of ablation debris left on the surface.

This ablation technique solved the issue of debris remaining on the surface after patterning (see Figure 3.2) and further samples showed that motility was unhindered on all areas of the final design.

3.1.2 PDMS preparation

Sylgard 184 Polydimethylsiloxane (PDMS), Dow corning corporation, is a silicone elastomer. It is supplied as a two part kit containing a base and curing agent that are mixed in a 10:1 mass ratio. When combined the two make a transparent viscous liquid that can be poured into a desired mold. Once the PDMS has been applied to the mold it is put under vacuum to remove the liquid of any gas bubbles formed in the reaction between base and curing agent, and also to aid in making a seal between the liquid and mold. When

completely degassed the PDMS is cured for 8 h at 65 ^{o}C to allow completion of the cross linking of the polymer chains.

To make the frames for the laser ablation method used to pattern the PNIPAM chips, a thin layer, approximately 2 mm, of PDMS was poured into a large petri dish. Once cured, frames measuring 18 x 12 mm^2 were cut.

3.1.3 Surface Functionalisation

The method for grafting PNIPAM onto surfaces was adapted from Ionov *et al*.[1] 200 nm thick gold-on-glass chips (20x14x1 mm^3, Ssens, Enschede, The Netherlands) were cleaned with Piranha solution (3:1 concentrated H_2SO_4 and H_2O_2; danger, extremely corrosive and explosive when mixed with organic solvents!). The clean substrates were then spin-coated (ramped at 500 rpm/s to 2000 rpm for 30 s) with a 0.01 % Poly(glycidyl methacrylate), (PGMA, M_n = 65000 g mol^{-1}, Polymersource Inc., Dorval, (Montreal), Canada) solution in chloroform. The PGMA was annealed at 130 °C for 20 min in a vacuum oven. After annealing, the substrates were placed in chloroform (70 °C) in order to remove unbound PGMA. After the deposition of the PGMA, the topographical structure and the electrodes were fabricated by laser microablation of the chip surface. Poly(N-isopropylacrylamide) (PNIPAM, Mn = 45000 g/mol, Polymersource Inc., Dorval (Montreal), Canada) was dissolved in chloroform (1% solution). The surface of the substrates was then completely covered with a droplet of the PNIPAM solution. After the chloroform evaporated, the substrates were placed in the vacuum oven at 160 °C for 60 min to anneal the PNIPAM. Unbound PNIPAM was removed by washing the substrates in hot chloroform (70 °C).

3.1.4 Motility Assay

Microtubules were polymerised from rhodamine-labeled porcine brain tubulin in BRB80 (80 mM PIPES, adjusted to pH 6.9 with KOH, 1 mM EGTA, 1 mM $MgCl_2$) with 5 mM $MgCl_2$,

1 mM GTP, 5 % DMSO at 37 °C for 30 min. The microtubules were stabilised and diluted 200-fold in BRB80 containing 10 µM taxol. Flow cells for motility experiments were assembled with the structured chips, two strips of parafilm across the surface and closed with a glass cover slip (Figure 3.3). The chips were then mounted onto a microscope stage that could be temperature-controlled using a Peltier element [1].

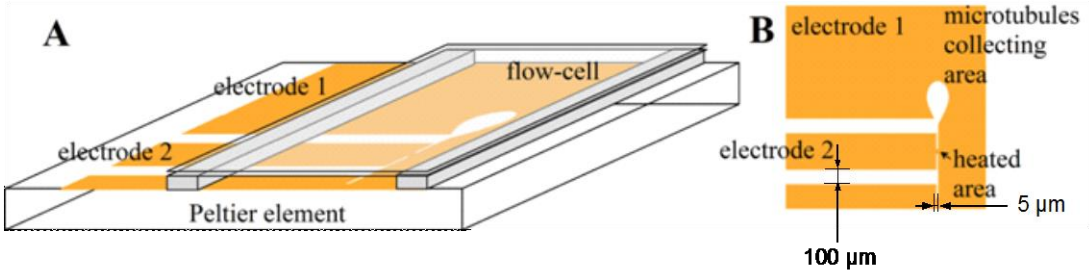

Figure.3.3 A, Scheme showing the layout of motility flow over the patterned surface making up the gliding assay. White areas show where the gold has been ablated away to leave 200 nm deep channel. B, There is a small area of gold between the channels where joule heating will occur.

A casein containing solution (BRB80 with 0.5 mg ml^{-1} casein) was perfused into the flow cell and allowed to adsorb for 5 min. This solution was exchanged for a kinesin solution (BRB80 with 10 µg ml^{-1} Kinesin-1, full length, from Drosophila melanogaster, expressed in bacteria[4]; 0.2 mg/ml casein, 1 mM ATP, 10 mM dithiothreitol), which was allowed to adsorb for 5 min. Finally, a microtubule containing solution (motility solution: BRB80 with 10 mM taxol, microtubules (equivalent of 32 nM tubulin), 1 mM ATP, 40 mM D-glucose, 55 µg ml^{-1} glucose oxidase, 11 mg ml^{-1} catalase, 10 mM dithiothreitol) was inserted and imaging was started. The imaging was performed using an Axiovert 200M inverted optical microscope (Zeiss) equipped with a back-illuminated CCD camera (MicroMax 512 BFT, Roper Scientific) in conjunction with a Metamorph imaging system (Universal Imaging Corp.).

3.2 Electrical motility device for the study of actin myosin motility on polymer and silane surfaces

The electrical motility device was used in the studies detailed in chapters 5 and 6 to examine filament guidance by electrical fields. By examining the effect of the field on motility on different surfaces the device has also been used to probe the protein adsorption properties of a number of polymers and silanes. The device set up described in the following section was used for the studies achieved in both chapters 5 and 6 of this thesis. An IVMA was modified using a large coverslip sealed at two sides with chambers attached at the open ends of the flow cell that allowed the application of electrodes. The electrodes were designed in a way that the distance between was defined by the size of the cover slip, 50 mm. Before assembling the flow cell the surface of the gliding assay was functionalised with the surface chemistries to be tested.

3.2.1 Surface functionalisation

The following polymers and silanes were used as surfaces with which to immobilise HMM to the surface of the electrical motility gliding assay, Nitrocellulose (NC), poly(methyl methacrylate) (PMMA), poly(tertbutyl methacrylate) (PtBMA), poly(butyl methacrylate) (PBMA), trimethylchlorosilane (TMCS) and Triehtlychlorosilane (TECS). Large coverslips measuring 50 x 22 mm^2 were functionalised prior to assembling the electrical motility flow cell. Solutions for spin coating the polymers were prepared as follows: NC 1% (w/v) in amyl acetate; PMMA (average M_w=120000) 2% (w/v) in PGMEA; PtBMA (average M_w=170000) 2% (w/v) in PGMEA; PBMA (average M_w=180000; Polysciences Europe) 1% (w/v) in toluene. The silane solutions when prepared as follows, TMCS 5 % in chloroform and TECS 5% in chloroform. For polymer functionalisation, glass cover slips were washed in ethanol and dried under a nitrogen flow before they were spin coated with the polymer solutions at

3600 rpm for 2 minutes (Figure 3.4). The cover slips were subsequently baked at 85^{o}C for 3 hours.

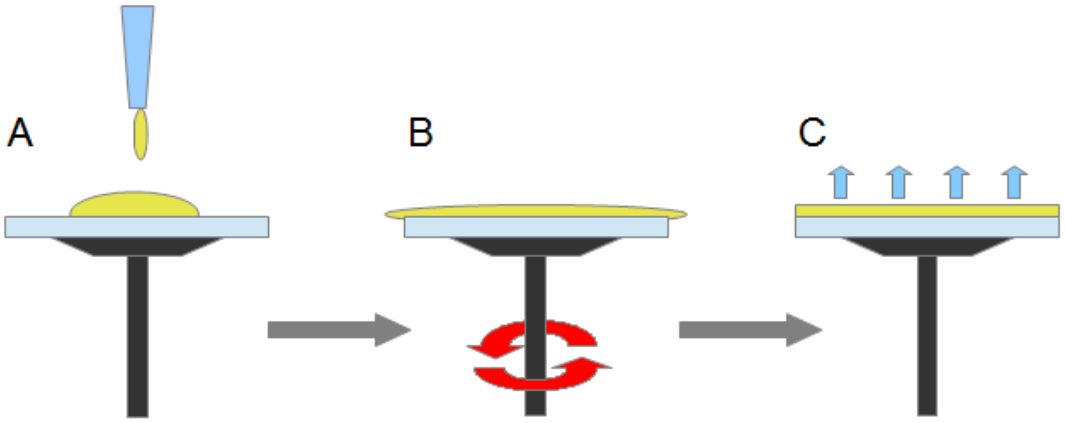

Figure.3.4 Schematic shows the process for spin coating. This was used to functionalise glass with NC, PMMA, PtBMA and PBMA. A, deposition of solution containing desired polymer. B, polymer is spread across surface as the sample is accelerated and spun at a given rpm. C, Sample is baked to allow evaporation of any residual solvent and to aid in adhesion to the glass.

For TMCS and TECS functionalisation, glass cover slips were soaked in dry acetone, followed by methanol and chloroform for 5 minutes then each soaked in a solution containing 5 % TMCS or TECS in dry chloroform for 5 minutes. After silanisation the cover slips were washed in dry chloroform, dried under a nitrogen flow and baked at 85 ^{o}C for 3 h. Figure 3.5 shows the reaction mechanism of the silanisation of the glass substrate.

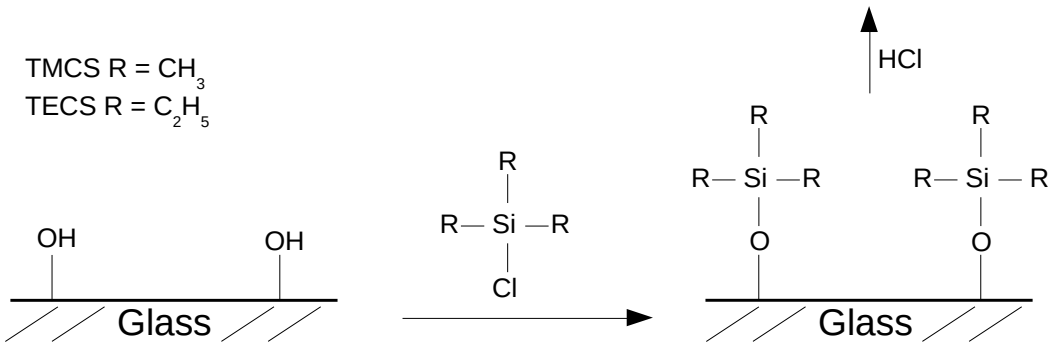

Figure.3.5 Schematic shows the functionalisation of glass with silanes TECS and TMCS. A silicon oxide bond is made at the surface with the release of hydrogen chloride.

All the surfaces chosen throughout this thesis have been previously shown to support myosin motility or are materials that are viable for use in lab-on-chip devices for protein adsorption.[5-8] A brief description of each surface chemistry and key characteristics follows.

PMMA is a homopolymer commonly used as a positive or negative photoresist for electron beam microscopy. The polymer has a glass temperature of 105 ^{o}C and low water absorption properties of around 0.2 – 0.4 % in standard room conditions.[9] The spin coating procedure used is expected to produce a flat, featureless surface.[10] PMMA is slightly hydrophobic with a measured contact angle of around 60 ^{o}. It has been used in previous studies for the immobilisation of myosin and has shown to adsorb the protein while retaining the motor function.[7, 11, 12] It has also been used in lab-on-chip designs for the confinement of myosin motility.[11]

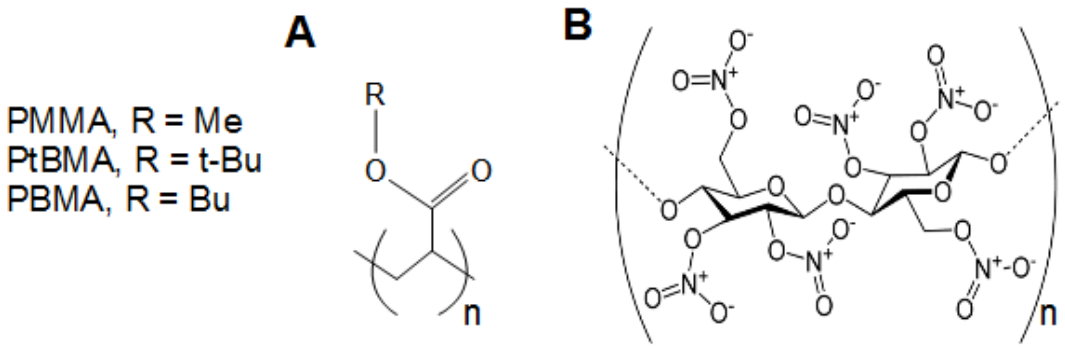

Figure.3.6. Structures of polymers used to functionalise the surface of the gliding assay. A, Methyl methacrylate polymers. B, Nitrocellulose.

NC (see Figure 3.6 B) is the nitrated form of cellulose, an important polymer found in the cell wall of plants. It is extremely flammable, so much so that it has found uses as a solid rocket fuel, flash paper and is responsible for a number cinema fires in the early 20th century due to its use in film stock.[13, 14] It has been used in a number of biological applications due to its protein and antibody binding characteristics.[15, 16] NC has long been used in actin myosin gliding assays and is regarded as the control surface in motility experiments.[17-20] The surfaces produced in the studies presented here are relatively hydrophobic (contact angle ~70^{o}). Contact angle measurements were achieved with nanopure water (5 µL) at room temperature (23-25^{o}C) in air using a Krüss drop shape analysis system DSA 10 Mk2. Higher contact angles show surfaces with higher hydrophobicity as the water droplet forms a structure closer to a bead on the surface. NC will readily absorb water into its structure. The spin coating and baking procedure used here will create a flat uniform surface. However, upon application of the assay solutions during the gliding assay the surface is likely to absorb water and become gel-like in nature.

Methacrylate polymers are widely used in scientific research (see Figure 3.6 A). PtBMA is used as a resist in semiconductor microlithography and although not extensively used in motility assays the surface has shown along with other resist polymers to readily adsorb

HMM.[11, 21] The PtBMA surfaces used here were very hydrophobic (contacts angles of 79 – 82 ^{o}) and much like PMMA, are flat and rigid with very little water absorption.

PBMA, though not widely used as a platform for actin myosin motility, has shown to support the protein with various degrees of success.[8, 22] The surfaces created here were slightly hydrophilic (contact angle around 58 ^{o} – 60 ^{o}). Much like NC the polymer has the propensity to absorb water into its structure leading to a gel-like surface when used in the gliding assay. Its use in this study is primarily down to its hydrophilicity and water absorption properties as a direct comparison to the more hydrophobic, but still gel like, structure that NC provides when utilised in the gliding assay.

Widely used in organic reaction as a means to protect functional groups during a reaction, silanes TECS and TMCS are used as coatings for glass and silcon surfaces and TMCS has also been applied in various microfabrication procedures as a resist.[23-25] Stable in the absence of water TMCS and TECS will form a self assembled monolayer on glass following reaction with the OH groups present at the surface. As such the resulting TMCS surfaces created in this study are expected to be flat, hydrophobic (contact angles of between 75^{o} – 80^{o}) and rigid with little water absorption. The TECS surfaces used here were again expected to form flat rigid surfaces with low water absorption, however, TECS creates highly hydrophilic surfaces with contact angles between 30^{o} – 35^{o}. Silanes have been shown to support actin myosin motility and more recent studies have shown preferable motility characteristics in terms of average filament velocity on TMCS over more traditional gliding assay surface chemistries such as NC. [6, 26, 27]

3.2.2 Electrical motility device

The electrical motility cell (EMC) is an extension of the standard *in vitro* motility flow cell. After surface functionalisation a large cover slip with dimensions of 50 x 22 mm^{2}, is sealed

on two sides to a microscope slide. Two pipette tips are then sealed at the centre of both open sections of the flow cell. These house the electrodes as well as the final assay solution which is applied before the electrodes are inserted (see Figure 3.7).

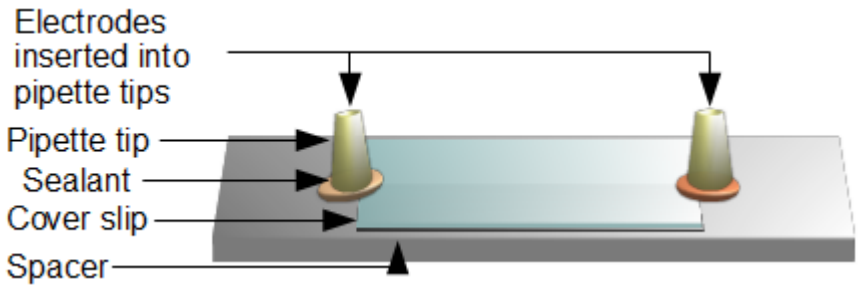

Figure.3.7. The pipette tips sealed at each end provide chambers that are first filled with the final assay solution of the motility assay and then electrodes are inserted.

The distance between the electrodes allows an oil immersion lens to be inserted between them in order to observe the motility in the centre of the flow cell. This is an important element of the design as in this section of the flow cell the field lines will be parallel allowing linear control of the filaments. This, coupled with the design of the electrode chambers, keeps any species harmful to the protein motors, e.g. gas bubbles and radicals, far from the area of analysis.

3.2.3 Motility assay

Apart from filling of the electrode reservoirs and the insertion of electrodes, the motility assays performed with the electrical motility device follows the same procedure as a standard *in vitro* motility assay. Each assay solution is perfused through the flow cell and allowed to incubate for a specific amount of time. The final solution containing the ATP is applied to both the flow cell and the electrode reservoirs.

Solutions for motility experiments

Assay solution; 1 mM MgATP, 10 mM DTT, 25 mM KCl and LISS with anti-bleach mixture containing 3 mg/ml^{-1} glucose, 20 units/ml glucose oxidase, 870 units/ml catalase and ATP regenerating system containing 2.5 mM creatine phosphate and 56 units/ml creatine kinase. Blocking solution; 1 mg ml^{-1} bovine serum albumin (BSA) in LISS buffer. Labelled actin; 10 µl of rhodamine phallodin labelled actin filaments (rhodamine phalloidin was purchased from Invitrogen and actin was labelled according to manufacturers protocol), 990 µl of L65. Blocking actin; 14 µl of unlabelled actin filaments, 986 µl of L65.

Motility assay procedure

60 µl of heavy meromyosin (HMM; 120 µg/ml in L65) was applied to a flow cell containing the functionalised cover slip and incubated for 2 minutes. At the end of this time, un-reacted binding sites on the cover slip were blocked by applying 60 µl of blocking solution to the flow cell. Following incubation for 30 seconds, the blocking solution in the flow cell was replaced with 60 µl of blocking actin in order to block non-functioning HMM heads. After 1 minute incubation, excess blocking actin was removed by flushing the flow cell with 60 µl of L65 and then 60 µl of labelled actin was applied for 30 seconds. At the end of this time excess labelled actin was removed by flushing the flow cell with 60 µl of L65 and 60 µl of assay solution was applied. The electrode chambers were filled with assay solution and the electrodes inserted. For each surface filament guiding was imaged at fields strengths 2 KVm^{-1} – 8 KVm^{-1} with an epifluorescence microscope (Zeiss Axio Imager.M1) fitted with an Andor iXon+ EMCCD camera at room temperature (23 - 35 ^{o}C).

Image acquisition and analysis

Videos were taken at a frame rate of 10 frames s^{-1}. Analysis of the videos was achieved in the open source image processing program imageJ and the filament movement tracked using

the plugin MtrackJ. Each experiment was repeated 3 times with an average of 10 filaments tracked per sample.

The electrical motility device was used in two separate studies utilising slightly different methodologies. In the first application, chapter 5, the device was used to guide the filaments across the surface and the average motility function, in terms of velocity and directionality, was recorded. The second motility study, chapter 6, was performed in two parts. The first section of the study performed in chapter 6 used the same electrical motility device but was performed and recorded slightly differently. In this experiment the movement actin filaments were recorded over a period of 30 seconds. After an initial period the filament were subjected to an electrical field to 'accelerate' the filaments across the protein surface. This was then terminated and the period after termination of the field analysed. A second study into the effect of blocking actin was performed in exactly the same fashion as the previous electrical motility study in chapter 5. The average motility function of guided actin filaments was measured on assays that did not contain blocking actin.

Where experiments were performed without the inclusion of blocking actin the assay procedure was performed as follows. 60 µl of heavy meromyosin (HMM; 120 µg/ml in L65) was applied to a flow cell containing the functionalised cover slip and incubated for 2 minutes. At the end of this time, 60 µl L65 was flowed through the cell. Following incubation for 30 seconds, the blocking solution in the flow cell was replaced with 60 µl of L65. This allowed the exclusion of blocking actin from the procedure without affecting the flushing of the flow cell. After 1 minute incubation, the L65 was then flushed from the flow cell with 2 x 60 µl of assay solution and then 60 µl of labelled actin was applied for 30 seconds. At the end of this time excess labelled actin was removed by flushing the flow cell with 60 µl of L65 and 60 µl of assay solution was applied to both the flow cell and the electrode chambers.

3.3 References

1. Ionov, L., Stamm, M. and Diez, S., "Reversible switching of microtubule motility using thermoresponsive polymer surfaces," *Nano Lett.* 6(9), 1982-1987 (2006)
2. Pethig, R., Burt, J. P. H., Parton, A., Rizvi, N., Talary, M. S. and Tame, J. A., "Development of biofactory-on-a-chip technology using excimer laser micromachining," *J. Micromech. Microeng.* 8(2), 57-63 (1998)
3. Pham, D., Tonge, L., Cao, J. N., Wright, J., Papiernik, M., Harvey, E. and Nicolau, D., "Effects of polymer properties on laser ablation behaviour," *Smart Materials & Structures* 11(5), 668-674 (2002)
4. Coy, D. L., Wagenbach, M. and Howard, J., "Kinesin takes one 8-nm step for each ATP that it hydrolyzes," *J. Biol. Chem.* 274(6), 3667-3671 (1999)
5. Suzuki, H., Yamada, A., Oiwa, K., Nakayama, H. and Mashiko, S., "Control of actin moving trajectory by patterned poly(methylmethacrylate) tracks," *Biophys J* 72(5), 1997-2001 (1997)
6. Sundberg, M., Rosengren, J. P., Bunk, R., Lindahl, J., Nicholls, I. A., Tagerud, S., Omling, P., Montelius, L. and Mansson, A., "Silanized surfaces for in vitro studies of actomyosin function and nanotechnology applications," *Analytical Biochemistry* 323(1), 127-138 (2003)
7. Nicolau, D. V., Solana, G., Kekic, M., Fulga, F., Mahanivong, C., Wright, J. and dos Remedios, C. G., "Surface Hydrophobicity Modulates the Operation of Actomyosin-Based Dynamic Nanodevices," *Langmuir* 23(21), 10846-10854 (2007)
8. Ramsey, L. C., Aveyard, J., van Zalinge, H., Persson, M., Månsson, A. and Nicolau, D. V., "Electric field modulation of the motility of actin filaments on myosin-functionalised surfaces," 85940R-85940R-85947 (2013).
9. "Matbase: the free and independent online materials properties resource."
10. Semaltianos, N. G., "Spin-coated PMMA films," *Microelectronics Journal* 38(6–7), 754-761 (2007)
11. Nicolau, D. V., Suzuki, H., Mashiko, S., Taguchi, T. and Yoshikawa, S., "Actin motion on microlithographically functionalized myosin surfaces and tracks," *Biophysical Journal* 77(2), 1126-1134 (1999)
12. Brunner, C., Ernst, K. H., Hess, H. and Vogel, V., "Lifetime of biomolecules in polymer-based hybrid nanodevices," *Nanotechnology* 15(10), S540-S548 (2004)
13. Gardiner, J., *The Thirties: An Intimate History of Britain*, Harper Press (2010).
14. "Nitrocellulose-based solid rocket propellant contg a carbamate|plasticizer," Aerojet General Corp.
15. Towbin, H., Staehelin, T. and Gordon, J., "Electrophoretic transfer of proteins from polyacrylamide gels to nitrocellulose sheets - procedure and some applications," *Proc. Natl. Acad. Sci. U. S. A.* 76(9), 4350-4354 (1979)
16. Tovey, E. R. and Baldo, B. A., "Protein binding to nitrocellulose, nylon and PVDF membranes in immunoassays and electroblotting," *J Biochem Biophys Methods* 19(2-3), 169-183 (1989)
17. Toyoshima, Y. Y., "How are myosin fragments bound to nitrocellulose film?," *Advances in experimental medicine and biology* 332(259-265 (1993)
18. Kron, S. J., Toyoshima, Y. Y., Uyeda, T. Q. P. and Spudich, J. A., "Assays for actin sliding movement over myosin-coated surfaces," *Methods Enzymol.* 196(399-416 (1991)
19. Persson, M., Albet-Torres, N., Ionov, L., Sundberg, M., Hook, F., Diez, S., Mansson, A. and Balaz, M., "Heavy Meromyosin Molecules Extending More Than 50 nm above Adsorbing Electronegative Surfaces," *Langmuir* 26(12), 9927-9936 (2010)
20. Spudich, J. A., "How Molecular Motors Work," *Nature* 372(6506), 515-518 (1994)

21. Wright, J., Ivanova, E., Pham, D., Filipponi, L., Viezzoli, A., Suyama, K., Shirai, M., Tsunooka, M. and Nicolau, D. V., "Positive and Negative Tone Protein Patterning on a Photobase Generating Polymer," *Langmuir* 19(2), 446-452 (2002)
22. Hanson, K. L., Solana, G. and Nicolau, D. V., "Effect of surface chemistry on in vitro actomyosin motility," in *Biomedical Applications of Micro- and Nanoengineering II* D. V. Nicolau, Ed., pp. 13-18, Spie-Int Soc Optical Engineering, Bellingham (2005).
23. Lercel, M. J., Whelan, C. S., Craighead, H. G., Seshadri, K. and Allara, D. L., "High-resolution silicon patterning with self-assembled monolayer resists," *J. Vac. Sci. Technol. B* 14(6), 4085-4090 (1996)
24. Chang, T. C., Liu, P. T., Mor, Y. S., Tsai, T. M., Chen, C. W., Mei, Y. J., Pan, F. M., Wu, W. F. and Sze, S. M., "Eliminating dielectric degradation of low-k organosilicate glass by trimethylchlorosilane treatment," *Journal of Vacuum Science & Technology B* 20(4), 1561-1566 (2002)
25. Wang, Q., Yang, B., Zhou, L., Gong, X., Yu, Q., Gao, J., Lu, Y. and Liang, P., "Preparation of paclitaxel involves performing acetylation on hydroxyl group of raw material in presence of cerium(III) chloride heptahydrate, protecting hydroxyl group with triethylchlorosilane, and performing condensation reaction," Jiangsu Yew Pharm Co Ltd.
26. Warrick, H. M., Simmons, R. M., Finer, J. T., Uyeda, T. Q. P., Chu, S. and Spudich, J. A., "In-vitro methods for measuring force and velocity of the actin-myosin interaction using purified proteins," *Methods in Cell Biology, Vol 39* 39(1-21 (1993)
27. Lard, M., ten Siethoff, L., Mansson, A. and Linke, H., "Tracking Actomyosin at Fluorescence Check Points," *Sci Rep* 3((2013)

Chapter IV: Guidance and Control of Kinesin Motility Using a Thermoresponsive Polymer

This chapter will focus on presenting a novel approach to the guidance and control of kinesin motility. A device design is presented that utilises topographic confinement and a thermoresponsive polymer to guide microtubules. A gliding assay containing a patterned surface is used to show how the movement of microtubules can be achieved. Specially created ‘Gates’ are positioned on the device where by localised heating using a thermoresponsive polymer in that region, motility is blocked.

4.1 Introduction

The following chapter will illustrate a novel approach to utilising motor proteins in lab-on-chip technologies. As stated in the introductory chapters, the main engineering goal for incorporating molecular motors into a device is control over the filament or microtubule movement. In this chapter a novel chip design is created so that the motility of microtubules can be topographically guided in predefined channels and a thermoresponsive polymer is used to create 'gates' at specific areas of these channels. Localised heating allows the selective inhibition of microtubule motility.

The kinesin microtubule system utilised in this device was chosen due to the surface binding nature of the protein. After the laser ablation of the Poly(glycidyl methacrylate) (PGMA) coated gold (see methods section 3.1.1) it is not possible to specifically functionalise the 'floors' of the channels in which the motility is to operate. Kinesin will attach to a variety of surface chemistries including glass.[1-6] As such there is no need for further functionalisation of the channels.

4.2 Application of the thermoresponsive polymer PNIPAM into a novel device for the control of microtubule motility

Kinesin is a robust motor protein which uses the energy generated by hydrolysing the nucleotide ATP to propel microtubules. *In vivo* the protein powers important processes such as cell division and vesicle transport. The movement of the microtubule is performed by the motor in a highly processive manner meaning, in the case of a gliding assay, that the protein can move the microtubule many steps before dissociating.[6-8] Alongside the previously stated surface binding characteristics of kinesin, this is a highly beneficial feature of the system and aids in the design of the gating device outlined in this chapter. It means that where the thermoresponsive polymer acts upon the motility will be highly specific as both the motor and the microtubule is in constant contact at each step in the ATPase cycle. This is important as in the final design of the device there are two defined areas where the motor protein attachment results in different densities of kinesin, where it is attached to glass and to PNIPAM coated regions on the chip. This characteristic of the kinesin system ensures that motility would be evident on both surface chemistries.

4.2.1 Previous kinesin motility applications

These benefits of the kinesin system have lead to it being implemented in a number of novel motility assays, all aimed at controlling the motility for a specific function. Perhaps the most common, and arguably the easiest to implement, methods of control has been the topographical guidance and isolation of kinesin motility.[9-14] In these examples the movement of the microtubules is confined in such a way that trajectories can only run in two directions, either up or down a channel. This has been shown in a number of studies to provide a simple route to confining motility to certain areas of a surface and also collecting the microtubules.[10, 14] As with all methods of guidance this technique has its limits, in this case being the directionality of the motility. Some studies have shown successful implementation

of ‘rectifiers’ into the motility channels. These collect microtubules that are moving in an undesired direction and return them to the channel flowing the correct way.[15] These, however, must be placed at specific regions of the chips and in many cases would involved more than one rectifier, rapidly increasing the complexity of the device.

The kinesin system has also shown some promise of being directed by the application of an electrical field.[10, 16, 17] Due to the negative charge held on the microtubules both electrophoresis and dielectrophoresis have been used to guide and ‘dock’ the motility. [18]

Other implementations of the kinesin system going beyond guidance, have seen the addition of cargoes to the microtubules and the use of these cargoes with surface bound entities to analyse the motility.[13, 19-21] In particular one study has used quantum dots attached to the filament to analyse the motility via 3D-nanometer tracking.[22]

The work in this chapter was done in collaboration with B CUBE - Center for Molecular Bioengineering, Technische Universität Germany and follows on from previous work performed there.

The thermoresponsive polymer PNIPAM was shown in a recent paper to provide a novel method for highly specific switching of kinesin motility.[23] In the initial implementation of the polymer, a globally heated PNIPAM coated surface was used to inhibit the attachment of microtubules to the motor protein. This inhibiting effect occurs at a specific temperature that is within the working temperature of kinesin and so does not risk the denaturing and therefore loss of function of the motor. Another paper has shown the successful implementation of this polymer switch to dynamically guide motility at a planer junction.[24] In the device presented here the PNIPAM switch is implemented into a chip design to provide a traffic-light type system with the addition of static topographical structures with which to guide the microtubules.

4.2.2 Response of motility to PNIPAM coating on globally heated surface

Poly(N-isopropylacrylamide) (PNIPAM) is a thermoresponsive polymer whose structure changes from a hydrated and extended state to one that is dehydrated and collapsed upon transition of the Lower Critical Solution Temperature (LCST) (see Figure 4.1). The polymer can be attached to specific regions of a surface via poly (glycidyl methacrylate) (PGMA). This creates a polymer surface with tuneable 'thickness'. It is this function that is utilised in the following device designs to remotely inhibit the motility by changing the temperature of the surface. The structural change of PNIPAM occurs at the LCST which is between 33 ^{o}C and 35 ^{o}C. This is within the operating temperature of kinesin in terms of avoiding any unwanted denaturing of the protein.

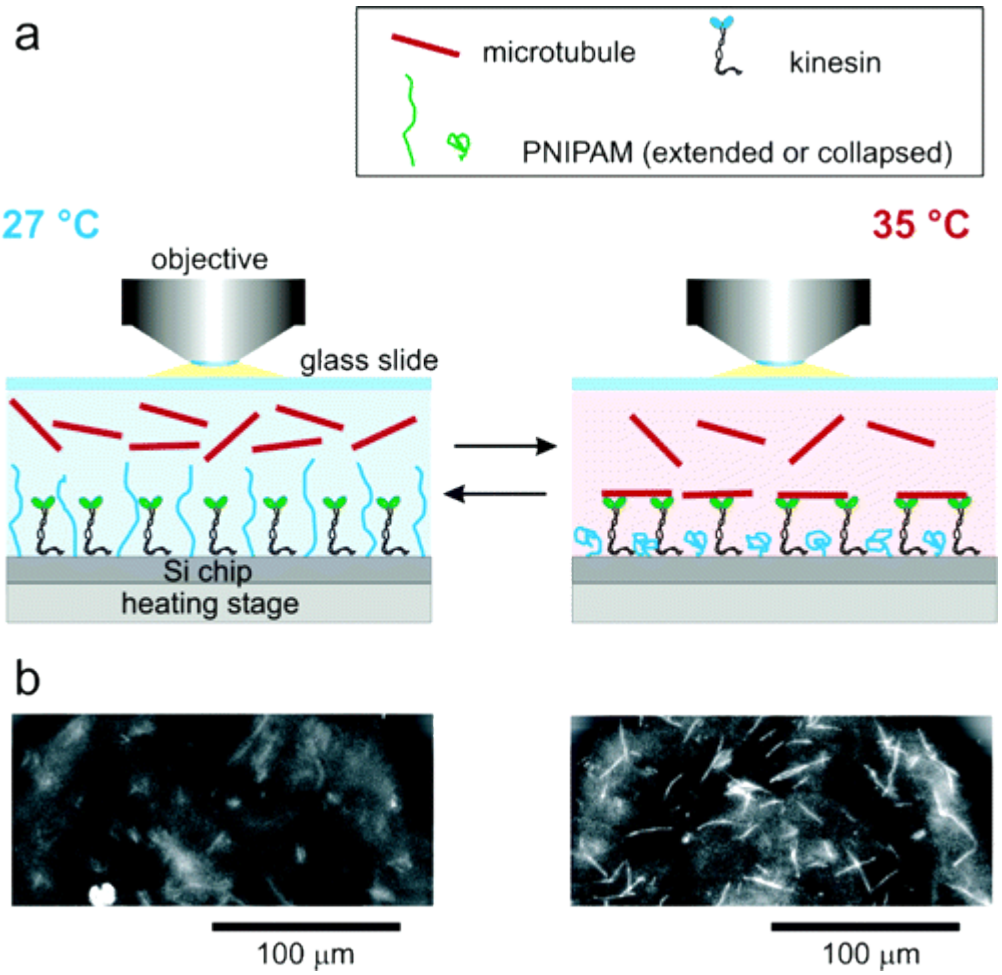

Figure.4.1. The image shows the operation of the PNIPAM at its functioning temperature. a, scheme shows how at the LCST (33 – 35°C) the polymer will collapse into its dehydrated state allowing the attachment of microtubules to the motors. Below this temperature the polymer extends, blocking any interactions between the motors and microtubules. b, resulting images from the globally heated sample.[23]

Work achieved to find the appropriate grafting density of the polymer in order to successfully inhibit the motility at temperatures below 33 – 35 °C can be found in Ionov et al 2006.[23]

4.3 Kinesin motility with functioning PNIPAM gate

The next section of this chapter focuses on the implementation of the PNIPAM into a chip design where the switching can be localised in a controlled manner. This will be presented in two generations of samples where a thermoresponsive gate is designed on a surface to create traffic light type junctions.

4.3.1 Combinatorial gating

The design of the first generation samples consisted of a number of planar gold electrodes on a surface with varying gate areas between. By applying a potential over the gold bridge the temperature at specific junctions can be controlled due to the increased resistance at the gate regions.

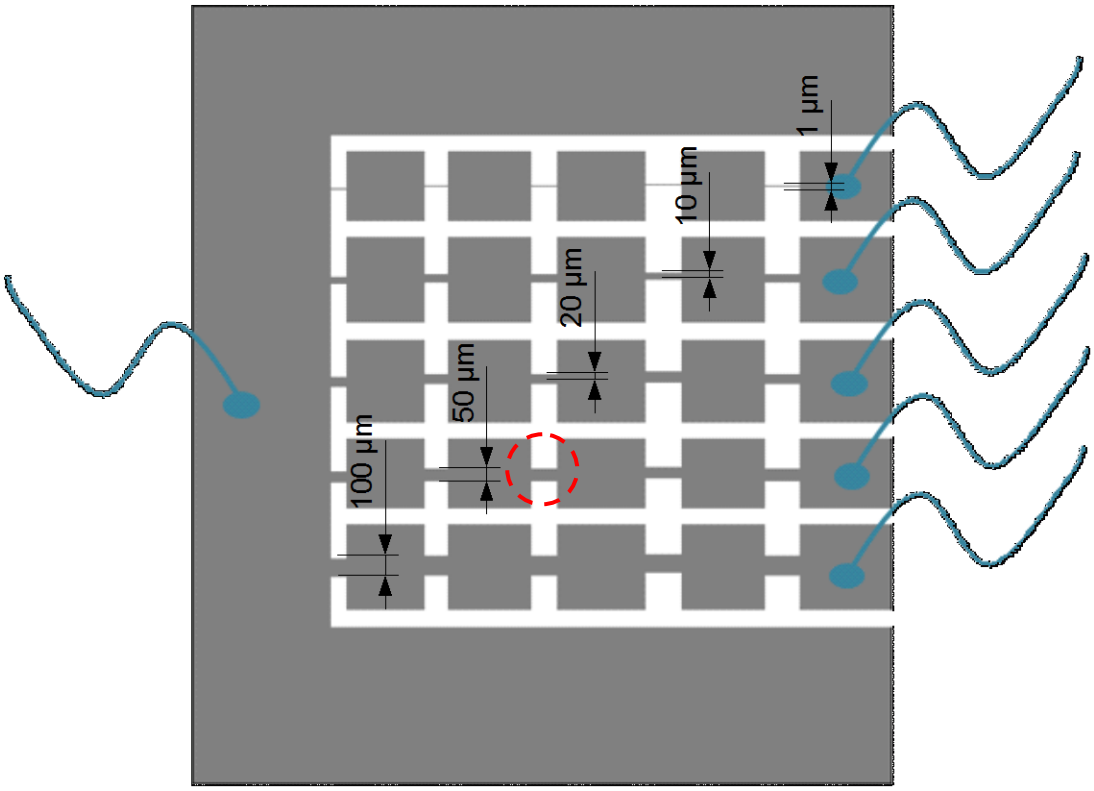

Figure.4.6. The structure of the gold electrodes on the surface of the device. The grey areas denote areas of 200 nm thick gold. The blue lines show where the connections are made in order to apply a potential over the device. The red circle highlights an area where increased resistance will result in an increase in temperature.

The structure of the gold electrodes is shown in Figure 4.6, where a 200 nm thick gold layer has been ablated using a laser mill to create the regions where high resistivity will occur. After the ablation, the entire chip is coated in a ‘planarisation layer’ by spin coating a 4% w/v PMMA solution over the sample.

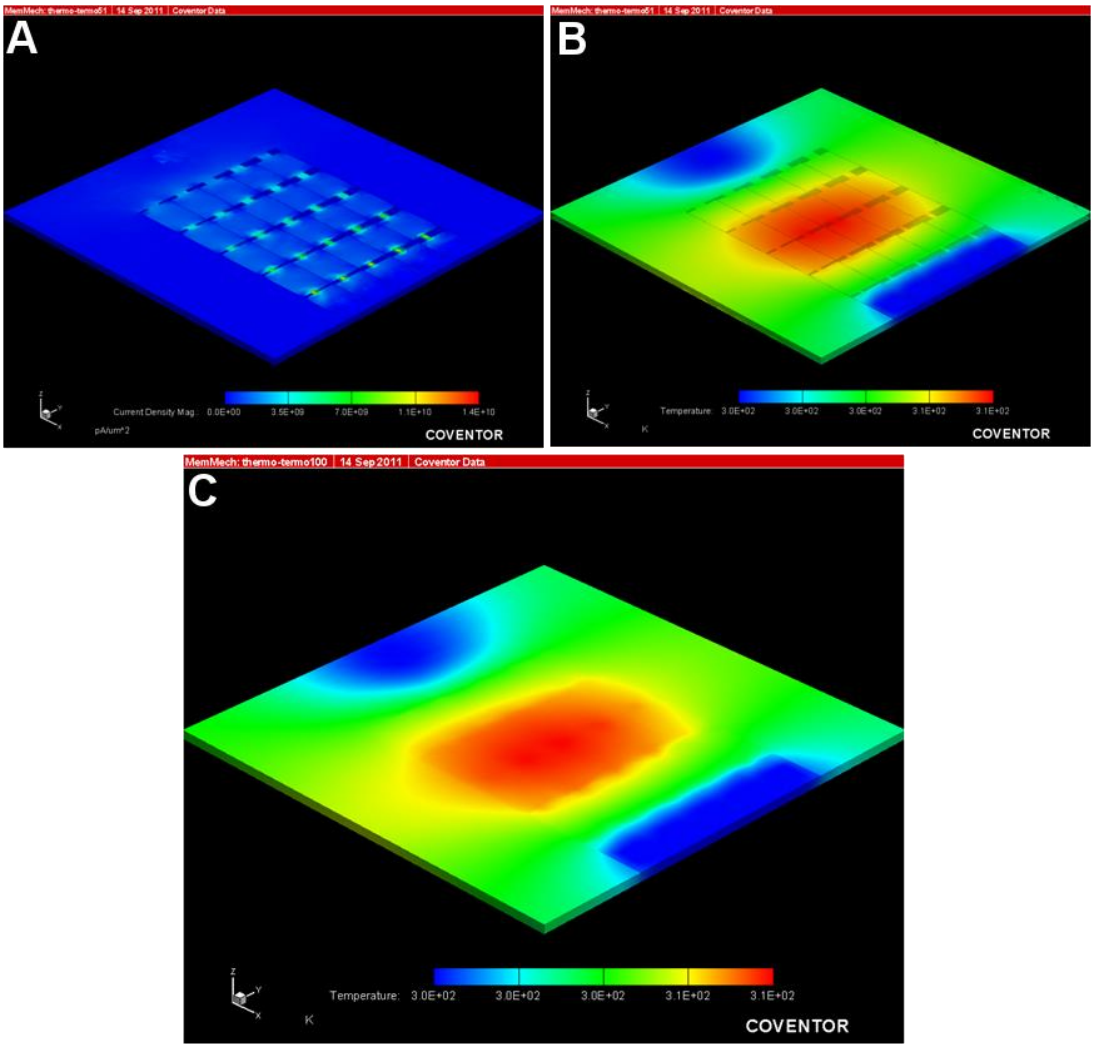

Figure.4.7. Meshed model of gold thermoelectrodes, the planarization layer and bottom glass substrates are not shown. A, The structure of the gold electrodes showing the current desnity across the gold. B, The heat distribution across the gold in the plane of the electrodes. C, The heat distribution in the plane of the electrodes with the addition of the PMMA planarisation layer. Figure courtesy of Dr Harm van Zalinge.

Simulations were performed to show the temperature behaviour of the device (Figure 4.7). In the simulation a constant temperature of 300 K was set at the gold pads in between the gate areas (the areas of high resistance where PNIPAM switching is to be localised). A potential of 35 mV is passed through the electrodes. The results suggest that upon

application of this voltage the maximum temperature of the electrodes and top PMMA layer rises to 43 °C.

Variations in the thickness of the glass substrate and the planarisation layer mean that the applied potential will be slightly different in order to obtain the required temperature differentiation. The results show that the magnitude of current density is higher in the regions of gold microelectrodes as represented in Figure 4.7 A. Therefore, it is expected that the gold gate regions (red circle Figure 4.6) will have a temperature higher than remaining surface of the gold layer and it is here that PNIPAM switching will occur.

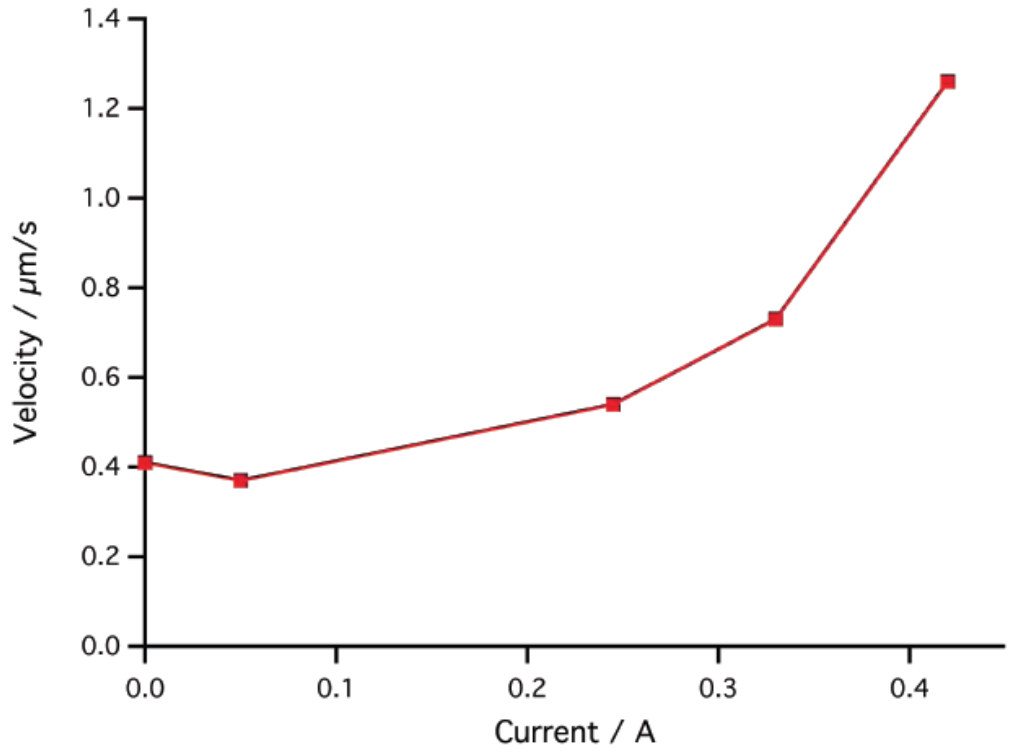

Figure.4.8. The graph outlines the relationship between the current applied to the device and the velocity of the kinesin motility.

The samples were integrated into an *in vitro* motility assay in the aqueous environment. The current dependent heating of the device was shown to directly influence the sliding velocity of microtubules (Figure 4.8) as seen in the previous experiments in section 4.2.2. The heat

generated by an Ohmic resistor is given by $Q=V^2R^{-1}t$. The best quadratic polynomial fit is indicated in Figure 4.9, where the offset is equal to the room temperature.

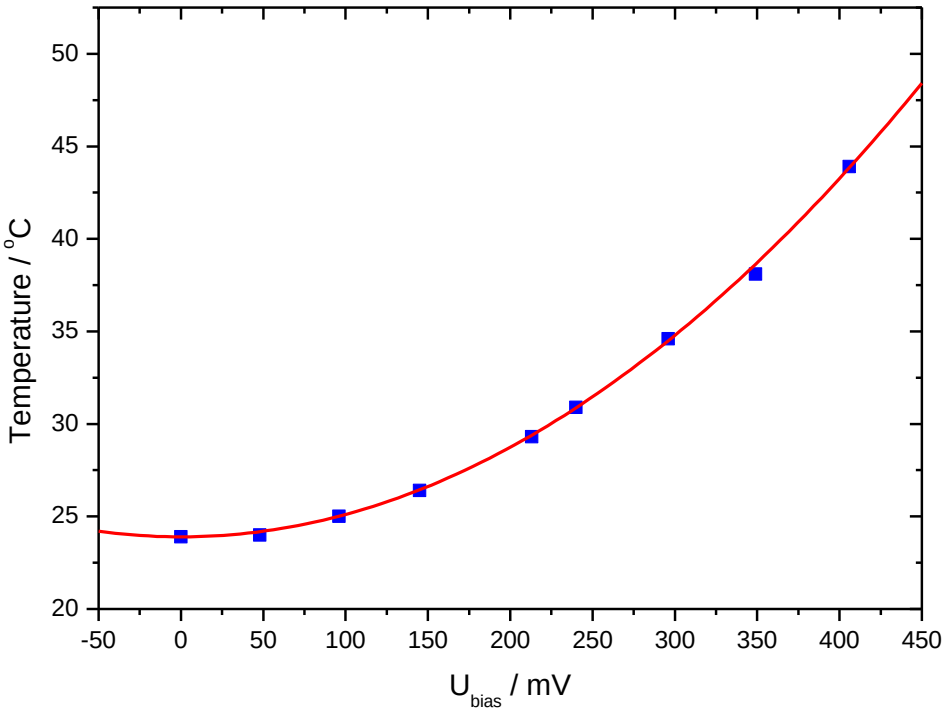

Figure.4.9. The graphs shows how the temperature increases as the bias potential is increased. The fitted curve shows a quadratic increase with bias potential increase.

Better localisation of the heating was obtained by connecting a single row of electrodes. The temperature dependence of the sliding velocity of microtubules was measured at two junctions, 1) on the row that is heated and 2) a junction on a row that is unheated, is shown in Figure 4.10.

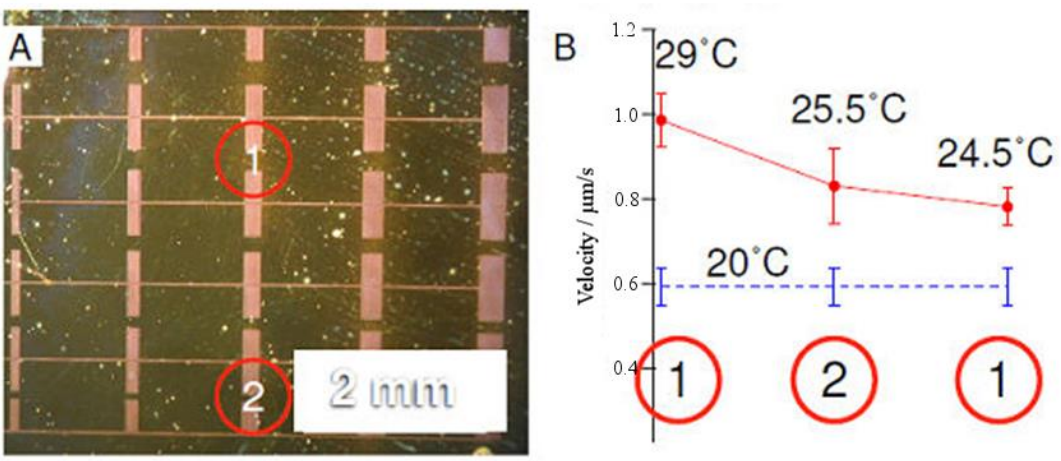

Figure.4.10. A, Confocal image of the gold structure used for local heating. A current was passed through the gold and measured at positions marked with circles labeled (1) and (2). B, Microtubule velocity at positions (1) and (2) the temperature corresponding to these temperatures is indicated. The temperature at position 1 was also measured before the experiment (dashed line) and directly after turning off the current (rightmost circle). Figure courtesy of Dr Harm van Zalinge.

The results showed a clear temperature difference between locations 1 and 2; however, localisation of the temperature was poor. The inability of this chip design to generate µlocalised heat means that the switching capability of PNIPAM will not only be achieved at 'gate' regions of the chip but also at undesired areas. The high thermal conductivity of the sample, exacerbated by the planarization layer covering the gold electrodes means that this design cannot be used to create functioning PNIPAM gates. Further simulation did suggest that cooling the back of the sample via a Peltier element would help in localising the heating.

4.3.2 Gating Device

In the second generation of the device a redesign of the gate area of the chip was created to improve the localisation of the heating which had been an issue in the previously used designs in combination with a Peltier element. Added to the design were topographical features which direct the microtubules towards the gate (Figure 4.11). The areas in which the motility is to function is in the channels patterned into the surface of the gold (1- 10 µm wide), as opposed to the first generation samples where the motility was functioning directly on top of the gold electrodes. Junctions where created by leaving small areas of gold (between 1-100 µm long) periodically along the channels. It is these areas that, due to increased resistance, will generate heat as a current is passed through the gold layer.

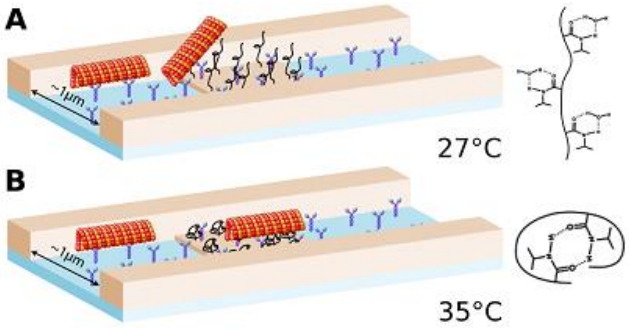

Figure.4.11. The schematic shows the operation of the PNIPAM 'gate' A, The PNIPAM at the 'gate' area remains unheated and therefore in its extended state. At this temperature the microtubules that come into contact with the 'gate' will detach into solution. B, A potential is applied to the 'gate' in order to heat the PNIPAM within the operating window where the molecule collapses but not so far as to cause damage to the protein layer. Microtubules will be able to pass freely over the PNIPAM.

A thin layer of PGMA was spin coated onto the 200 nm gold surface of the samples. The samples were then patterned by laser ablation of the gold to leave glass floored channels in which to isolate the motility. The areas of gold left after patterning allowed the attachment

of PNIPAM via the spin coated PGMA. The design of the electrodes shown in (see materials and method figure 3.3) allowed the collection of motility (white areas of the diagram) and left the remaining areas of the chip free for electrodes to be attached and a current passed through the gold.

Initially the motility was performed on patterned samples prior to annealing with PNIPAM (Figure 4.12). This was done to study the motility function both in the channel and the area surrounding the ‘gates’. The results highlighted issues with the debris left around the ablated areas of the gold. Microtubules are seen over the entire chip, however, at the edges of the areas where patterning has taken place the amount of debris left by the ablation was sufficient to hinder the motility. It was found that various washing techniques did not improve the surface of the channels and that there was still sufficient debris left by the ablation to hinder the motility.

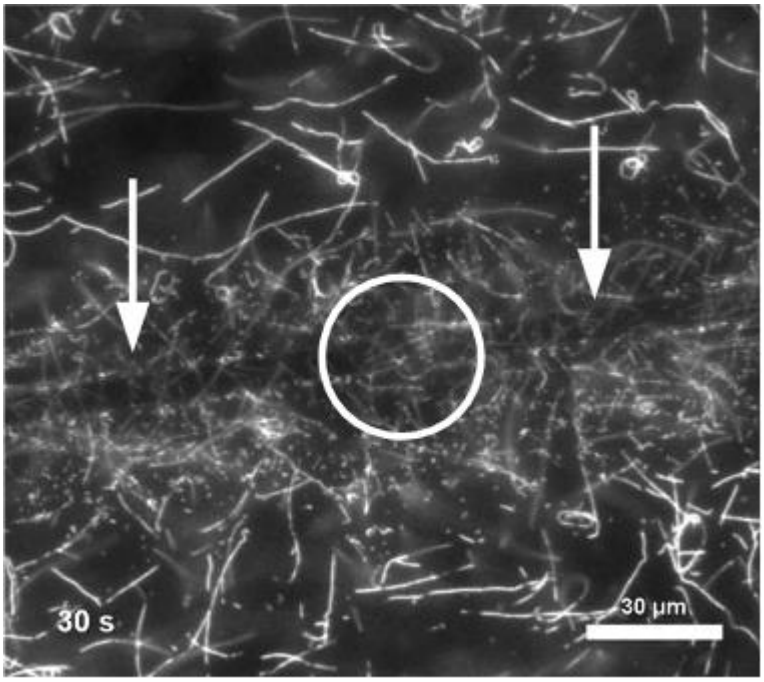

Figure.4.12. The image shows kinesin motility on a PGMA coated sample. The white arrows show the position of the channels. The white circle shows the position of the ~10 µm 'gate'. Motility was present on unpatented areas of the chip. Clearly shown, however, is the inhibiting nature of the debris left after patterning at the edges of the channels and around the gate.

In the first generation samples a PMMA planarisation layer was spin coated on top of the ablated gold and this will have helped in avoiding the issues with ablation debris inhibiting smooth sliding. However, due to the issues caused by the planarisation layer discussed in section 4.3.1 an alternative ablation technique was created to negate the issue (see chapter 3 section 3.1.1). The patterning was performed in a specially made water cell. It was found that ablating the gold through the rear of the chip helped create more clearly defined channel walls. The water cell meant that debris created by the ablation of the gold fell into solution rather than being deposited onto the surface. Images taken after the new ablation technique confirmed the absence of debris at the edges of the channels (Figure 4.13).

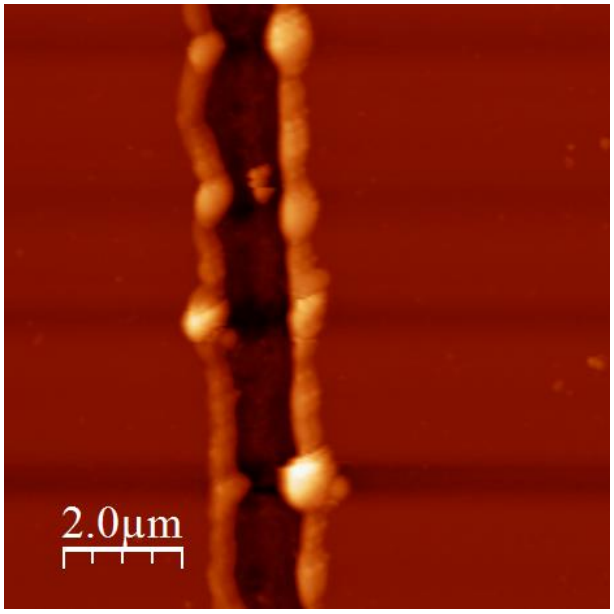

Firgure.4.13. The AFM images shows an example of the channels created by the water cell laser ablation technique. The areas around the channel are free of debris and so will not hinder smooth gliding motility.

Samples were made by first spin coating the PGMA and then applying the new ablation technique. The PNIPAM was subsequently annealed to the samples as per the grafting protocol set out in section 4.2 using a grafting density of ~6 mg/m^2 which was shown to exhibit the appropriate level of control over the motility. To test the PNIPAM layer and the switching ability of the polymer close to the channels and gate areas of the samples the chips were first placed on a Peltier element so that the temperature of the entire surface could be controlled (Figure.4.14.).

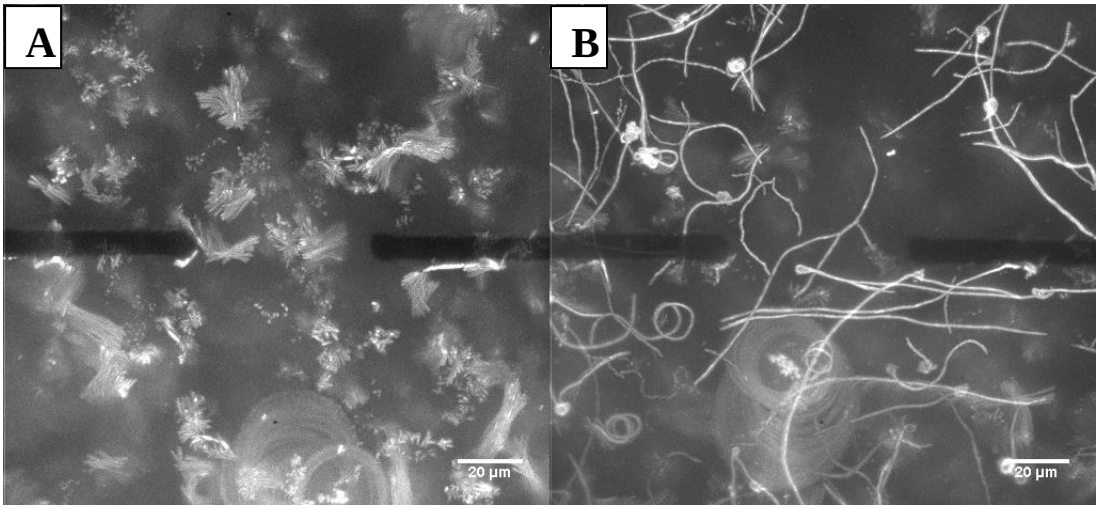

Figure.4.14. The time integrated images show the motility performed on PNIPAM coated patterned samples while the surface temperature is controlled via a Peltier element. A, The sample is held at approximately 27 ^{o}C, the PNIPAM in its extended state does not allow interaction between microtubules and kinesin to occur. B, The surface temperature is held at approximately 35 ^{o}C. At this temperature the PNIPAM collapses as its structure is dehydrated. This allows the microtubules to attach to the motors on the surface and so motility is clearly visible (Whites lines in image B show the movement of filaments due to motor attachment).

The results showed that the new ablation technique had cleared the areas around the channels and gates and that motility functioned uniformly on all areas of the sample. The annealing of PNIPAM to the PGMA coated surface of the gold was also unaffected by the laser ablation. In Figure 4.14 the switching ability of the PNIPAM is clearly evident in all areas, with the exception of the channels where polymer is not present. The halos seen in Figure 4.14 A are a result of microtubules moving due to Brownian motion and are unable to attach to the kinesin. Figure 4.14 B shows the time integrated movement of microtubules across the surface (white lines) as the surface is heated allowing motor attachment. Both Figures show that the PNIPAM coating was functioning as expected and inhibiting motility when the surface temperature was below 33-35 ^{o}C.

To test the local heating ability of the gate areas, the samples were placed on a Peltier element that was held at a temperature of 23 ^{o}C to limit heat exchange to undesired regions of the chip. A potential was applied to the gold layer (0.3 V at 52 mA) which resulted in 15.6 mW of heat being generated at the gate.

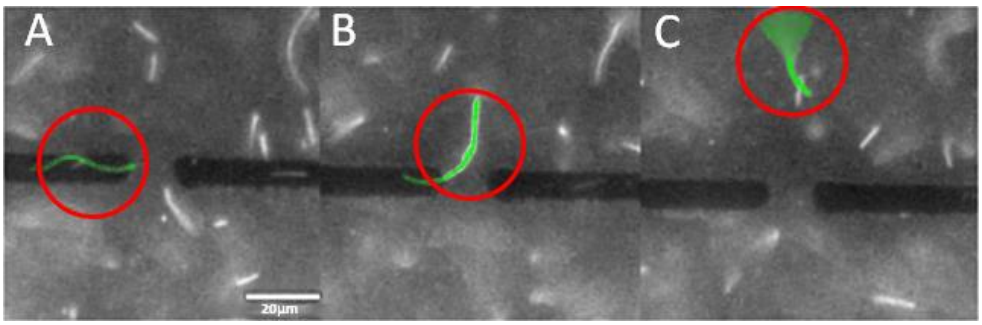

Figure.4.15. Key Frames from a video taken of filament movement. A, Image show the topographical confinement of a motile microtubule. B, The microtubule comes into contact with the heating 'gate' region of the chip where the PNIPAM is in its collapsed state, which allows the continuation of motility. C, The filament reaches the edge of the heated area of the chip, the PNIPAM in this area is in its extended state and so the attachment of microtubule to the motor heads is inhibited and hence the microtubule begins to detach from the surface.

In Figure 4.15 the potential is applied to the gold gate from top to bottom in the images shown. Highlighted in green and with a red circle is the path taken by a single microtubule. The microtubule can be seen gliding unhindered inside the channel. Image B shows that the heated PNIPAM gate allows the interaction between motor microtubule to occur. Important to note are the areas either side of the channel where microtubules can be seen slightly out of focus. These are microtubules present in solution, due to the extended state of PNIPAM in these areas of the chip they are unable to attach to the kinesin. The slight movement, shown by the blurring of their outlines is due to Brownian motion. In the final image (C) the microtubule can be seen to make a turn while moving in the locally heated area. Clearly shown here is the boundary of the heated area. As the microtubule continues to move away

from the gate the front of the filament reaches an area of the chip where PNIPAM is in its extended state as so begins to drift into solution as it can no longer attach to other motors. In figure 4.15C this can be seen by the blurring of a portion of the filament as its movement begins to be defined by Brownian motion rather than the kinesin motors. While this highlights the functioning of the gate it also shows that, due to the thermal conductivity of the materials used, the area of localised heating is still relatively large (approximately diameter of 40 – 50 μm). This meant that instead of moving from one channel across the gate and back into the other, the microtubules can make turns and move onto other areas of the chip which in turn resulted in the dissociation of the filaments into solution as they reached the extended PNIPAM chains.

4.4 Conclusions

This chapter has shown the use of the thermoresponsive polymer PNIPAM in selectively switching kinesin motility. The polymer has been confined to areas on a chip and via the localised heating of these areas a functioning gate has been created. The function of the polymer at these gate regions was seen to perform just as reliably as in the original samples where the entire surface of the samples was temperature controlled. There are two remaining issues of the design that in future iterations will have to be addressed. Firstly the gold is extremely conductive. This creates issues with the localisation of the heating. Perhaps another material can be used that while still allowing heating via a current potential, is less susceptible to transfer the heat generated to the surrounding area. Another factor to consider is the height of the PNIPAM gate structures. If these could be lowered in height this may help in transferring the microtubules from one channel to the other as opposed to the current situation where they turn to other areas of the chip. If for example the gate were 100 nm high, this would provide a channel across the gate with walls of 100 nm which should be sufficient to guide the motility. The best way to perform this may be a threefold ablation

procedure. In the first step the channels would be ablated as stated in the final section of this chapter. At this stage laser pulses of much reduced power and utilising a specifically shaped aperture could then be applied to the top of the gate areas of the chip. This would ablate some but not all of the gold and could reduce the height of the metal in these areas.

The results of this study have shown that PNIPAM can be used as a method of gating microtubule motility at specific junctions on a patterned gliding assay. One possible design that could utilise these gates is a structured surface that contains roundabouts where the PNIPAM gates are contained at specific areas at the edge of the circle. This would mean that while the PNIPAM was in its extended state the microtubules would continue to move around the channel until they reached a gate that had been heated. The lowered PNIPAM in these sections would then allow the microtubules to pass out of the structure.

The studies performed in this chapter has lead to a publication in Biomedical Microdevices:

Control and gating of kinesin-microtubule motility on electrically heated thermo-chips

L.C. Ramsey, V. Schroeder, H. van Zalinge, M. Berndt, T. Korten, S. Diez, D.V. Nicolau

Biomedical Microdevices, DOI: 10.1007/s10544-014-9848-2 (2014)

4.5 References

1. Howard, J., Hunt, A. and Baek, S., "Assay of Microtubule Movement Driven By Single Kinesin Molecules," *Methods in Cell Biology, Vol 39* 39(137-147 (1993)
2. Hunt, A. J., Gittes, F. and Howard, J., "The Force Exerted By A Single Kinesin Molecule Against A Viscous Load," *Biophysical Journal* 67(2), 766-781 (1994)
3. Dennis, J. R., Howard, J. and Vogel, V., "Molecular shuttles: directed motion of microtubules slang nanoscale kinesin tracks," *Nanotechnology* 10(3), 232-236 (1999)
4. Kawaguchi, K. and Ishiwata, S. i., "Temperature Dependence of Force, Velocity, and Processivity of Single Kinesin Molecules," *Biochemical and Biophysical Research Communications* 272(3), 895-899 (2000)
5. Hess, H., Matzke, C. M., Doot, R. K., Clemmens, J., Bachand, G. D., Bunker, B. C. and Vogel, V., "Molecular Shuttles Operating Undercover: A New Photolithographic Approach for the Fabrication of Structured Surfaces Supporting Directed Motility," *Nano Lett.* 3(12), 1651-1655 (2003)
6. Block, S. M., Goldstein, L. S. B. and Schnapp, B. J., "Bead Movement By Single Kinesin Molecules Studied With Optical Tweezers," *Nature* 348(6299), 348-352 (1990)
7. Coy, D. L., Wagenbach, M. and Howard, J., "Kinesin takes one 8-nm step for each ATP that it hydrolyzes," *J. Biol. Chem.* 274(6), 3667-3671 (1999)
8. Manfred, S., *Molecular Motors*, Wiley-VCH, Weinheim (2003).
9. Bakewell, D. J. G. and Nicolau, D. V., "Protein linear molecular motor-powered nanodevices," *Aust. J. Chem.* 60(5), 314-332 (2007)
10. van den Heuvel, M. G. L., De Graaff, M. P. and Dekker, C., "Molecular sorting by electrical steering of microtubules in kinesin-coated channels," *Science* 312(5775), 910-914 (2006)
11. Uppalapati, M., Huang, Y. M., Shastry, S., Jackson, T. N. and Hancock, W. O., *Microtubule Motors in Microfluidics*, Artech House, Norwood (2010).
12. Moorjani, S. G., Jia, L., Jackson, T. N. and Hancock, W. O., "Lithographically patterned channels spatially segregate kinesin motor activity and effectively guide microtubule movements," *Nano Lett.* 3(5), 633-637 (2003)
13. Korten, T., Mansson, A. and Diez, S., "Towards the application of cytoskeletal motor proteins in molecular detection and diagnostic devices," *Curr. Opin. Biotechnol.* 21(4), 477-488 (2010)
14. Clemmens, J., Hess, H., Doot, R., Matzke, C. M., Bachand, G. D. and Vogel, V., "Motor-protein "roundabouts": microtubules moving on kinesin-coated tracks through engineered networks," *Lab Chip* 4(2), 83-86 (2004)
15. Hiratsuka, Y., Tada, T., Oiwa, K., Kanayama, T. and Uyeda, T. Q. P., "Controlling the direction of kinesin-driven microtubule movements along microlithographic tracks," *Biophysical Journal* 81(3), 1555-1561 (2001)
16. Kim, E., Byun, K. E., Choi, D. S., Lee, D. J., Cho, D. H., Lee, B. Y., Yang, H., Heo, J., Chung, H. J., Seo, S. and Hong, S., "Electrical control of kinesin-microtubule motility using a transparent functionalized-graphene substrate," *Nanotechnology* 24(19), 195102 (2013)
17. Dujovne, I., van den Heuvel, M., Shen, Y., de Graaff, M. and Dekker, C., "Velocity modulation of microtubules in electric fields," *Nano Lett* 8(12), 4217-4220 (2008)
18. van den Heuvel, M. G., Butcher, C. T., Lemay, S. G., Diez, S. and Dekker, C., "Electrical docking of microtubules for kinesin-driven motility in nanostructures," *Nano Lett* 5(2), 235-241 (2005)
19. Schmidt, C., Kim, B., Grabner, H., Ries, J., Kulomaa, M. and Vogel, V., "Tuning the “Roadblock” Effect in Kinesin-Based Transport," *Nano Lett.* 12(7), 3466-3471 (2012)

20. Bachand, G. D., Rivera, S. B., Carroll-Portillo, A., Hess, H. and Bachand, M., "Active capture and transport of virus particles using a biomolecular motor-driven, nanoscale antibody sandwich assay," *Small* 2(3), 381-385 (2006)
21. Korten, T. and Diez, S., "Setting up roadblocks for kinesin-1: mechanism for the selective speed control of cargo carrying microtubules," *Lab Chip* 8(9), 1441-1447 (2008)
22. Nitzsche, B., Bormuth, V., Bräuer, C., Howard, J., Ionov, L., Kerssemakers, J., Korten, T., Leduc, C., Ruhnow, F. and Diez, S., "Chapter 14 - Studying Kinesin Motors by Optical 3D-Nanometry in Gliding Motility Assays," in *Methods Cell Biol* W. Leslie and J. C. John, Eds., pp. 247-271, Academic Press (2010).
23. Ionov, L., Stamm, M. and Diez, S., "Reversible switching of microtubule motility using thermoresponsive polymer surfaces," *Nano Lett.* 6(9), 1982-1987 (2006)
24. Schroeder, V., Korten, T., Linke, H., Diez, S. and Maxirnov, I., "Dynamic Guiding of Motor-Driven Microtubules on Electrically Heated, Smart Polymer Tracks," *Nano Lett.* 13(7), 3434-3438 (2013)

Chapter V: Manipulation of Actin Myosin Motility with DC Fields and Study of Protein Adsorption

The study within this chapter focuses on the actin myosin motor protein system. DC electrical fields are used to guide the negative charge filaments across the surface of a gliding assay. Several surface chemistries are used within the electrical motility device to immobilise the motor protein. The motility function exhibited during application of an electrical field is analysed in terms of velocity and directing ability. This is then used to derive the protein adsorption properties of the surface chemistries used.

5.1 Introduction

The aims of this chapter are twofold. Initially the ability to guide actin myosin motility by uniform electrical fields will be presented to evaluate this as a viable method of directional control. This experimental procedure will then be used to probe into the HMM adsorbing properties of six surfaces. The study will concentrate on how surface rigidity and the hydrophobicity and charge held by each of the surfaces impacts the adsorption of HMM. By comparing the motility function observed when a range of fields are applied to the motility assays it will be possible to draw conclusions on the adsorption mechanism of HMM and the cause of any loss in the function of the motor protein. The study of motor proteins in novel *in vitro* environments is important in further elucidating the complex nature of these systems and to explore ways in which their properties may be exploited. This study is also important as an insight into the viability of such a guidance technique if the system was to be used in any future bionanodevices.

The actin myosin system is important as it is ubiquitous in eukaryotic cells providing a platform for a great many biological functions and has been the subject of many studies into its biological and chemical functions. Since the development of the *in vitro* motility assay the study of the system in an array of environments has become widespread.[1] The lure of exploiting such an efficient nanomachine has seen a large number of studies using a variety of different engineering solutions with which to utilize the system.[2-5]

It is not hard to imagine the potential for such a system to be used as means to transport chemical or biological cargo around a lab-on-chip device, or as a switch or signal activator in a sensing device. [6, 7] The principle guidance of actin filaments by uniform electrical fields has been achieved in previous work by other research groups, namely Riveline et al.[8] This work follows on to provide a practical analysis of the effect that different surface chemistries has on the motility function. In particular the investigation focuses on the different

characteristics that the motility function displays when the protein is immobilised on a variety of surfaces and what can in turn be inferred about the mechanism of this immobilisation. The six surfaces investigated in this study were, Nitrocellulose (NC), poly(methyl methacrylate) (PMMA), poly(tertbutyl methacrylate) (PtBMA), poly(butyl methacrylate) (PBMA), trimethylchlorosilane (TMCS) and triehtlychlorosilane (TECS).

5.2 Actin myosin motility

In order to study the effects of an electrical field on the motility function, initial experiments are required to provide a base line of what is classed as 'normal' motility characteristics. Experiments were run on nitrocellulose (NC) as this has been the typical surface chemistry used for running *in vitro* motility assays.[9, 10]

NC is a highly flammable polymer used in a wide range of applications. Since the 1980's it has been used as a protein membrane due to its ability to bind protein while allowing the immobilised protein to retain its function.[11] Although extensively used the precise mechanism of binding is still unknown although it is thought to be a combination of hydrogen bonding and electrostatic and hydrophobic interactions.[11, 12] The NC surfaces produced from this procedure give contact angle measurements between $65^{o} - 70^{o}$.

The movement of 20 - 30 filaments were tracked as this accounted for all the fully motile filaments in the field of view (see Figure 5.1). The tracking was obtained for a 5 second period of the experiment which relates to 50 frames. This was deemed enough to make statistically valid assessment of the velocity and directionality of the filaments. The average velocity of filaments along with data obtained of the angle of trajectory was used to analyse the typical motility function the actin myosin system displays in a standard NC *in vitro* motility assay under the environmental conditions that the electrical motility experiments are to be performed in.

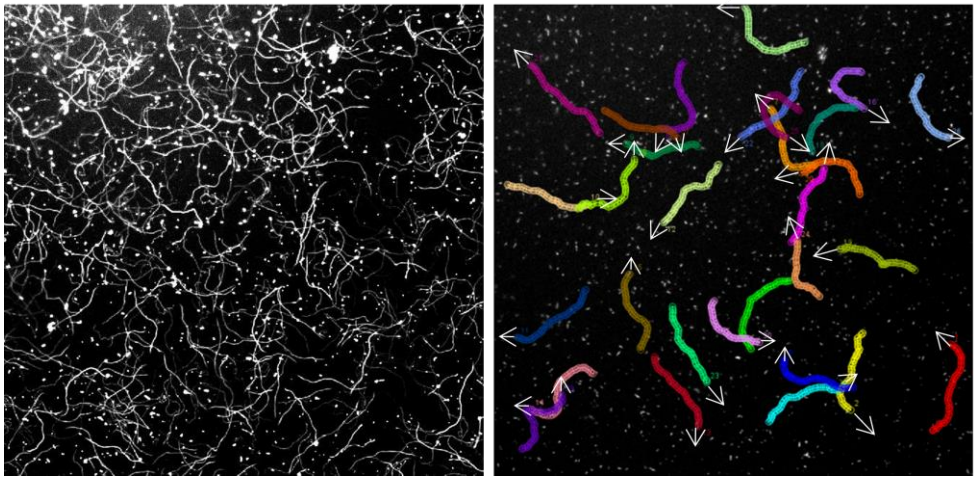

Figure.5.1. Images show actin myosin motility on NC coated surface. Left, Integrated pixel intensity image of the motility over 5 s, white lines show the movement of individual actin filaments. Right, tracking overlaid on the final frame of a 5 s video stream with arrows denoting the direction of movement. Notice that the direction of filament movement is random when in the absence of a directing element such as an electrical field. Both images obtained via fluorescence microscopy.

The ambient room temperature (~24 ^{o}C) was recorded at all times to ensure that this did not deviate significantly during the course of the experiments.

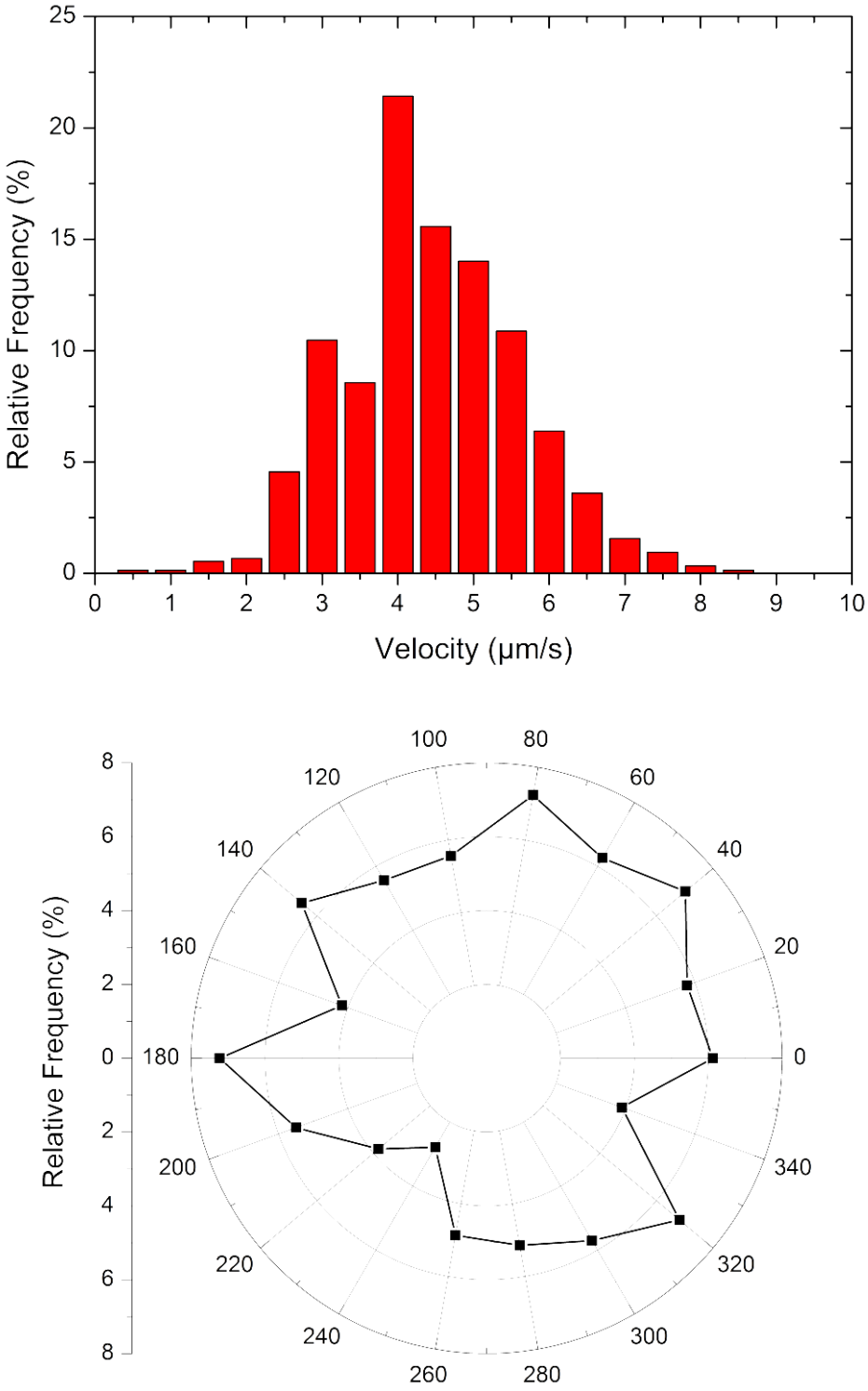

Figure.5.2. Graphs showing motility function on NC. A, Plot shows a frequency count of the velocity of 30 filaments each making a total of 50 individual movements. B, The radial plot shows a frequency count of the angle of trajectory of 30 filaments, 0-360 representing the 360^{o} of movement.

The initial experiments showed that the motility function was within previously reported ranges with respect to the velocity and the general direction of travel.[10, 13, 14] Filaments moved in a random fashion with the angle of trajectory being dependent largely upon Brownian motion and presumably the way in which the motors, available to interact with the actin, are positioned (see Figure 5.2).[15]

Table.5.1. Descriptive statistics of actin myosin motility on NC. Data represents the tracking of 30 filaments

	Velocity (μm/s)	Change in angle of trajectory (^{o})
Average	4.1	16.4
Maximum value	8.1	168.7
Minimum Value	0.7	0.0
Standard deviation	1.2	14.8
Median	4.2	12.7

5.3 The effects of electrical guidance of actin on nitrocellulose immobilised HMM

After the base line experiments were achieved on nitrocellulose, the same surface was used and an electrical field was applied in order to study the guidance effects of this external force and the general changes in the motility function as fields of increasing strengths were applied.

The length dependent charge on the actin filaments gives rise to the ability to guide the motility via electrical fields.[8, 16, 17] In the electrical motility experiment the motility assays were performed in an adapted flow cell that allowed the application of a uniform field across the surface. The field range of 0 – 8 kV/m was chosen as previous experiments by this group and other groups showed this to be the optimum range of operation for guiding actin myosin motility.[8, 17]

5.3.1 Electrically guided motility on nitrocellulose

In order to remove filament length as a variable in this study a strict tracking protocol was followed. It was important that the filaments chosen for tracking were done so by characteristics other than purely being the most visible in the field of view, these most likely being the larger filaments. A procedure was therefore created so that the filaments would be chosen due to their motility function. Firstly, only filaments that were 'fully motile' for the entire 50 frames of the video were tracked, i.e. filaments that did not stop, or start moving, part way through the video. Note here that filaments that displayed hindered motility were still included in the data as this was an important characteristic in this study. As previously mentioned 20-30 filaments were tracked for each sample which in the field of view (80 x 80 μm^2) accounted for all the fully motile filaments on the sample. Therefore velocity and directionality data are largely independent of the length as average filament length for all samples was ~1.3 µm (see Figure 5.3).

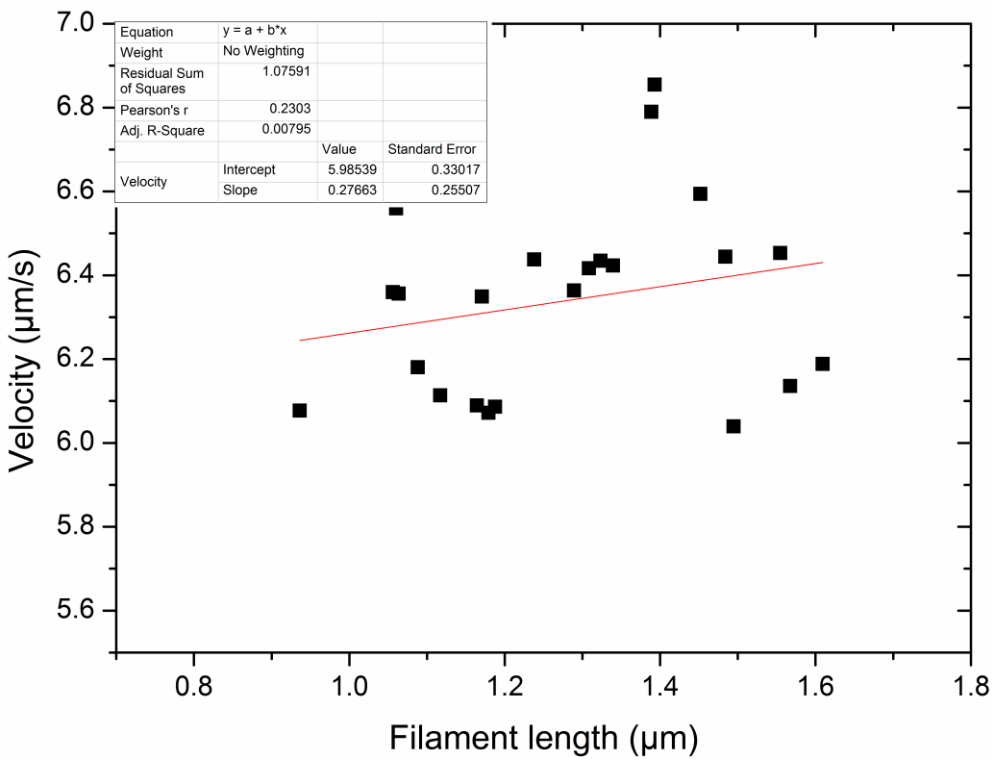

Figure.5.3. The graph shows the relationship between the filament length and average velocity on NC when a 6000 V/m field is applied. Data shows the average velocity of 22 filaments of varying lengths.

Upon application of an electrical field to the motility assay a change is seen in two aspects of the motility function. Firstly an increase in the velocity of the actin filaments and secondly the general direction of travel of actin filaments changes towards the positive electrode.

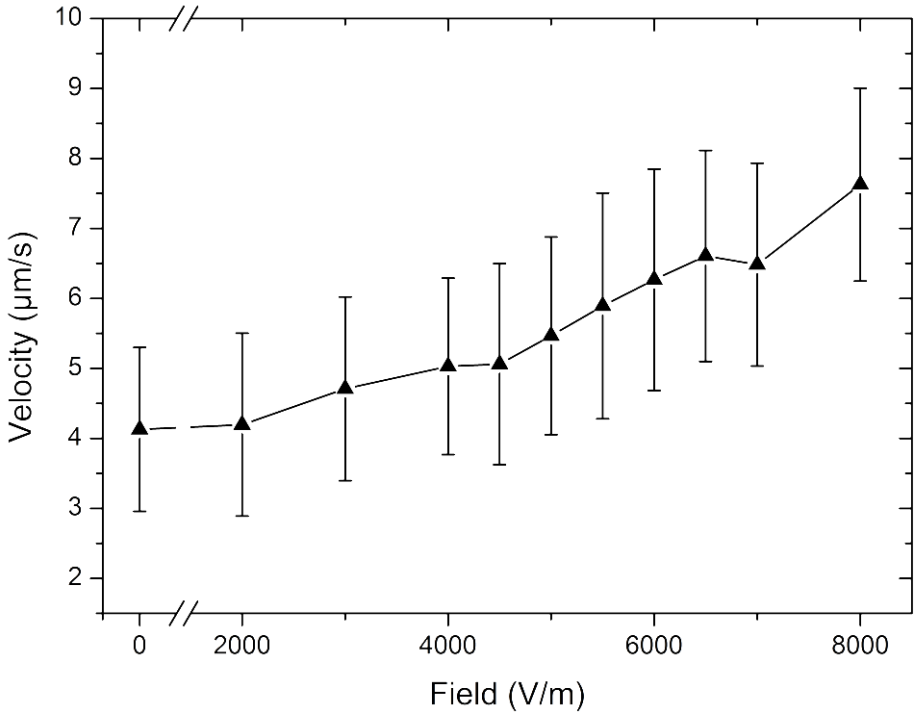

Figure.5.4. Plot shows the increase in the average velocity of actin filaments as the electric field increases on nitrocellulose. Error bars show the standard deviation of velocity. Each data point represents the tracks of 30 filaments over 3 samples.

As seen in the graph (Figure 5.4) there is an almost two fold increase in the average velocity at 8 kV/m compared to that seen in the absence of a field. It can also be observed that the increase in velocity is accelerated between 4.5 – 5 kV/m. A Theory for this sudden increase is that the pulling force of the field overcomes a specific obstacle to filament movement such as inactive HMM on the surface.

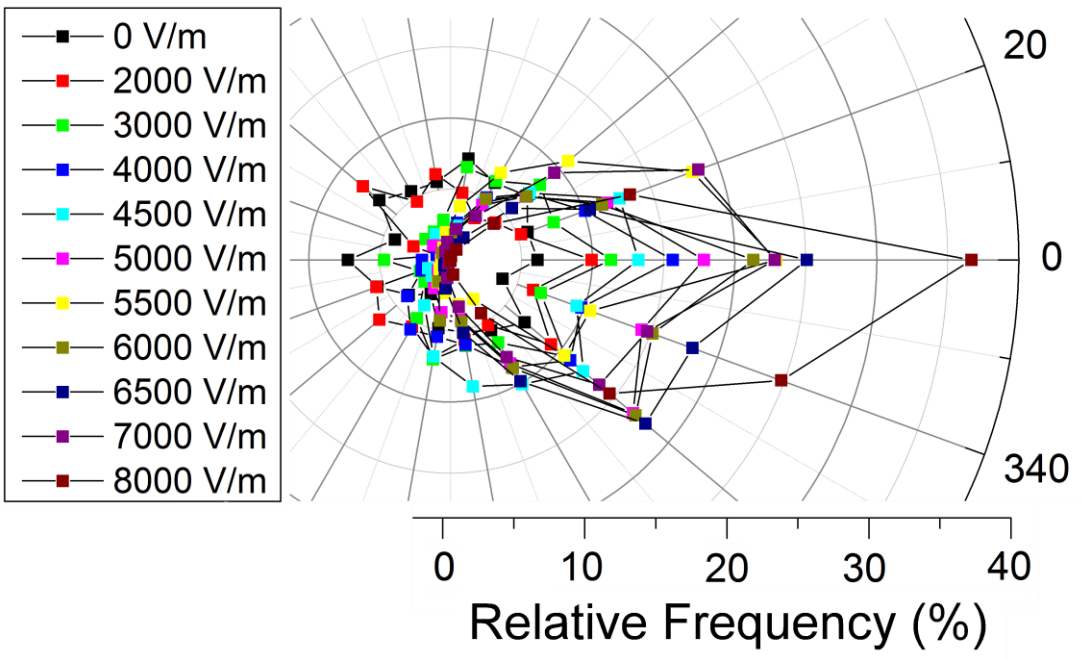

Figure.5.5. Radial plot shows a frequency count of the angle of trajectory on nitrocellulose. 0 – 360 represent the angle of frame by frame movement of the actin filaments with 0 showing the position of the positive electrode. The graph represents the movement of 30 filaments tracked over 3 samples at each of the fields tested.

As the field is increased the percentage of filaments moving against the field dramatically reduces until; at 8 kV/m there are no recorded movements that strayed more than 90^{o} from the direction of the positive electrode (0^{o}). In the middle range between 4 – 6 kV/m filaments were seen travelling against the direction of the field but most of these eventually made U-turns (Figure 5.6). At 5 kV/m filaments moving against the field displayed an average velocity 87% of those moving in line with the field.

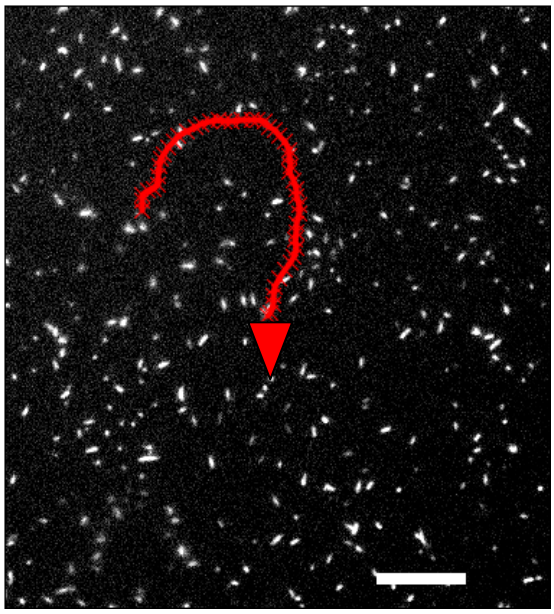

Figure.5.6. Fluorescence microscopy image shows the tracks made by a filament when a U-turn is observed during the application of a 6 kV/m electrical field on nitrocellulose. Arrow head shows direction of movement. Scale bar equals 5 µm. Tracking achieved in program ImageJ.

The percentage of motile filaments increased along with the field. From 0 – 8 kV/m the percentage of motile filaments more than doubled from 27.9 % to 66.9 % respectively. The largest increase was seen at 6 - 8 kV/m from 34.3 % to 66.9 %. This characteristic was mirrored in the velocity data where a rapid increase in the average velocity of filaments is seen between 5 and 8 kV/m.

Table.5.2 Descriptive statistics of the motility function on NC. Standard deviation is given in brackets, Data represents the tracking of 30 filaments.

Electrical field (kV/m)	Percentage of motile filaments (%)	Percentage of filaments moving within 40^{o} of the positive electrode (%)	Average velocity (µm/s)
0	27.9	15.8	4.1(1.2)
4	30.6	35.5	5.0(1.3)
6	34.3	47.8	6.3(1.6)
8	66.9	74.9	7.6(1.4)

It is important to note that upon termination of the field the motility function returns to that of a sample that has not been exposed to a field (see also chapter 6).

5.4 The effect of surface rigidity on the motility function while under the influence of an electrical field

The surface rigidity was investigated as a potential source of any changes seen in the characteristic behaviour when the actin filaments are guided by a range of fields. For this investigation two surfaces, nitrocellulose and TMCS, were chosen due to their similarities, in terms of hydrophobicity, and the large differences in surface rigidity. The gel like structure of nitrocellulose, that forms due to uptake of water, provides this study with a direct comparison to the highly planar and rigid surface structure of TMCS.

5.4.1 Motility function of electrically guided actin filaments on TMCS

Silanes are extensively used in the chemical industry as precursors to a number of chemical processes and also as a resist in some microfabrication procedures.[18, 19] TMCS is reactive towards neucleophiles, the chlorine atom is replaced and it is this reaction which allows attachment to the glass slides (see chapter 3 section 3.2.1). It is important to keep the reaction between the silane and glass surface anhydrous in order to prevent the silane from preferentially reacting with water.

The samples produced with TMCS exhibited the least hindered gliding motility of all the surfaces tested. TMCS has previously been studied as a substrate for actin myosin assays and shows generally good motility function.[4, 20-23] The samples prepared were hydrophobic with contact angles measuring between 75 – 80^{o}.

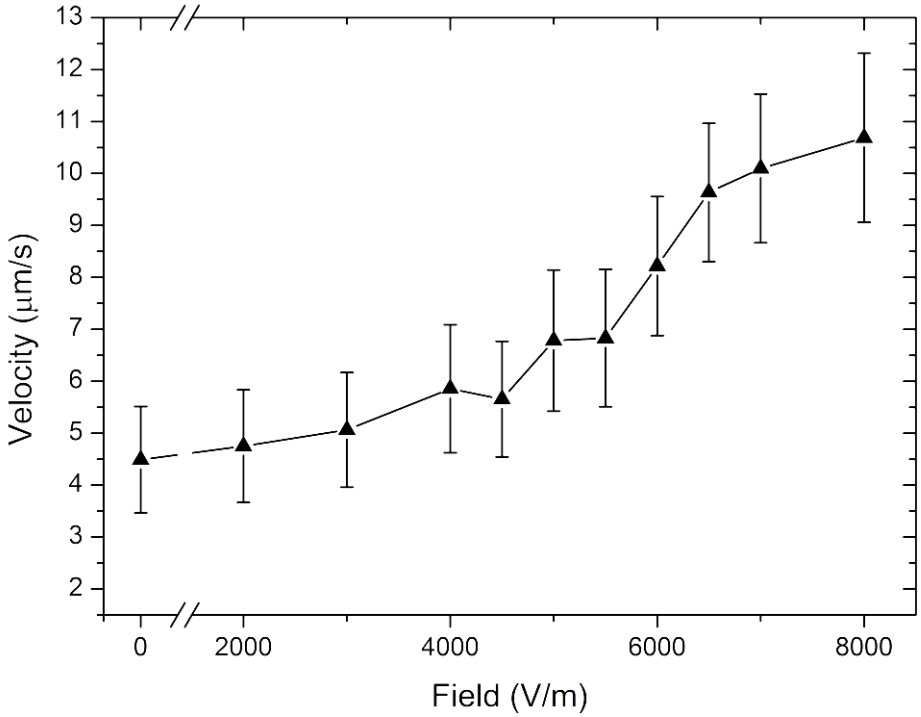

Figure.5.7. Plot shows the increase in the average velocity of actin filaments as the electric field increases on TMCS. Error bars show the standard deviation of velocity. Each data point represents the tracks of 30 filaments over 3 samples.

The motility function on these samples was of a high quality in terms of uninterrupted filament movement. TMCS exhibited a high percentage of motile filaments, above 80 % at 8 kV/m. As seen in Figure 5.7 the velocity increases with increasing field strength and there is a proportionally large increase in the mid range, here between 4.5 – 5 kV/m. After this there is a rapid increase in the average velocity. The motility on TMCS also exhibited a much larger increase in velocity from 0 to 8 kV/m (~ 6 µm/s) compared with the increase seen on NC.

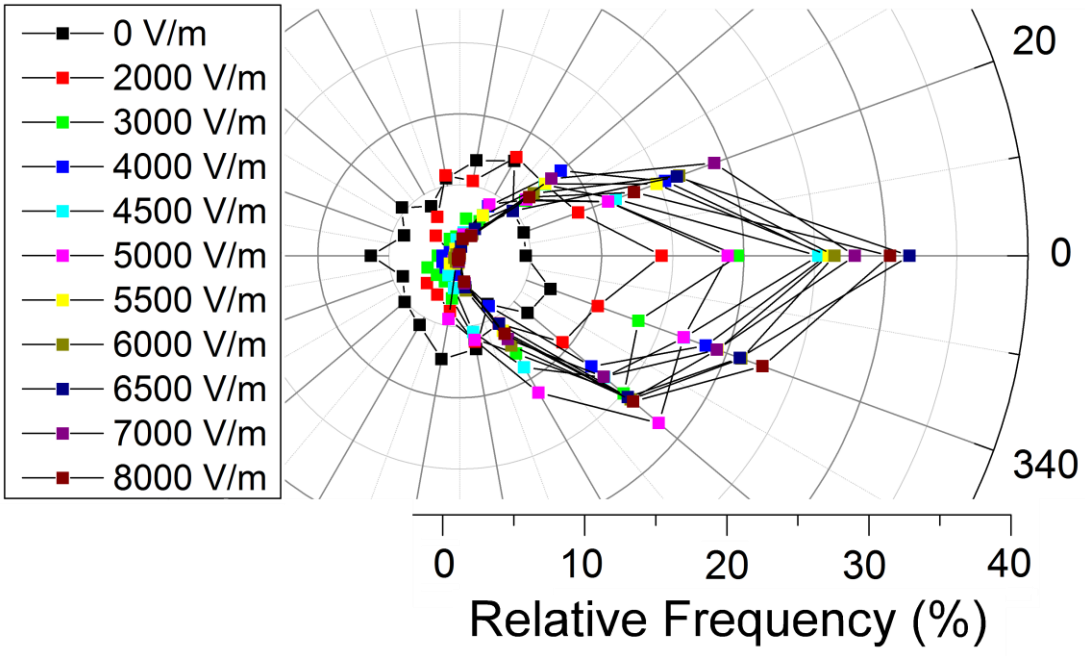

Figure.5.8. Radial plot shows a frequency count of the angle of trajectory on TMCS. 0 – 360 represent the angle of frame by frame movement of the actin filaments with 0 showing the position of the positive electrode. The graph represents the movement of 30 filaments tracked over 3 samples at each of the fields tested.

Following on from the velocity data, directionality on TMCS was also very strong with filament trajectories being affected in the lower field range. At 8 kV/m there were no filaments observed that move against the direction of the field; even at fields as low as 4 kV/m filaments that move against the field quickly made U-turns. At 8 kV/m over 60 % of the filaments were moving within 40^{o} of the positive electrode.

Table.5.3. Descriptive statistics of the motility function on TMCS. Standard deviation is given in brackets. Data represents the tracking of 30 filaments over 3 samples.

Electrical field (kV/m)	Percentage of motile filaments (%)	Percentage of filaments moving within 40^{o} of the positive electrode (%)	Average velocity (µm/s)
0	31.1	16.2	4.5(1.0)
4	38.7	59.6	5.9(1.2)
6	44.4	63.9	8.2(1.3)
8	80.5	66.1	10.7(1.6)

5.4.2 Effects of surface rigidity on electrically guided motility on TMCS and nitrocellulose

The difference in the rigidity of these two surfaces lies in the ability of each to absorb water into their structure. NC will absorb water into the polymers structure upon application of the assay solutions creating a gel like layer for the protein to adsorb on. Conversely TMCS is a hard flat surface. Functionalisation of the surface with TMCS creates a largely uniform layer absent of large polymer chains for water molecules to infiltrate. Though the rigidity of these two surfaces will be largely similar in their dry state, the application the assay solutions rapidly changes the characteristics of the two due to the swelling of NC. This is illustrated in Figure 5.9 where upon protein adsorption the definition between the HMM layer and the polymer, in the case of NC, becomes blurred due to polymer swelling.[24] It is important to note, however, that upon protein adsorption and addition of ATP, QCM experiments have shown the resulting rigidity, of both surface and protein layer, on both TMCS and NC to be similar.[24]

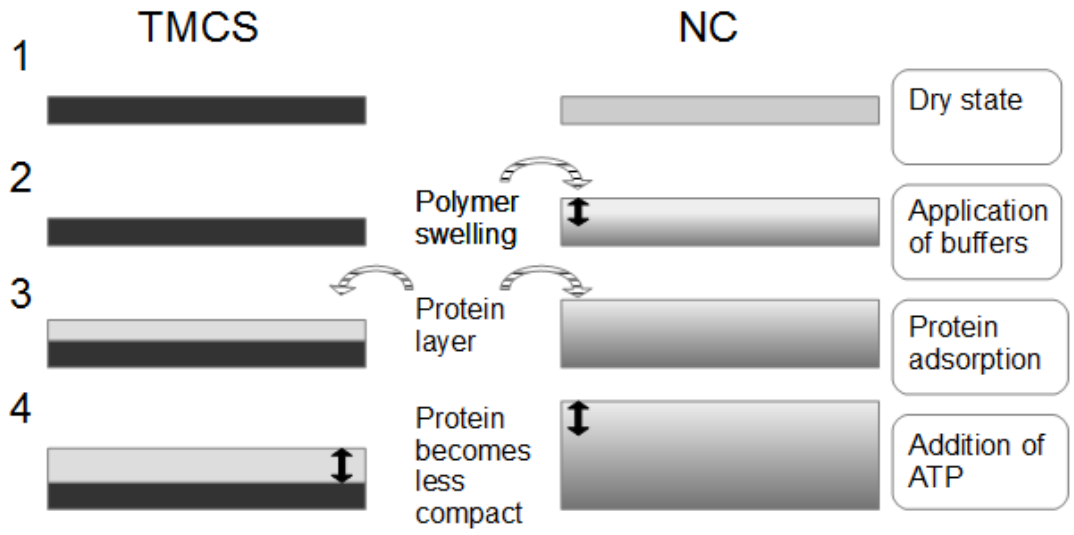

Figure.5.9. Schematic shows the stepwise process of the motility assay and the evolution of the two surface chemistries TMCS and NC. Note here that upon addition of the final assay solution containing ATP, motility will begin and as a result this movement the protein layer itself becomes less compact.

The protein layer itself will also become less compact as the ATP is added to the system and the motors begin to move. Conversely on TMCS the hard surface does not swell and upon the addition of ATP the difference in density make the definition between the surface and protein layer much more obvious.

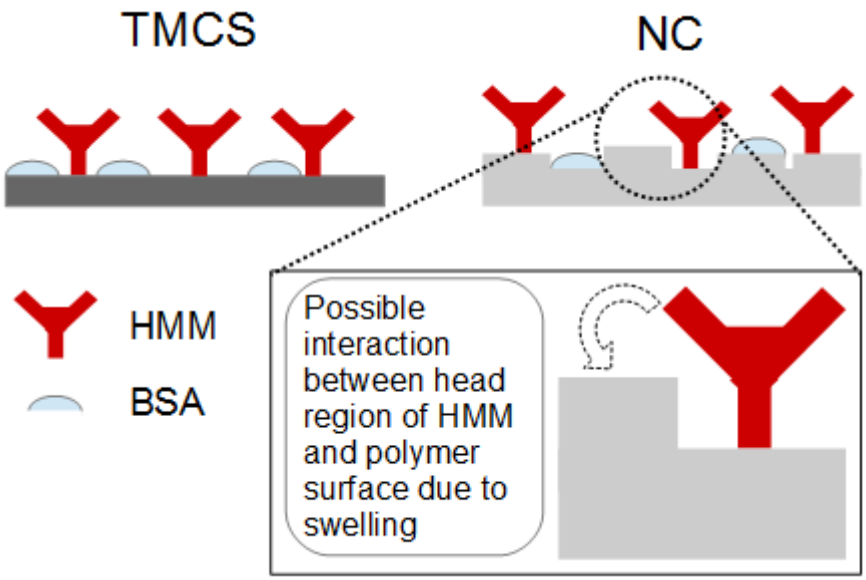

Figure.5.10. Due to the possibility of uneven swelling of the polymer surface, in the case of nitrocellulose there is opportunity for the polymer chains to interact with regions of the bound HMM. One example is shown here where the head region of the HMM could interact with the swelled polymer layer potentially hindering motility.

Figure 5.10 outlines one particular scenario where the polymer rigidity could have an effect on the motor protein function. In the case of NC the swelling of the surface is unlikely to be even. The gel-like behaviour of the polymer when hydrated means that there could be potential for protein interactions with the surface after the initial immobilisation.

The visually observed quality of motility behaviour on both NC and TMCS was very similar. Both surfaces produced gliding assays that exhibited unhindered motility with a high

percentage of motile filaments. The velocity data obtained on the samples coated with TMCS showed a larger increase from 0 – 8 kV/m when compared to NC. Given the similar hydrophobicity of the two surfaces it is therefore assumed that the gel like nature of NC may slightly impair the smooth gliding of filaments. However, as will be shown in the later sections of this chapter, the effect on motility function due to the surface rigidity seems to be minor in comparison to the effects of hydrophobicity on the adsorption of HMM.

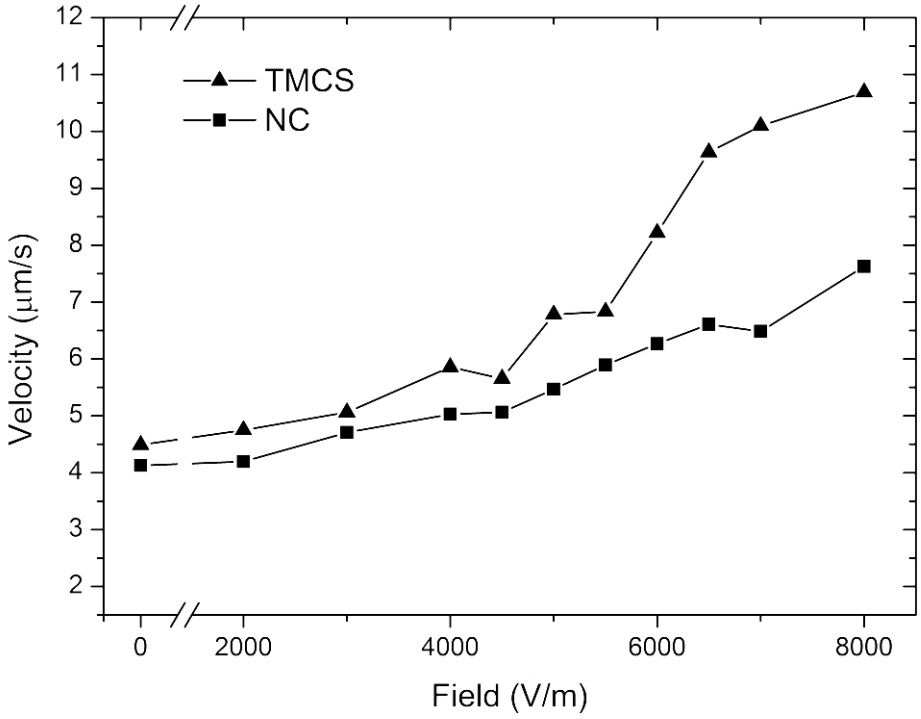

Figure.5.11. The average velocity of actins filaments on TMCS and NC vs. electrical field strength. Each data point presented shows the tracks of 30 filaments over 3 samples.

As shown in Figure 5.11 both have very similar velocities when not under the influence of a field. It is only when a substantial field is applied that the two surface start to show a differences in the motility function. TMCS seems to show slightly less hindered motility than NC as shown by the larger increase in velocity from 0 to 8 kV/m. This may be due to the previously described interactions between the polymer surface and the protein motors and the undefined nature of the polymer-protein layer described in Figure 5.9. Another

aspect to consider is the height of the HMM when immobilised on NC and TMCS. The NC layer is unlikely to swell in a uniform way and as such the heights of the attached HMM will differ slightly as the protein is adsorbed to the polymer, which may affect the resulting motility due to straining filament attachment. This would not be the case on TMCS as it is considered to create a largely flat surface and so the heights of fully active HMM should all be comparable.

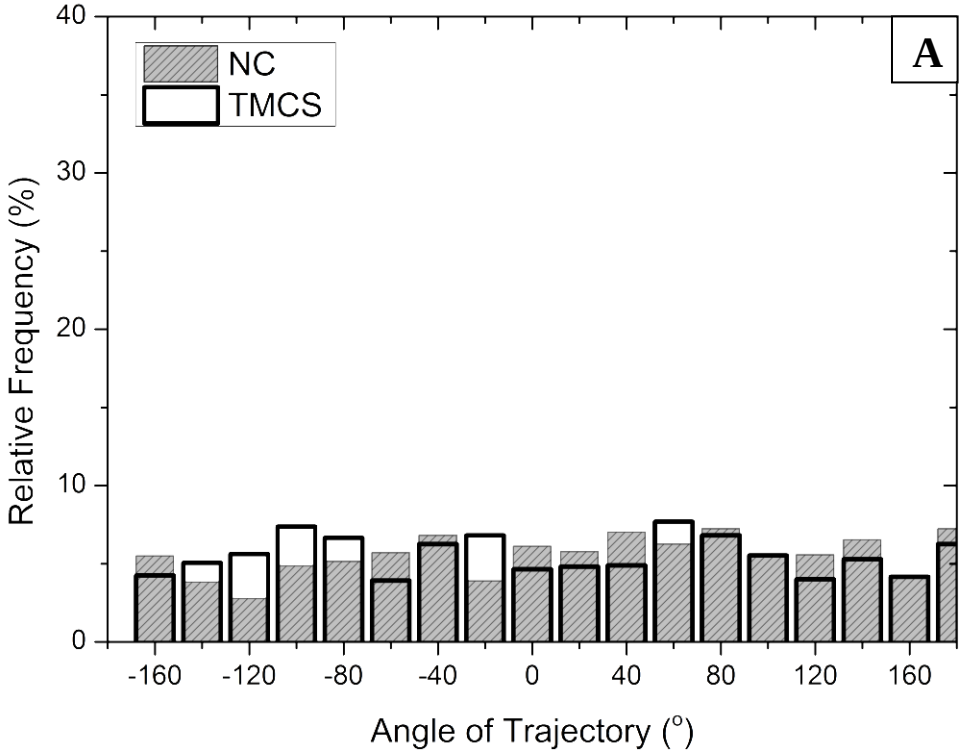
A
NC
TMCS
Relative Frequency (%)
0
10
20
30
40
-160
-120
-80
-40
0
40
80
120
160
Angle of Trajectory (°)

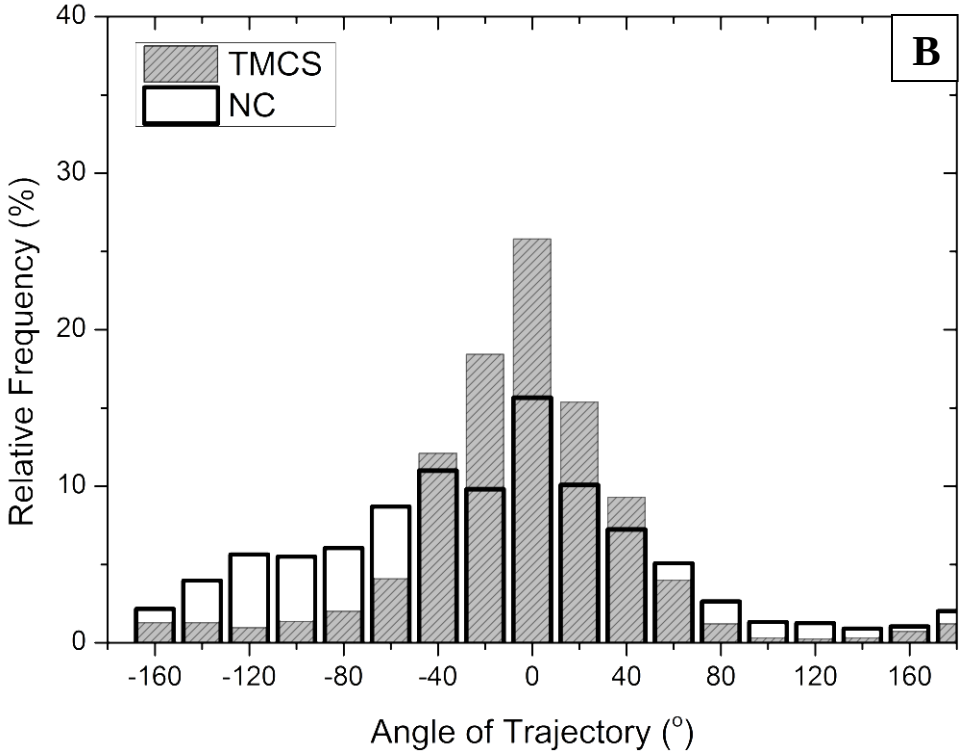
B
TMCS
NC
Relative Frequency (%)
0
10
20
30
40
-160
-120
-80
-40
0
40
80
120
160
Angle of Trajectory (°)

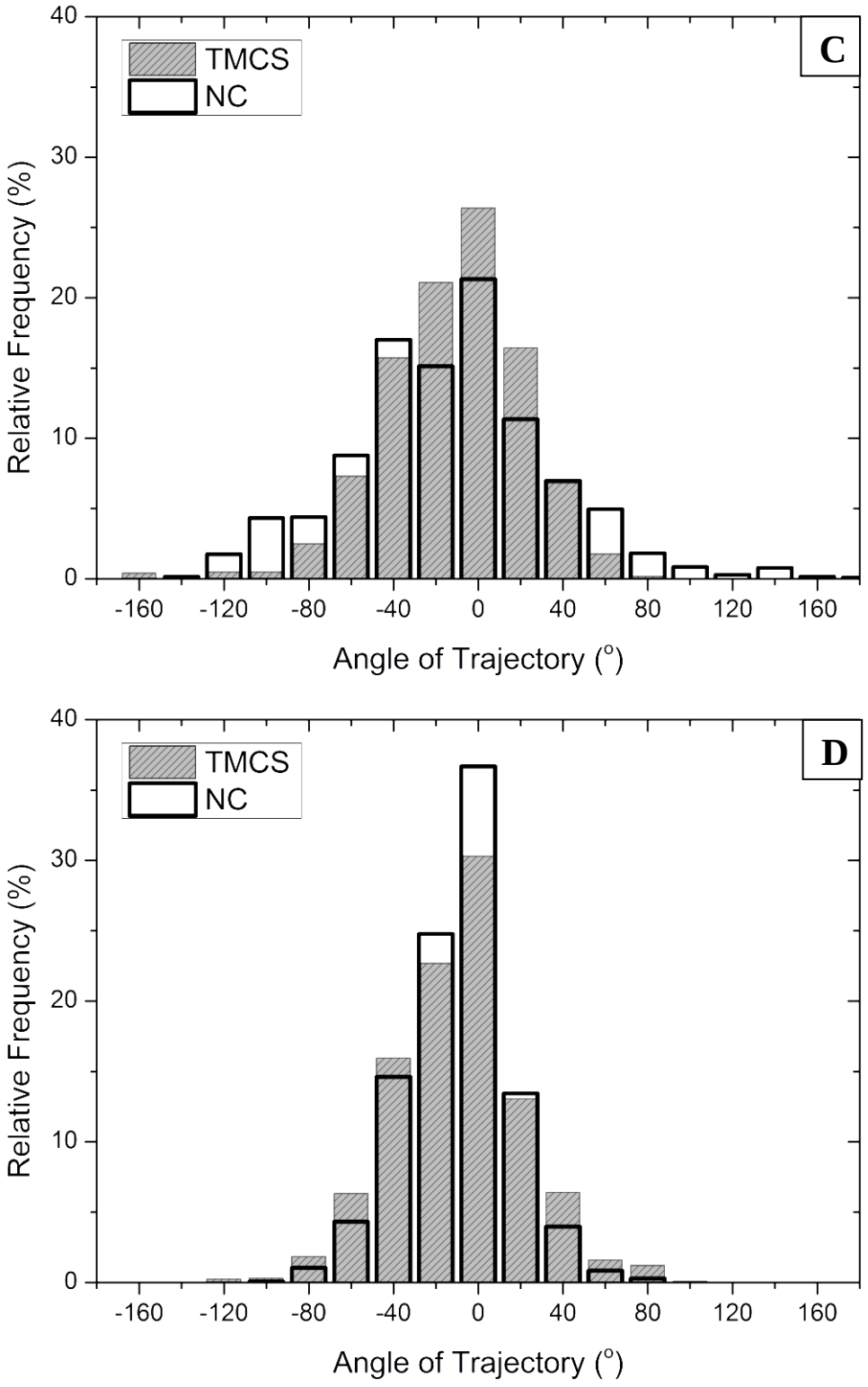

Figure.5.12. Graphs show the angle of trajectory of actin filaments on NC and TMCS. 0 degrees represents the position of the positive electrode. A, No field applied , B, 4000 V/m, C, 6000 V/m and D, 8000 V/m. Each graph represent to movement of 30 filaments over 3 samples.

Figure 5.12 again looks very similar with both displaying characteristics at the final 8 kV/m field. Though NC seems to have a larger number of filaments moving within 40^{o} of the positive electrode at 8 kV/m (~70%), at field strengths lower than this TMCS displays a higher level of guidance. This again could be attributed to the gel-like nature of NC making the polymer slightly more erratic in its behaviour than the highly planar TMCS. It is clear, however, that by looking at both sets of data and taking into account the comparable motility function observed during the experiment that both surfaces perform to a high degree with very little hindrance to motility. This may be due to the large surface area afforded to a swelled polymer such as NC. Any interactions between the bound HMM and the swelled polymer that would otherwise negatively impact the motility function may be negated by the density of HMM that is available due to the increased surface area of the swelled NC.

Therefore while the rigidity of the surface chemistry used to immobilise the HMM will have some influence as to retaining the function of the protein, other surfaces properties effecting protein adsorption such as hydrophobicity need to be examined. The next section of this chapter will concentrate on this in relation to the adsorption mechanism of the protein.

5.5 The effect of surface hydrophobicity on actin myosin motility while under the influence of an electrical field

Surface hydrophobicity and charge have been discussed in many studies to be the most important factors not only in the attachment of a protein to a surface but also the effect on the protein structure (the potential to denature) and as a result its functioning.[25-32] Section 5.4.2 outlined the effect that surface rigidity plays on the retention of unhindered motility, here the focus is on the remaining major aspects of HMM attachment. In 5.5 the motility function exhibited on a range of surfaces will be analysed in terms of their hydrophobicity and the overall charge held on each of the surfaces. This will be followed by an evaluation

of the HMM structure with the aim of correlating the displayed motility function with a number of geometries available to the HMM on a given surface.

5.5.1 Comparison of motility behaviour on silanes TMCS and TECS

Although TMCS and TECS are structurally similar, the carbon chains only differ by one, the chemical properties of the resulting surfaces are very different (Figure 5.13). TECS was the most hydrophilic of the surfaces tested in this study. Contact angle measurements gave readings between 32 – 35^{o}. Upon incubation with the assay solutions HMM was attaching to the surface as can be concluded from the presence of actin filaments, which are attached to the HMM.

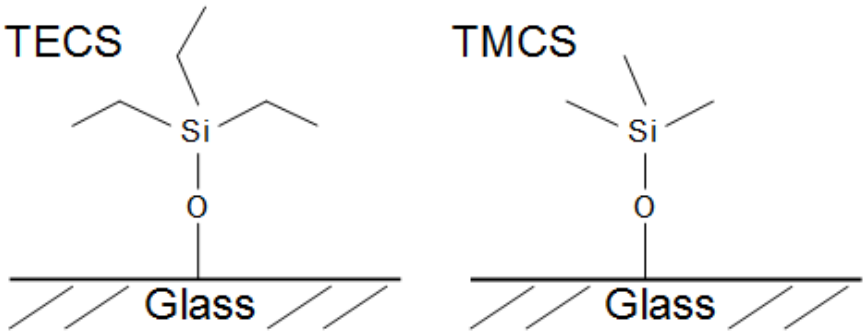

Figure.5.13. Schematic shows the structures of TECS and TMCS when attached to a glass surface. Although the difference in carbon chain is only by one, the result is a dramatic change in hydrophobicity and HMM immobilisation properties.

Motility on TECS without an electrical field was present but extremely sporadic and untrackable. Upon application of a field (2 kV/m) the filaments seen attached to the surface were quickly stripped off. Further samples were prepared with the final assay solution containing ATP replaced with the L65 wash solution (see chapter 3 section 3.2.4). These samples on average exhibited the same number of filaments present on the surface as the ATP containing assays. Upon application of 2 kV/m filaments were again stripped from the

surface. Both ATP containing and non ATP containing assays were then tested at lower fields (1 kV/m, 0.5kV/m and 0.25kV/m) all of which stripped the filaments from the surface. These experiments showed that there was an absence of attachment points, HMM molecules with heads available for attachment to the filaments, which not only support fully functional motility, but also anchor the filaments to the surface. TECS was deemed to have such poor HMM binding characteristics that no further study was achieved with this surface chemistry. This could be due to a propensity for the HMM to denature upon immobilisation owing to the hydrophilicity of TECS or perhaps an all round low density of HMM present. Another possibility is that the HMM is binding to the surface at the head domain leaving no active HMM for the filaments to bind to.

5.5.2 Motility function on methacrylate polymers, poly (methyl methacrylate) (PMMA), poly (tert-butyl methacrylate)(PtBMA) and poly (butyl methacrylate)(PBMA)

The backbones of these polymers are identical but the difference in the carbon chain in each of the polymers significantly changes the hydrophobicity of the resulting surfaces produced in this study. Together with the previous two surface chemistries tested, TMCS and nitrocellulose, conclusions can be drawn as to the main contributing factors in HMM binding and the reason the motility function differs on each substrate. The motility exhibited in terms of velocity and the tendency of the filaments to move towards the positive electrode on each surface will be analysed. This will be used to assess the HMM adsorption properties of surfaces based on their hydrophobicity.

5.5.2.1 Poly (methyl methacrylate) (PMMA)

PMMA is a polymer that is widely used in the medical sector due to its compatibility with human tissue and in photolithography as a high resolution mask. It exists as a strongly cross linked duroplastic polymer with high aging stability and relatively good chemical resistance. Although not extensively used as such, PMMA has been used to immobilise HMM and is an important material in lab-on-chip device technologies.[30, 33-36]

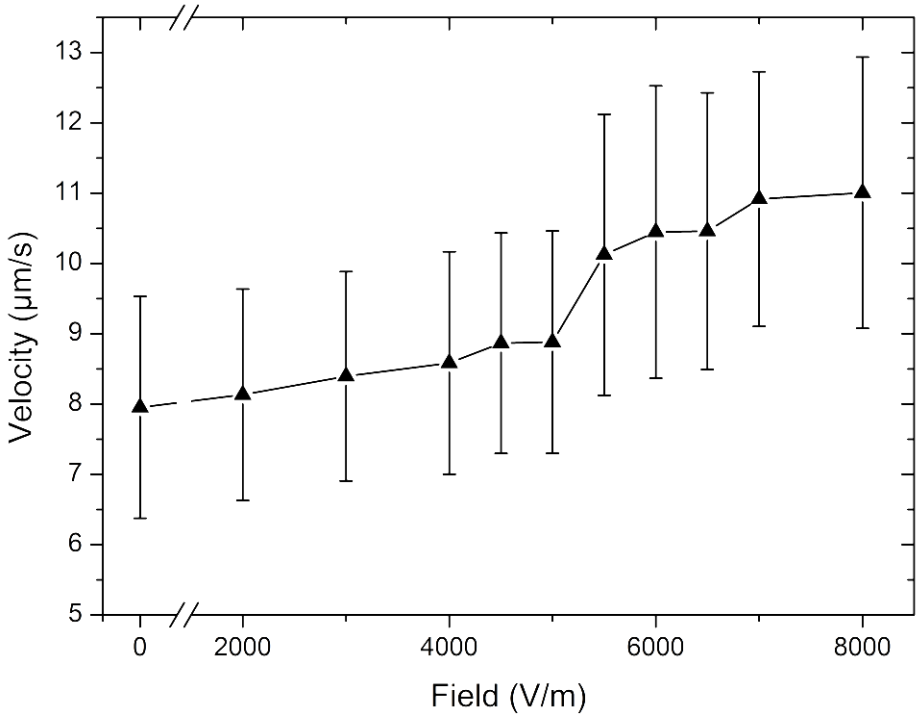

Figure.5.14. Plot shows the increase in the average velocity of actin filaments as the electric field increases on PMMA. Error bars show the standard deviation of velocity. Each data point represents shows the tracks of 30 filaments over 3 samples.

The PMMA surfaces have contact angles between 60^{o} – 63^{o} showing reasonable wettability. As seen in Figure 5.14 the velocity increases with the applied field and an increase in velocity can be observed in the mid range (5.5 - 6 kV/m) followed by a rapid increase. From 0 to 8 kV/m there was increase in the average velocity of 39%, a large portion of this comes from the jump at 5.5 kV/m.

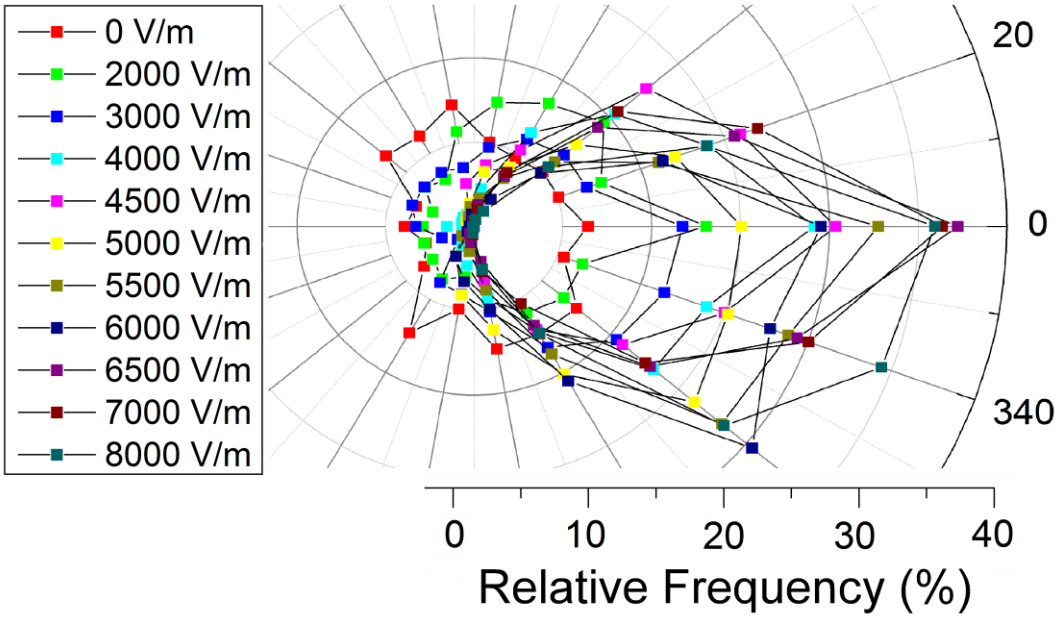

Figure.5.15. Radial plot shows a frequency count of the angle of trajectory on PMMA. 0 – 360 represent the angle of frame by frame movement of the actin filaments with 0 showing the position of the positive electrode. The graph shows the movement of 30 filaments over 3 samples for each of the fields tested.

Directionality was generally poor on these samples, although at 8 kV/m all filaments moving against the field made a U-turn. From 0 to 8 kV/m the percentage of motile filament increased from 39.5 to 60.3 %.

Table.5.4. Descriptive statistics of the motility function on PMMA. Standard deviation is given in brackets. Data represents the tracking of 30 filaments over 3 samples.

Electrical field (kV/m)	Percentage of motile filaments (%)	Percentage of filaments moving within 40o of the positive electrode (%)	Average velocity (µm/s)
0	39.5	16.8	8.0(1.6)
4	42.1	47.1	8.6(1.6)
6	46.3	48.5	10.4(2.0)
8	60.3	64.2	11.0(1.9)

5.5.2.2. Poly (tert-butyl methacrylate)(PtBMA)

PtBMA is used in microfabrication technologies as a positive photoresist, and lithographical resists in general have had an increase in interest for creating addressable protein surfaces over the recent years.[37, 38] PtBMA is highly hydrophobic; samples produced contact angles between 79^{o} - 81^{o}. Although no extensively used in motility assays, the surface has been used to attach HMM and shown reasonable motility function.[39]

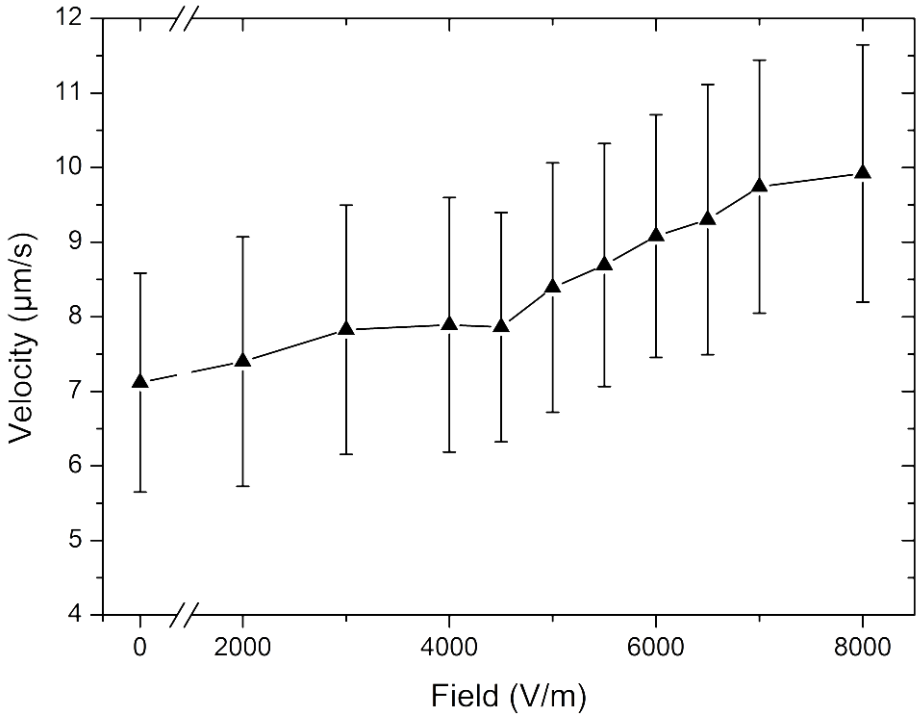

Figure.5.16. Plot shows the increase in the average velocity of actin filaments as the electric field increases on PtBMA. Error bars show the standard deviation of velocity. Each data point represents the tracks of 30 filaments over 3 samples.

As seen in Figure 5.16 there is a sudden increase in the average velocity of filament movement this time between 4.5 and 5 kV/m with a rapid rise following.

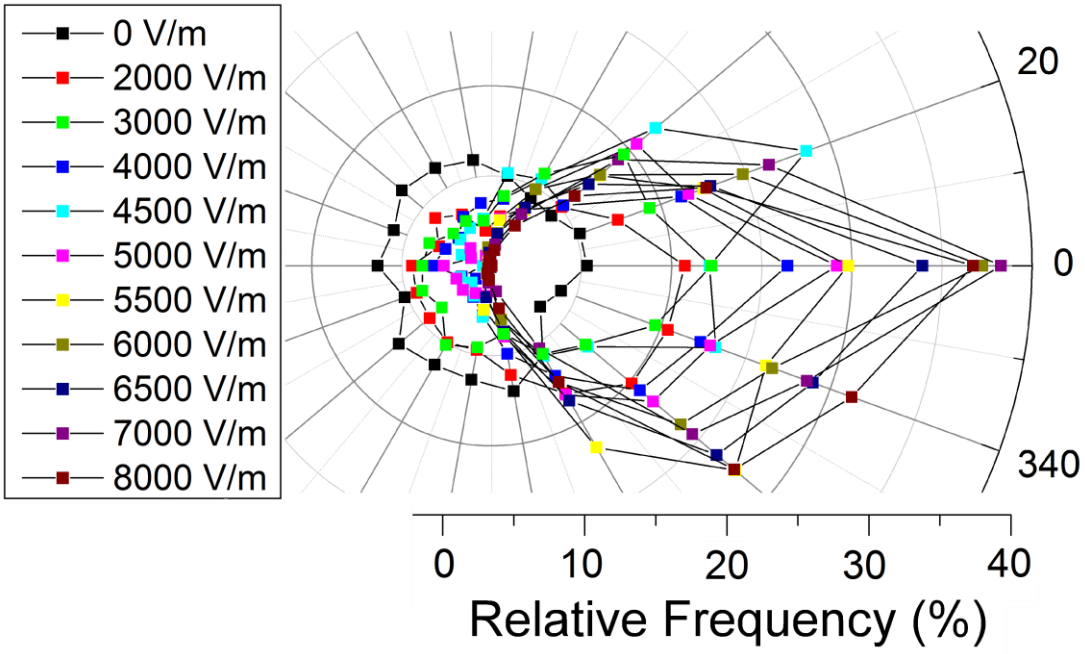

Figure.5.17. Radial plot shows a frequency count of the angle of trajectory on PtBMA. 0 – 360 represent the angle of frame by frame movement of the actin filaments with 0 showing the position of the positive electrode. Data presented shows the tracks of 30 filaments over 3 samples for each of the fields tested.

Directionality on PtBMA was poor. Both PtBMA and PBMA (see section 5.5.2.3) had comparable characteristics in terms of motility function. Even at the highest field strength tested the percentage of filaments moving within 40^{o} of the positive electrode was below 40%, comparatively lower than that of NC (over 60 %).

Table.5.5. Descriptive statistics of the motility function on PtBMA. Standard deviation is given in brackets. Data represents the tracking of 30 filaments over 3 samples.

Electrical field (kV/m)	Percentage of motile filaments (%)	Percentage of filaments moving within 40o of the positive electrode (%)	Average velocity (µm/s)
0	31.0	14.6	7.1(1.4)
4	31.9	39.9	7.9(1.7)
6	33.8	58.6	9.1(1.6)
8	51.6	60.7	9.9(1.7)

5.5.2.3. Poly (butyl methacrylate)(PBMA)

PBMA was used in this study due to the similarities in structure with both PtBMA and PMMA. It is not generally used as a substrate for protein immobilisation although it has been shown previously to support actin myosin motility.[30] Its inclusion here is one of scientific interest due to its structural similarities to PtBMA and contrasting chemical properties. Due to the long carbon chains PBMA has the ability to uptake more water in its structure than the other two methacrylate polymers used in this study and the surfaces produced with this polymer are thought to be much more like the NC surfaces in that they will turn gel-like and less rigid upon application of the assay solutions.

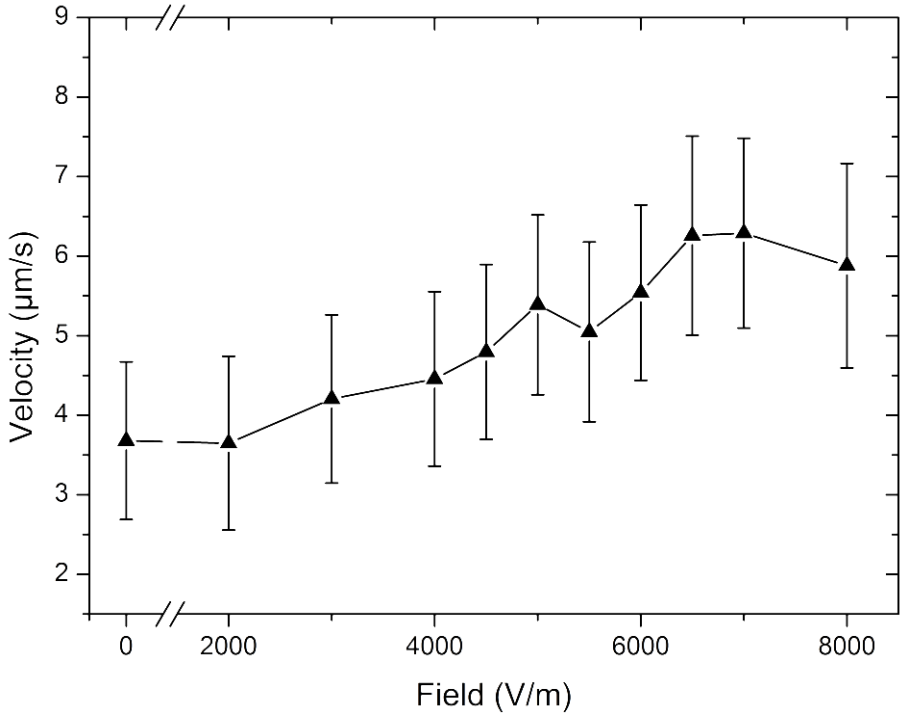

Figure.5.18. Plot shows the increase in the average velocity of actin filaments as the electric field increases on PBMA. Error bars show the standard deviation of velocity. Each data point represents the tracks of 30 filaments over 3 samples.

The motility function on PBMA was by far the most erratic of all the surface chemistries in this study. While Figure 5.18 suggests that the data follows on with what has been seen with

the previous surfaces, with a proportionally large increase in velocity between 4.5 and 5 kV/m, there is also much more irregularity to the motility function. The velocity increase on PBMA from 0 to 8 kV/m was also the smallest of all the surfaces studied.

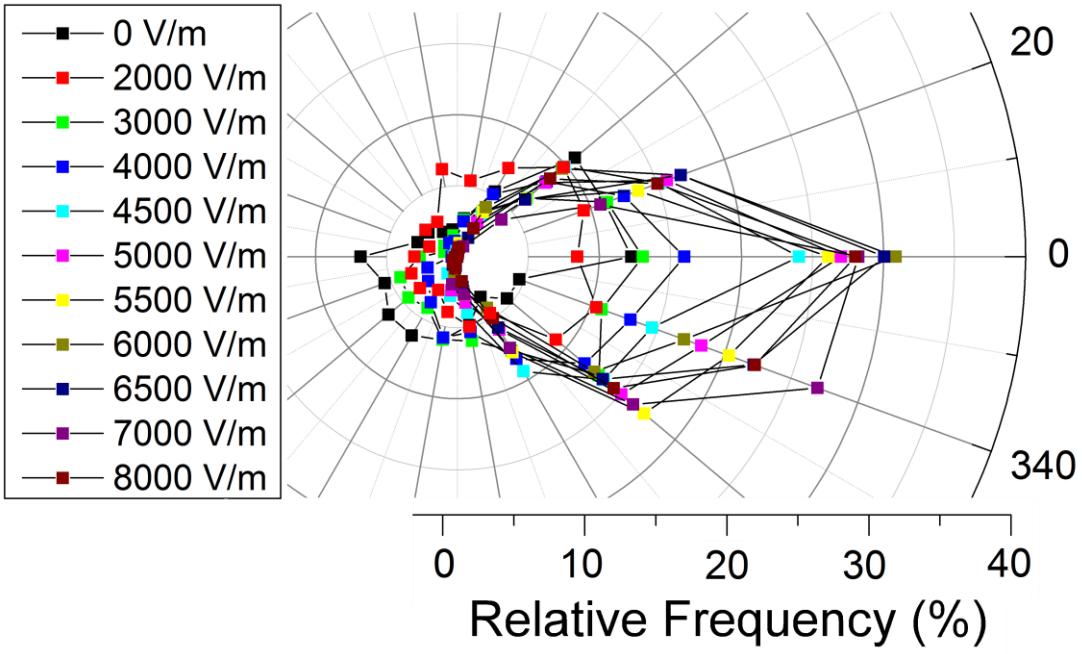

Figure.5.19. Radial plot shows a frequency count of the angle of trajectory on PBMA. 0 – 360 represent the angle of frame by frame movement of the actin filaments with 0 showing the position of the positive electrode. The data presented shows the movement of 30 filaments over 3 samples for each of the fields tested.

Following on from what was seen in the velocity data, the directionality of the motility on PBMA was irregular. Even at higher field strengths filaments were seen, if only briefly, to move against the field. It is important to note that no surface defects were visible on any of the samples produced and the contact angle measurements were also consistent. With this in mind it would seem that the erratic movement of the filaments on this surface is caused by the adsorption mechanism of the HMM on the different surfaces.

Table.5.6. Descriptive statistics of the motility function on PBMA. Standard deviation is given in brackets. Data represents the tracking of 30 filaments over 3 samples.

Electrical field (kV/m)	Percentage of motile filaments (%)	Percentage of filaments moving within 40o of the positive electrode (%)	Average velocity (µm/s)
0	22.1	28	3.7(1.0)
4	25.0	41.5	4.5(1.0)
6	27.1	64.5	5.5(1.1)
8	42.0	65.3	5.9(1.3)

5.5.3 Discussion on the effects of hydrophobicity and the protein adsorption properties of NC, TMCS, TECS, PMMA, PtBMA and PBMA

The adsorption of proteins to surfaces is an extremely complex and important area of study, and one that is still not yet fully understood. The mechanisms of immobilisation and the exact forces at work in the attachment of a protein to a given surface chemistry can have huge implications to the activity of the protein. Lab-on-chip technologies that wish to utilise immobilized proteins in their designs must first elucidate this relationship if highly specific devices are to be implemented.

5.5.3.1 Protein surface interactions

22 amino acids of varying hydrophobicity are the building blocks from which proteins are made.[40] The resulting complex structures contain heterogeneous hydrophobic and charge domains. Their three dimensional structure is a result of intramolecular forces and the interaction of the molecule with its environment. Any change to this structure can substantially change the functioning of the protein.[25, 26, 28] This can result in attachment sites being blocked or even almost complete denaturing of the protein.[25, 26] The importance of studying the interactions of proteins and surfaces is vast and has many implications in a range of industries including food and medical sciences.[26] It is thought that the enrichment of proteinacious material at soil particles played an essential role in the creation of life.[28] The

amphiphilic character of proteins also determines their functioning at biological membranes and the adsorption of proteins may affect microbial life in a variety of habitats.

In medical and technical applications the interactions between proteins and surfaces is important as they can lead to both desired and undesired consequences. For example the adherence of biological cells, such as bacteria, to protein layers is an issue for the food industry.[28] Proteins are also extensively used in pharmaceuticals and cosmetics as stabilisers in colloidal dispersions. More recently, the development of protein arrays for high throughput testing of antibodies is reliant upon better understanding of protein-surface interactions. These technologies have not seen the advancement that DNA microarrays have due to the sheer diversity of proteins.[41]

This fragile nature of the protein structure in terms of retaining its function upon absorption is a key issue if they are to be implemented in lab-on-chip technologies. Proteins have multiple attachment sites and will react differently depending not only on the surface chosen for immobilisation, but also on the conditions at the point of immobilisation. Changes in pH and ionic activity can affect the electrostatic interactions between protein and surface. Though these interactions tend to be weaker and more reversible than the hydrophobic interactions, they are also thought to be important first line forces that may affect the overall protein orientation on the surface.[25] The much stronger hydrogen bonding and hydrophobic interactions are the key interactions in terms of changes in the protein structure. It is these interactions that will most likely be the cause of any partial denaturing of protein at attachment sites.[25, 26] It is therefore important to know how a chosen protein will interact with a surface in order to keep the desired functionality. HMM is a prime example, where in order to keep full functioning of the molecular motor, immobilisation must occur at a certain region of the molecule so that the attachment and propulsion of actin filaments is kept intact. As previously stated, the exact mechanism of protein adsorption is still debated. In addition

to fluorescence microscopy there are many techniques that have been used to evaluate motor protein surfaces. Quartz crystal microbalance (QCM) has been used to measure the density of motor protein layers and also to distinguish individual steps in an *in vitro* motility assay.[21, 32, 42] This is done by measuring minute differences in the resonant frequency of a quartz crystal on which the protein is immobilised. Total internal reflection fluorescence microscopy (TIRF) has also been used to study the extent of motor protein layers and their catalytic activity using fluorescent analogues of ATP.[31, 32, 42] Each of these methods has given further insight into the geometry of attachment to a variety of surfaces and also the activity of the immobilised HMM. However it is here that it must be noted, that although much knowledge has been gained in the area, no definitive explanation of the adsorption mechanism has been given. It is therefore important to continue to study this mechanism in new and novel ways such as the method used in this study. Only by using alternative techniques such as the electrical motility assay will we step closer to a clear understanding of the relationship between HMM immobilisation, surface chemistry and motor function. An important stepping stone in the realisation of lab-on-chip technologies utilising molecular motors.

5.5.3.2 Attachment of HMM to surfaces

The HMM motor has three main regions, head, neck and tail, each of which carries different charges and properties in terms of hydrophobicity.[9, 40, 43] As stated previously, the incubation step of immobilising the HMM on the surface of the *in vitro* motility assay is highly random with no specific positioning in terms of the orientation of the HMM on the surface. When the solution containing HMM is applied the motor protein is simply allowed to diffuse through the solution with a percentage of the total concentration attaching to the surface. In reality the HMM molecules will attach to most surfaces the solution comes in contact with including the plastic of the pipette and the glass ‘ceiling’ of the flow cell, though to what

degree will depend on the surface properties. [22, 30-32, 42, 44-46] This means that as opposed to the highly ordered fashion in which the myosin system works *in vivo*, the motility function exhibited on a standard NC coated motility assay is highly irregular. This is due to a number of reasons. One of which is the lateral positioning of the HMM. Firstly, assume that all the HMM has been positioned on a given surface with both head domains available to propel an actin filament. The direction that each motor propels a filament, without outside influence, will be decided by the direction in which the HMM is facing, and the force of Brownian motion applied to the filament. In this sense it would be attractive if one could position HMM molecules in an ordered fashion to create a track on which filaments could be propelled in a highly directed way similar to the arrangement *in vivo*. This particular issue is solved in this study by the application of an external field to exert an additional force on the filaments to negate the directing effect of this HMM positioning and Brownian motion.

Another reason as to why the motility on a standard NC coated assay is random is the attachment of the HMM to the surface in terms of the region of the motor that binds with the surface. In order for the attachment of HMM to a surface to result in a motor that is fully active the protein must be immobilised by the tail region, at the C-terminus. It is only in this conformation that both motor heads are available to attach and propel the actin filament.

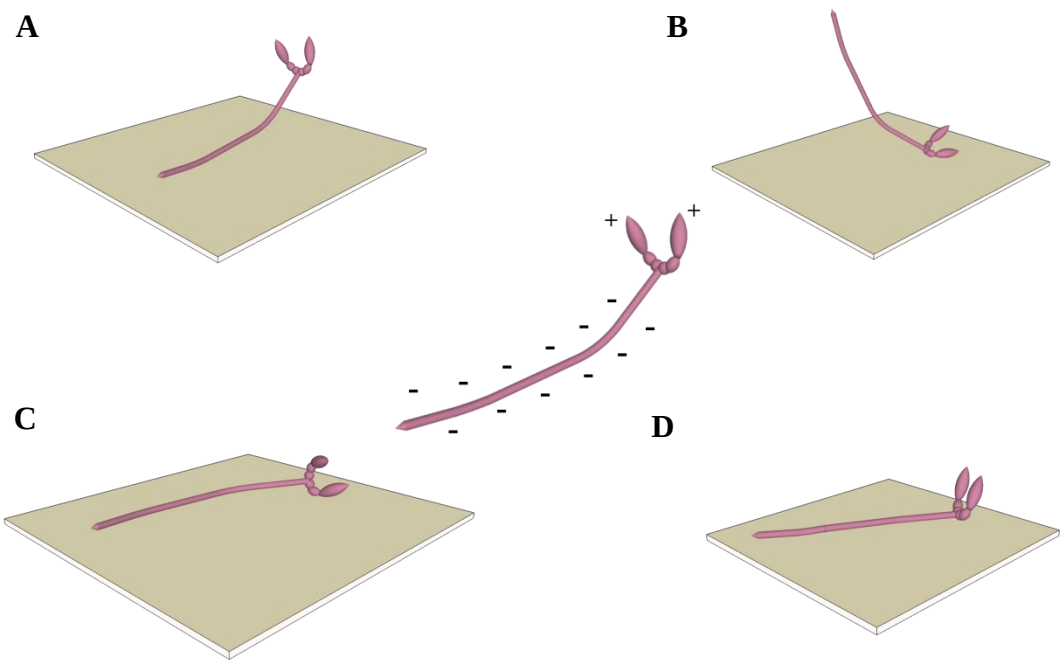

Figure.5.20. An illustration of four different conformations of HMM on a surface. The image at the center show a molecule of HMM and the associated charges. A, This is HMM attached to the surface in its fully active state with both head regions available to attach and propel an actin filament. B, In this state the HMM molecule is attached via the head region. In this example the head regions are unavailable for attachment to a filament and the tail region will protrude a significant distance above the surface. C, The motor is immobilised on the surface via one of the head regions. This would leave one head available for attachment. D, in this case the HMM is bound to the surface via the neck region.

In Figure 5.20 there is a representation of four conformations of HMM attached to a surface that are thought to be available to the protein. The charges held by the different regions of the HMM will impact on the mechanism of immobilisation as well as the hydrophobic nature of the different regions. One might assume that a surface that carries a negative charge is more likely to have attachment of the protein via the head and neck regions leaving the HMM unable to function properly. Conversely one would expect the propensity for the protein to attach via the tail region on a surface carrying a positive charge. Electrostatic

interactions, however, are often reversible and are affected by any changes in pH and ionic activity.

The adsorption of proteins involves multiple forces, with surface charge being one contributing factor in a wider mechanism which can have profound effects on the protein structure upon adsorption. The fact is that one cannot rely upon electrostatic interactions alone as a clear indication of the mechanism of protein binding.

5.5.3.3 Analysis of surfaces

In order to study the immobilisation of HMM and the protein activity, six surfaces with a range of hydrophobicities and surface charges were used to support the motility. NC, PtBMA, PBMA, PMMA, TMCS and TECS surfaces were used in motility assays that had a range of electrical fields applied to them. In this way it is possible to study the differences in the motility function on all six surfaces while an external force is applied to the filament. The result was a map of motility function due to surface chemistry.

NC has been used extensively as a surface to study motor proteins. It is relativity hydrophobic and carries an overall positive charge. It has been shown in numerous motility studies to exhibit fully functioning myosin motors.[10, 13, 30, 31, 44, 47]. TMCS has been used extensively as a substrate for actin myosin motility assay studies. As a hydrophobic surface with low surface charge, HMM binding characteristics have been previously reported which show the density of fully functioning motors to be high.[22] See Chapter 3 for details on surface chemistry. The following discussions will be based upon how these surface characteristics affect the motility function and in turn what this tells us about the HMM adsorption.

An important characteristic in the velocity data, mentioned briefly in previous research of electrically guided motility, is the increase in the average velocity of actin filaments in the

mid range (4.5 - 6 kV/m).[8] The positioning of this increase on the graph is particularly interesting as it seems to support the hypothesis of tail hindered motility where the sudden increase signifies the overcoming of restrictive forces acting against motility. In the case of PMMA this jump occurs in a slightly higher range than NC, TMCS and PtBMA. One might assume that this alone would indicate a higher proportion of head attached HMM and thus a higher force is needed to be applied to the filaments in order to overcome the hindrance to motility. In the case of NC, TMCS and PtBMA the increase seems to be in the same region. Giving the impression of at least similar attachment geometries offered to the HMM. PBMA, however, shows no such relationship. On this surface the immobilisation of HMM on the surface is so unfavourable for free gliding motility that the velocity graph only shows a small effect of an increasing field. The motility on these samples was highly erratic, presumably due to head attachment of HMM. There is also the possibility in this case for the formation of a second protein layer due to the protruding heads, further hindering motility (Figure 5.22 C).

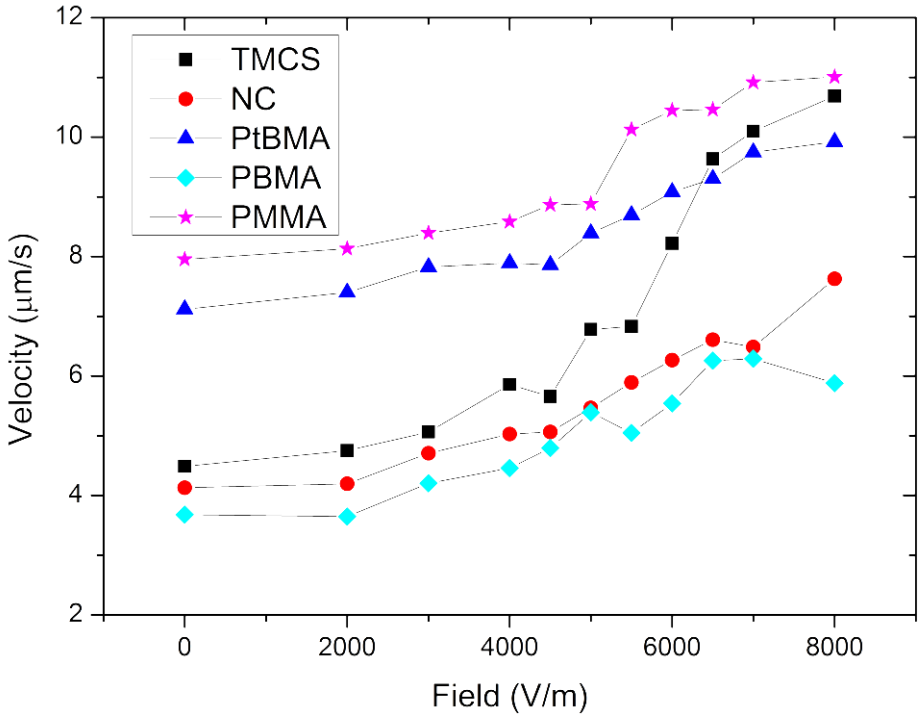

Figure.5.21. Plots of Average velocity vs. field for all five surfaces tested with the scales adjusted to highlight the motility function seen as a result of surface chemistry. Note the characteristic increase in velocity seen in all the plots at around 4.5 – 5.5 kV/m. Each experiment was repeated 3 times with an average of 10 filaments tracked on each sample.

The overall increase in velocity also gives insight to the density of fully active motors on each surface. NC and TMCS exhibit the largest increase, at 3.5 and 6.2 μms^{-1}, respectively. This would point towards a large proportion of the HMM immobilised on these surfaces being available to attach and propel actin filaments. Conversely PBMA shows an increase of only 2.2 μms^{-1}. This indicates that the availability of active motors on this surface is low and also that the attachment geometry of HMM to the surface is actually further hindering motility. This hindrance could be caused either by inactive motor heads or protruding tails of head bound motors.

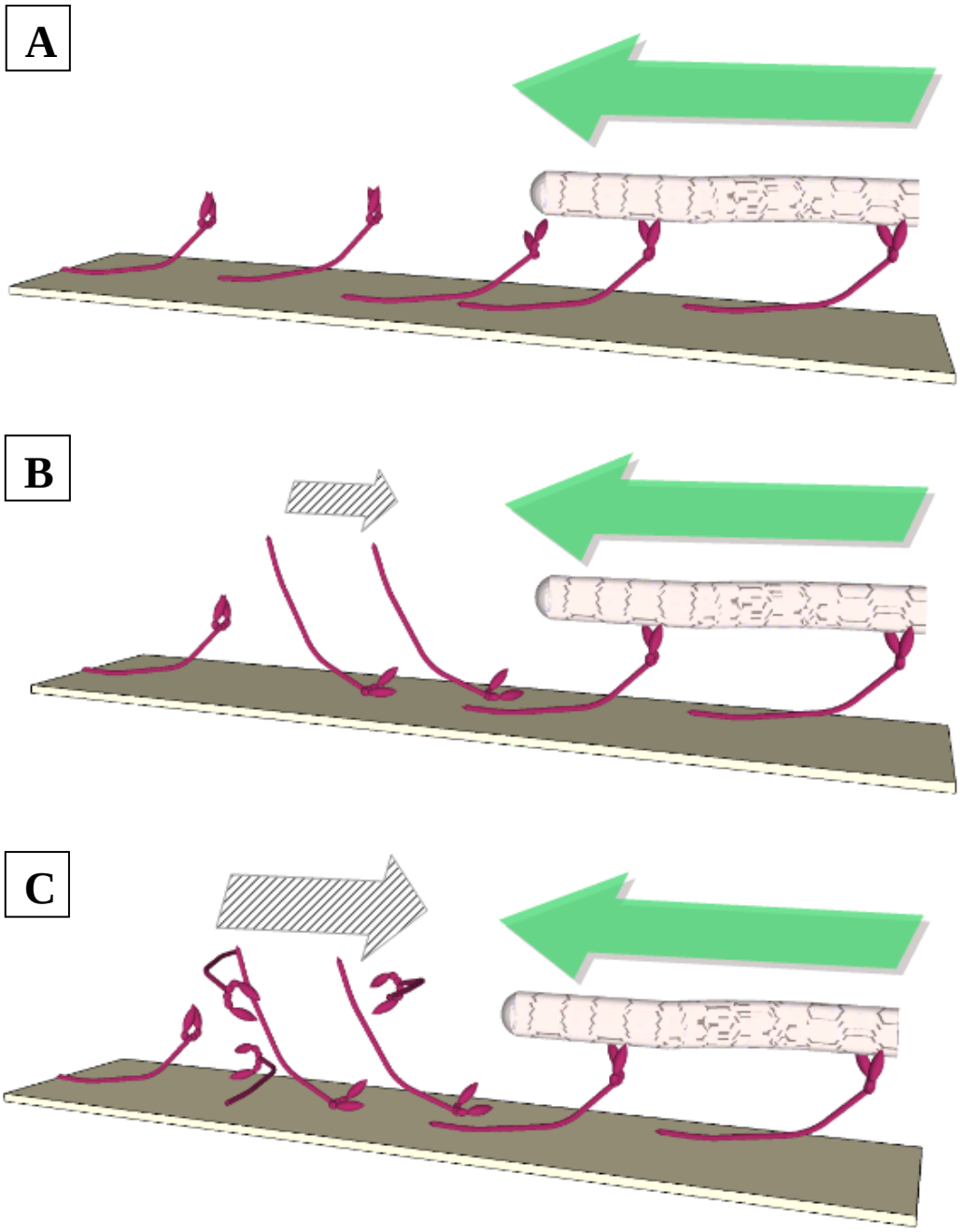

Figure.5.22. This scheme shows examples of three situations where the orientation of HMM on a surface effects the overall motility function. A, In this case the HMM is immobilised via the tail for unhindered motility. B, The motility in this case is hindered by a proportion of HMM that cannot aid in the propelling of the filaments and adds a restrictive force against filament movement. C, This represents a surface where the HMM is bound to the surface in orientations that would prove very restrictive to motility.

In Figure 5.22 a scheme is shown to highlight the possible hindrances to motility due to different HMM orientations. A surface that has good HMM adsorption properties will immobilise the motor at its tail region (Figure 5.22 A). This leaves both head regions available for interaction with the actin filaments. This orientation also ensures that any partial denaturing of the protein due to adsorption does not occur at the function regions of the motor i.e. the head or neck domains.

When adsorption of the protein occurs at the head region of the motor it eliminates the function of the protein. This is due to the inability of a filament to attach, but immobilisation at the head region may also involve partial denaturing of the actin binding sites. There is evidence to show that HMM bound in this state can actually protrude above the surface of tail bound HMM.[42] This is shown in Figure 5.22 B where the protruding tails of head bound HMM impacts on the motility function. Resistive forces due to the obstruction of filaments would impact the movement of actin on the motor protein layer. The negatively charged tail region may also act unfavourable with the negatively charge filaments and obstruct the interaction of the actin with surrounding HMM.

On surfaces where adsorption occurs at unfavourable sites i.e. head, neck or a combination of the two, there is evidence to suggest the possibility of multiple protein layers forming.[21, 32, 42] Figure 5.22 C shows how this might work and the hindrance it would place on motility.

There is a possible arrangement where only one head could attach to the actin filament, as shown in Figure 5.20 C. Propulsion of actin filaments can be achieved by a single head of HMM, however, this is at a reduced step size and force, around 6 nm and 0.7 pN respectively, compared to around 10 nm and 3.4 pN of a motor with two functioning heads.[48] It is therefore obvious that in this situation unhindered translocation of actin would still be inhibited by attachment to motors where only one head can supply force. There is room for argument that in this orientation, filament attachment would be unlikely. Assuming that the

other head region is adsorbed to the surface, due to the height of any surrounding HMM bound at either the head, with the tail protruding above the level of fully active HMM,[42] or at the tail with both heads active, actin filaments are unlikely to manoeuvre close enough to interact with the single headed HMM. In either situation, HMM bound via a single head region with one head still active would not effectively contribute to gliding due to either the inability to interact with the filaments or reduced force and step size upon attachment.

Another contribution to the overall motility function, though arguably minor, is ATP insensitive HMM i.e. HMM that is able to bind but not propel actin. These are motors that are either tail bound, but ATP insensitive, or bound in an orientation that has lead to the partial denaturing of the protein but still able to bind to actin. In the first instance, the ratio of ATP insensitive HMM in the HMM solution before incubation with the sample surface has to be low. An inactive motor head can hold a filament with a force of around 9.2 pN.[49] Given that an active motor will propel with a combined force of around 3.4 pN, the ratio of active to inactive must be in a state where there are very few inactive motor heads otherwise motility to any observable degree would not occur.[50] Since motility of varying degrees has occurred on all the samples tested we can assume the protein solution used in this study had a low ratio of ATP insensitive HMM prior to immobilisation. Secondly, any HMM that becomes insensitive to ATP upon immobilisation, has probably done so due to protein-surface interactions at the neck or head regions as it is these that contain the catalytic site for the hydrolysation of ATP. This in turn means that this portion of HMM molecules are likely to be bound to the surface at a lower height then that of fully functioning tail bound HMM, ~38 nm.[40, 42] It is therefore unlikely that actin filaments will manoeuvre close enough to these motors to interact with the actin binding sites.

Table.5.7. Percentage of motile filaments and the percentage of filaments moving within 40^{o} of the positive electrode at fields 4, 6 and 8 kV/m. Surfaces are ordered by hydrophobicity, PMMA being the most hydrophilic, PBMA the least. Data represents the tracking of 30 filaments over 3 samples for each surface.

	Field					
	4000 V/m		6000 V/m		8000 V/m	
	Filaments moving within 40^{o} of positive electrode (%)	motile filaments (%)	Filaments moving within 40^{o} of positive electrode (%)	motile filaments (%)	Filaments moving within 40^{o} of positive electrode (%)	motile filaments (%)
PMMA	47.1	42.1	48.6	46.3	64.3	60.3
NC	35.5	30.6	47.8	34.3	74.9	66.9
TMCS	59.6	38.7	63.9	44.4	66	80.5
PtBMA	40	31.9	58.7	33.8	60.7	51.6
PBMA	41.4	25	64.6	27.1	65.3	42

The directionality data is harder to interpret. In table 5.7 there is clearly a strong relationship between the velocity data presented previously and the percentage of motile filaments at each field. Direct comparisons can be made on each surface in relation to these two data sets and the possible mechanism of adsorption of HMM. The directionality data, however, seems a little more complex. While there is a relationship showing an increased tendency for filaments to move towards the positive electrode with increasing field, there are instances in the data that seem at first not to follow the previous assumptions made with respect to the HMM adsorption mechanism on these surfaces. The issue here is that the velocity data, and the qualitative visual observation of the motility, can be explained relatively simply in terms of fully functional motility, or varying degrees of motility function, due to the orientation of HMM. That is to say a surface that presents visibly smooth gliding and velocity data suggests a high percentage of active HMM along with a high percentage of motile filaments, e.g. TMCS, would point to a surface with the propensity to adsorb myosin motors at the tail

region. Conversely a surface that displays erratic motility with a poor ratio of motile filaments and velocity data suggesting a lower density of active HMM, e.g. PBMA, indicates HMM immobilisation at regions of the motor that does not support unhindered gliding i.e. head and neck region, or a combination of the two. How strongly the motility is directed towards the positive electrode seems to be a combination of two aspects for the adsorption characteristics of each surface. Both surfaces with fully a functioning HMM layer, and surfaces with a partially functioning HMM layer, have characteristics that would aid in the directing of filaments.

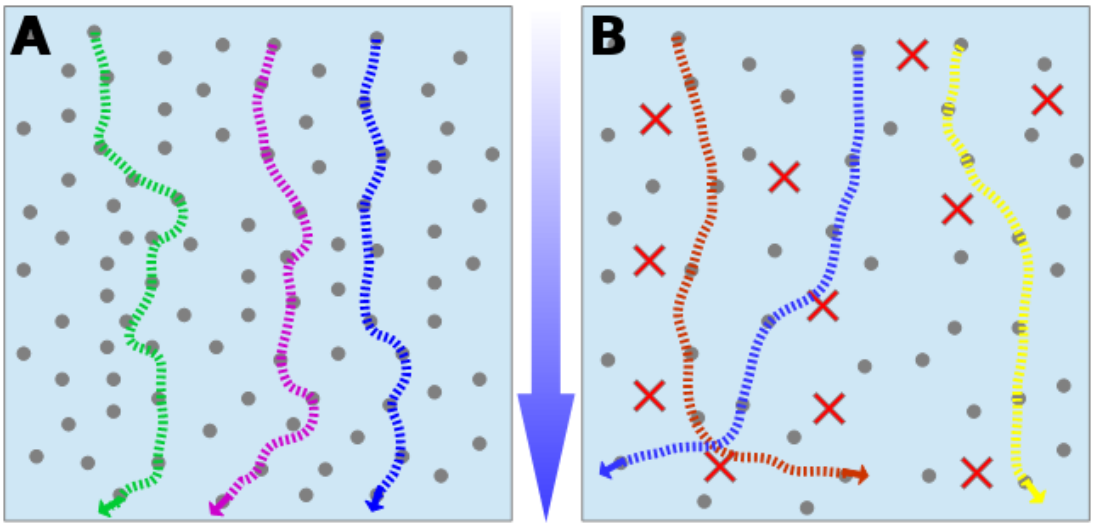

Figure.5.23. The Figure shows the directing influence of active HMM and obstacles on two types of surfaces. The grey dots represent active motors while the red crosses show areas where obstructions occur due to HMM bound in unfavourable orientations for actin motility. The center arrow represents the direction of the electrical field. A, HMM is adsorbed in a favourable orientation for the attachment and propulsion of actin. The relatively close confinement of the motors in this example means that the field has less time between the motor attachments to influence the direction of the filament. B, the density of active HMM is lower and therefore the time between motor attachments is greater. This means the head of the filament is greatly influenced by the force of the electrical field. However, due to the protein binding nature of such a surface, extended HMM tails and potential dual protein layers will cause obstructions around which the filaments must navigate.

First consider a fully functional HMM layer with no obstacles to motility (Figure 5.23 A). In this instance the filament movement is at least partially dictated by the direction in which the HMM is facing. Now consider the converse surface type, where HMM is adsorbed in an orientation that hinders the attachment of actin filaments the HMM and the propulsion of said filaments (Figure 5.23 B). In this case the field will have to overcome the Brownian motion. However, on this surface there are fewer active HMM molecules that can influence the direction of the filament via their lateral positioning. This means the time spent where the head of the filament is unattached to a motor, and therefore more heavily influenced by the electrical field, is longer. This type of behaviour can be observed in the directionality data. Compare the percentage of filaments moving within 40^{o} of the positive electrode at 6 and 8 kV/m on PBMA and TMCS in table 5.7 PBMA has previously exhibited adsorption properties that hinder motility function. TMCS, however, has shown a high density of active HMM through analysis of the velocity data and the percentage of motile filaments. Despite this both show comparable statistics with respect to the directionality of the actin filaments.

This is an important result as it highlights the impact of the lateral positioning of HMM on directionality. The directing ability of this positioning seems to be much greater than previously thought, as most sources highlight Brownian motion to be the chief factor in the trajectories of unguided actin myosin motility.[15] This, however, should not come as much of a surprise as *in vivo* the very nature of molecular motor function is highly ordered. Depending on the motor and cystoskeletal filament involved there is a predefined mechanism where the motor will move from a given end of a filament to the opposite.[9, 40, 43] In the actin myosin system the motor will move towards the positive end. This means that when the negatively charged end of the actin filament, which is being directed by the electrical field, interacts with an immobilised HMM, the motor itself has a predominant role in determining the direction of movement.

From the above analysis it is possible to draw conclusion on the adsorption properties of the six surfaces in this study due to the motility function observed during the electrical motility experiment. The data also shows evidence of the complex nature of protein binding as there is more to the immobilisation characteristics of each surface than just hydrophobicity. The surface charges and relative hydrophobicity of NC and TMCS seem to favour the immobilisation of HMM at the tail region of the motor. These two surfaces showed visibly smoother gliding than the others tested and the data presented point to the presence of a high density of active HMM. The hydrophilic nature of TECS meant that protein binding on this surface was extremely poor. The experiments performed on this surface point to a limited amount of active HMM available for interaction with actin filaments. It would be interesting to follow up with experiments on this surface to see if this characteristic is down to protein orientation or general lack of bound protein. PBMA and PtBMA exhibited HMM binding characteristics that severely hindered motility. These can be explained by the preference for the surfaces to bind the protein at the head or neck region. The results from PMMA showed that hydrophobicity is not the only participant in protein binding. This slightly hydrophilic surface, a chemical property said to repel protein adsorption,[25, 26, 28] actually showed reasonable motility function. It is thought that the electrostatic interactions with PMMA as the HMM approaches, which are likely to be the initial interactions,[25, 28, 40, 41] help to keep the protein function upon adsorption.

As a side note it is also important to mention Bovine Serum Albumin (BSA), if not just to discount it from this chapter's conclusions. BSA is a protein most commonly purified from the blood of cattle protein and used in the actin myosin motility assay to block surface sites that do not hold HMM after the initial incubation with the solution containing the motor protein (See chapter 3 section 3.2.4). BSA is used extensively as a blocking agent to prevent the attachment of protein and enzymes to the walls of reaction vessels.[51, 52] A surface functionalised with BSA will exhibit increased hydrophilicity; as a result BSA can also be

used to aid in the filling of micro fluidic systems.[51, 53, 54] BSA will adsorb to an extensive range of surfaces and in the concentration used in this study will occupy all the available sites left after HMM incubation.[25, 55, 56] As a result, the adsorption of BSA and any differences there may be in its protein adsorption mechanism on the surfaces in this study, are not thought to affect the motility function seen. The conclusions in this chapter are based purely upon the interaction between the surface and HMM.

5.6 Conclusions

Presented in this chapter is a detailed analysis of the HMM immobilisation characteristics on six surfaces, NC, TMCS, TECS, PtBMA, PBMA and PMMA. The motility function exhibited by each when used in an electrical motility assay can be explained based upon the orientation of the molecule motors adsorbed on the surface. Studies such as this one are important stepping stones in the development of lab-on-chip technologies utilising molecular motors. It also helps in building a better interpretation of the surface interactions with HMM and which characteristics are preferable, not only for the unhindered motility of actin but also for directing motility using electrical fields. The results presented in this chapter point to substrates that hold low surface charge and are in the range of hydrophobicities that is occupied by NC and TMCS, will favour attachment of HMM at the tail region. The directionality data has shown that a surface with preferential HMM binding characteristic does not necessarily preferentially contribute to the directing of the filaments. In order to have maximum directionality while minimizing restrictive components of the protein layer one should not only consider the ratio of fully functional HMM : inactive or inhibiting HMM be considered, but also the density of HMM itself.

In terms of the viability of utilising electrical guidance within a device to control the motility there are several issues with long term exposure of DC electrical fields on the motor protein system. In the electrical motility device used in this study, the issue of heat and species created at the electrodes that would disrupt the protein have been negated by the spacing of the electrodes and the chambers used to contain them. If this was to be used within a device specifically to guide the filaments it may be preferable to have the electrodes contained within structures on the surface of the gliding assay so that the field only need be applied for a short amount of time for the desired effect. For example, if the electrodes were contained within a Y junction of a channel so the filaments could be steered to one direction or another the field need only be applied when a filament comes within a certain distance of the junction. This would mean the field would be applied for a fraction of the time it has been in this study and the likelihood of damaging the protein system would be reduced. The directionality results in this study have shown that guidance of filaments does occur at relatively low field strengths which again will reduce the possibility of damaging the protein if used within a lab-on-chip device.

5.6 References

1. Kron, S. J. and Spudich, J. A., "Fluorescent actin filaments move on myosin fixed to a glass surface," *Proceedings of the National Academy of Sciences* 83(17), 6272-6276 (1986)
2. Bakewell, D. J. G. and Nicolau, D. V., "Protein linear molecular motor-powered nanodevices," *Aust. J. Chem.* 60(5), 314-332 (2007)
3. van den Heuvel, M. G. L. and Dekker, C., "Motor Proteins at Work for Nanotechnology," *Science* 317(5836), 333-336 (2007)
4. Sundberg, M., Bunk, R., Albet-Torres, N., Kvennefors, A., Persson, F., Montelius, L., Nicholls, I. A., Ghatnekar-Nilsson, S., Omling, P., Tagerud, S. and Mansson, A., "Actin filament guidance on a chip: Toward high-throughput assays and lab-on-a-chip applications," *Langmuir* 22(17), 7286-7295 (2006)
5. Hess, H., Bachand, G. D. and Vogel, V., "Powering nanodevices with biomolecular motors," *Chem.-Eur. J.* 10(9), 2110-2116 (2004)
6. Hess, H., Clemmens, J., Qin, D., Howard, J. and Vogel, V., "Light-controlled molecular shuttles made from motor proteins carrying cargo on engineered surfaces," *Nano Lett.* 1(5), 235-239 (2001)
7. Takatsuki, H., Rice, K. M., Asano, S., Day, B. S., Hino, M., Oiwa, K., Ishikawa, R., Hiratsuka, Y., Uyeda, T. Q. P., Kohama, K. and Blough, E. R., "Utilization of Myosin and Actin Bundles for the Transport of Molecular Cargo," *Small* 6(3), 452-457 (2010)
8. Riveline, D., Ott, A., Julicher, F., Winkelmann, D. A., Cardoso, O., Lacapere, J. J., Magnusdottir, S., Viovy, J. L., Gorre-Talini, L. and Prost, J., "Acting on actin: the electric motility assay," *Eur. Biophys. J. Biophys. Lett.* 27(4), 403-408 (1998)
9. Manfred, S., *Molecular Motors*, Wiley-VCH, Weinheim (2003).
10. Spudich, J. A., "How Molecular Motors Work," *Nature* 372(6506), 515-518 (1994)
11. Přistoupil, T. I., Kramlová, M. and Štěrbíková, J., "On the mechanism of adsorption of proteins to nitrocellulose in membrane chromatography," *Journal of Chromatography A* 42(0), 367-375 (1969)
12. Jones, K. D., "Troubleshooting protein binding in nitrocellulose membranes," in *IVDTechnology magazine* (1999).
13. Sellers, J. R., "In Vitro Motility Assay to Study Translocation of Actin by Myosin," in *Current Protocols in Cell Biology*, John Wiley & Sons, Inc. (2001).
14. Hooft, A. M., Maki, E. J., Cox, K. K. and Baker, J. E., "An accelerated state of myosin-based actin motility," *Biochemistry* 46(11), 3513-3520 (2007)
15. Li, G. and Tang, J. X., "Diffusion of actin filaments within a thin layer between two walls," *Physical Review E* 69(6), 061921 (2004)
16. Hosek, M. and Tang, J. X., "Polymer-induced bundling of F actin and the depletion force," *Physical Review E* 69(5), (2004)
17. Hanson, K. L., Solana, G. and Nicolau, D. V., "Electrophoretic control of actomyosin motility," in *Microtechnology in Medicine and Biology, 2005. 3rd IEEE/EMBS Special Topic Conference on*, pp. 205-206 (2005).
18. Lercel, M. J., Whelan, C. S., Craighead, H. G., Seshadri, K. and Allara, D. L., "High-resolution silicon patterning with self-assembled monolayer resists," *J. Vac. Sci. Technol. B* 14(6), 4085-4090 (1996)
19. Chang, T. C., Liu, P. T., Mor, Y. S., Tsai, T. M., Chen, C. W., Mei, Y. J., Pan, F. M., Wu, W. F. and Sze, S. M., "Eliminating dielectric degradation of low-k organosilicate glass by trimethylchlorosilane treatment," *Journal of Vacuum Science & Technology B* 20(4), 1561-1566 (2002)

20. Bunk, R., Rosengren, J., Forlander, K., Sundberg, M., Montelius, L., Nicholls, I. A., Omling, P., Tagerud, S. and Mansson, A., "Actomyosin motility on nanostructured resist polymers and silanes," *Biophysical Journal* 84(2), 327A-327A (2003)
21. Albet-Torres, N., O'Mahony, J., Charlton, C., Balaz, M., Lisboa, P., Aastrup, T., Mansson, A. and Nicholls, I. A., "Mode of heavy meromyosin adsorption and motor function correlated with surface hydrophobicity and charge," *Langmuir* 23(22), 11147-11156 (2007)
22. Sundberg, M., Rosengren, J. P., Bunk, R., Lindahl, J., Nicholls, I. A., Tagerud, S., Omling, P., Montelius, L. and Mansson, A., "Silanized surfaces for in vitro studies of actomyosin function and nanotechnology applications," *Analytical Biochemistry* 323(1), 127-138 (2003)
23. Bunk, R., Sundberg, M., Mansson, A., Nicholls, I. A., Omling, P., Tagerud, S. and Montelius, L., "Guiding motor-propelled molecules with nanoscale precision through silanized bi-channel structures," *Nanotechnology* 16(6), 710-717 (2005)
24. van Zalinge, H., Aveyard, J., Hajne, J., Persson, M., Mansson, A. and Nicolau, D. V., "Actin filament motility induced variation of resonance frequency and rigidity of polymer surfaces studied by quartz crystal microbalance," *Langmuir* 28(42), 15033-15037 (2012)
25. Nakanishi, K., Sakiyama, T. and Imamura, K., "On the adsorption of proteins on solid surfaces, a common but very complicated phenomenon," *J. Biosci. Bioeng.* 91(3), 233-244 (2001)
26. Gray, J. J., "The interaction of proteins with solid surfaces," *Curr. Opin. Struct. Biol.* 14(1), 110-115 (2004)
27. Kasemo, B., "Biological surface science," *Surf. Sci.* 500(1-3), 656-677 (2002)
28. Norde, W., "Adsorption of proteins from solution at the solid-liquid interface," *Advances in Colloid and Interface Science* 25(0), 267-340 (1986)
29. Vasina, E. N., Paszek, E., Nicolau, D. V. and Nicolau, D. V., "The BAD project: data mining, database and prediction of protein adsorption on surfaces," *Lab Chip* 9(7), 891-900 (2009)
30. Hanson, K. L., Solana, G. and Nicolau, D. V., "Effect of surface chemistry on in vitro actomyosin motility," in *Biomedical Applications of Micro- and Nanoengineering II* D. V. Nicolau, Ed., pp. 13-18, Spie-Int Soc Optical Engineering, Bellingham (2005).
31. Balaz, M., Sundberg, M., Persson, M., Kvassman, J. and Monsson, A., "Effects of surface adsorption on catalytic activity of heavy meromyosin studied using a fluorescent ATP analogue," *Biochemistry* 46(24), 7233-7251 (2007)
32. Albet-Torres, N., Gunnarsson, A., Persson, M., Balaz, M., Hook, F. and Mansson, A., "Molecular motors on lipid bilayers and silicon dioxide: different driving forces for adsorption," *Soft Matter* 6(14), 3211-3219 (2010)
33. Bunk, R., Klinth, J., Montelius, L., Nicholls, I. A., Omling, P., Tagerud, S. and Mansson, A., "Actomyosin motility on nanostructured surfaces," *Biochemical and Biophysical Research Communications* 301(3), 783-788 (2003)
34. Suzuki, H., Yamada, A., Oiwa, K., Nakayama, H. and Mashiko, S., "Control of actin moving trajectory by patterned poly(methyl methacrylate) tracks," *Biophysical Journal* 72(5), 1997-2001 (1997)
35. Stefan Diez, J. H., "Nanotechnological Applications of Biomolecular Motor Systems," *La Physique au Canada* 65(1), 7-12 (2009)
36. Korten, T., Mansson, A. and Diez, S., "Towards the application of cytoskeletal motor proteins in molecular detection and diagnostic devices," *Curr. Opin. Biotechnol.* 21(4), 477-488 (2010)

37. Schwarz, A., Rossier, J. S., Roulet, E., Mermod, N., Roberts, M. A. and Girault, H. H., "Micropatterning of Biomolecules on Polymer Substrates," *Langmuir* 14(19), 5526-5531 (1998)
38. Wright, J., Ivanova, E., Pham, D., Filipponi, L., Viezzoli, A., Suyama, K., Shirai, M., Tsunooka, M. and Nicolau, D. V., "Positive and Negative Tone Protein Patterning on a Photobase Generating Polymer," *Langmuir* 19(2), 446-452 (2002)
39. Nicolau, D. V., Suzuki, H., Mashiko, S., Taguchi, T. and Yoshikawa, S., "Actin Motion on Microlithographically Functionalized Myosin Surfaces and Tracks," *Biophysical Journal* 77(2), 1126-1134 (1999)
40. Howard, J., *Mechanics of motor proteins and the cytoskeleton*, Sinauer Associates, Inc., sunderland Massachusetts (2001).
41. Nicolau, D. V. and Muller, U. V., *Microarray Technology and Its Applications*, Springer-Verlag Berlin Heidelberg Germany (2005).
42. Persson, M., Albet-Torres, N., Ionov, L., Sundberg, M., Hook, F., Diez, S., Mansson, A. and Balaz, M., "Heavy Meromyosin Molecules Extending More Than 50 nm above Adsorbing Electronegative Surfaces," *Langmuir* 26(12), 9927-9936 (2010)
43. Kreis, T. and Vale, R. D., *Guidebook to the Cytoskeletal and Motor Proteins*, Oxford University Press Inc., New York (1993).
44. Nicolau, D. V., Solana, G., Kekic, M., Fulga, F., Mahanivong, C., Wright, J. and dos Remedios, C. G., "Surface Hydrophobicity Modulates the Operation of Actomyosin-Based Dynamic Nanodevices," *Langmuir* 23(21), 10846-10854 (2007)
45. Sundberg, M., Balaz, M., Bunk, R., Rosengren-Holmberg, J. P., Montelius, L., Nicholls, I. A., Omling, P., Tagerud, S. and Mansson, A., "Selective spatial localization of actomyosin motor function by chemical surface patterning," *Langmuir* 22(17), 7302-7312 (2006)
46. Albet-Torres, N., O'Mahony, J., Charlton, C., Balaz, M., Lisboa, P., Aastrup, T., Månsson, A. and Nicholls, I. A., "Mode of heavy meromyosin adsorption and motor function correlated with surface hydrophobicity and charge," *Langmuir* 23(22), 11147-11156 (2007)
47. Warshaw, D. M., "The in vitro motility assay: A window into the myosin molecular motor," *News in Physiological Sciences* 11(1-7 (1996)
48. Tyska, M. J., Dupuis, D. E., Guilford, W. H., Patlak, J. B., Waller, G. S., Trybus, K. M., Warshaw, D. M. and Lowey, S., "Two heads of myosin are better than one for generating force and motion," *Proc. Natl. Acad. Sci. U. S. A.* 96(8), 4402-4407 (1999)
49. Nishizaka, T., Miyata, H., Yoshikawa, H., Ishiwata, S. and Kinosita, K., Jr., "Unbinding force of a single motor molecule of muscle measured using optical tweezers," *Nature* 377(6546), 251-254 (1995)
50. Finer, J. T., Simmons, R. M. and Spudich, J. A., "Single myosin molecule mechanics – piconewton forces and nanometer steps," *Nature* 368(6467), 113-119 (1994)
51. Zhou, J. W., Ellis, A. V. and Voelcker, N. H., "Recent developments in PDMS surface modification for microfluidic devices," *Electrophoresis* 31(1), 2-16 (2010)
52. Towbin, H., Staehelin, T. and Gordon, J., "Electrophoretic transfer of proteins from polyacrylamide gels to nitrocellulose sheets – procedure and some applications," *Proc. Natl. Acad. Sci. U. S. A.* 76(9), 4350-4354 (1979)
53. Binz, M., Lee, A. P., Edwards, C. and Nicolau, D. V., "Motility of bacteria in microfluidic structures," *Microelectron. Eng.* 87(5–8), 810-813 (2010)
54. Held, M., Lee, A. P., Edwards, C. and Nicolau, D. V., "Microfluidics structures for probing the dynamic behaviour of filamentous fungi," *Microelectron. Eng.* 87(5–8), 786-789 (2010)
55. Suzawa, T. and Murakami, T., "Adsorption of bovine serum albumin on synthetic polymer latices," *J. Colloid Interface Sci.* 78(1), 266-268 (1980)

56. Suzawa, T., Shirahama, H. and Fujimoto, T., "Adsorption of bovine serum-albumin onto homo-polymer and co-polymer lattices," *J. Colloid Interface Sci.* 86(1), 144-150 (1982)

Chapter VI: Deceleration Study of Electrically Stimulated Actin Filaments

Where in the previous chapter the focus was on the effect of an electrical field on the steady state in this chapter the aim is to look at the dynamics when applying the electrical field. The results are used in conjunction with the discussion in chapter 5 to further elucidate the protein adsorption properties of three surface chemistries. Coupled with the electrical motility experiments is a study on the impact of ‘blocking actin’ on the motility function when an electrical field is applied to the gliding assay.

6.1 Introduction

In the previous chapter the actin myosin motility on six different surface chemistries was analysed. The guidance of active filaments by an electrical field was presented and an investigation into the difference in motility function vs. field strength. This was analysed as an average of the motility function seen over the course of the experiment. A correlation between the differences in this relationship and the surface characteristics upon which the HMM had been immobilised was discussed. In order to further the hypothesis made, that the orientation of HMM bound to a surface can be directly correlated to motility function and that certain surface chemistries have a preference for immobilisation in a certain motor orientation, supplementary investigations are required.

Results shown in the previous chapter, as well as a multitude of previous studies, show that the electrostatic interaction between the motor protein and the surface is part of a much more complicated mechanism.[1-3] It was sugested that the binding of myosin at the tail region, the region preferred for retaining full functionality, was much more prolific on surfaces that exhibited low overall surface charge density along with relatively high hydrophobicity. This hypothesis was reached by comparing the different motility characteristics exhibited while the system was influenced by an external force, an electrical field. By comparing the velocity and directionality data accumulated while directing the actin filaments in a field, the influencing factors in terms of motor orientation were discussed. It was found that the relationship of smooth gliding motility was due to the number of fully active motors available on the surface coupled with the obstructing force that certain motor orientations have on smooth gliding motility. The influencing nature of several HMM orientations was discussed and there appears to be a preference for specific HMM binding orientation due to certain surface characteristics.

In this chapter a method will be formulated to further test the hypothesis made. The actin motility on three different surface chemistries is analysed as a field is applied and then terminated in order to observe the response in terms of filament velocity.

In this chapter the motility function will be studied as a function of time while the motility is accelerated by the electrical field and then allowed to decay back to the motility function seen before being exposed to the field. The relationship between the maximum velocities reached in the time frame of electrical field exposure and the time taken for the motility to decay back to the initial function, in terms of velocity, will be analysed. In addition to this 'deceleration study', the influence of the blocking actin in the experimental procedure used in both chapter 5 and 6 was investigated. The electrical motility experiment detailed in chapter 5 was repeated at significant electrical field strengths using the three surfaces chosen for this chapter, PMMA, NC and TMCS.

The procedure was altered so that each experiment was repeated with and without the use of blocking actin, the unlabelled actin filaments used to block ATP inactive HMM. This was done in order to gain an insight into the number of ATP inactive motors on a particular surface chemistry and also to investigate the hypothesis detailed in chapter 5 that stated that the additional crowding caused by these unlabelled filaments contributes to the motility characteristics seen on each surface and aided in the indication of whether the surface had preferable binding characteristics or not. Both procedures will be used to shed further light on the HMM binding properties of the three surface chemistries chosen for this study and the influence that HMM orientation has on smooth gliding motility.

6.2 Investigation of post field motility function

In the following experiments the same electrical motility set-up is used as described in chapter 3. PMMA, TMCS and NC were used to immobilise the motor protein in the electrical motility cell. These three surfaces were selected due to the chemical properties in order to study the adsorption properties of each and how this affects the motility function. NC and TMCS are similar in hydrophobicity but have vastly different water absorption and surface rigidity. TMCS and PMMA have similar water absorption properties and both will form a flat rigid surface. They do, however, differ greatly in the hydrophobicity of the resulting surface. All three have slightly different charge densities and it was for this combination of varying properties that they were chosen.

6.2.1 Outline for the 'deceleration' study

In the following study the electrical motility device has been utilised to analyse the movement of actin filaments. Unlike the procedure used in chapter 5 the main aim of this study was to see the behaviour of the motility before, during and after the application of an electrical field. The motility in each gliding assay is recorded for a total of 30 seconds. After an initial period of 5 seconds a field is applied to the sample as in the previous electrical motility procedure for a total of 5 seconds. After this time the field is terminated and the video capture of the motility continues for a further 20 seconds. This 5 second 'acceleration' phase was chosen as it would give enough data points so that after averaging statistically sound results were obtained. Within this time frame the motility will be unable to reach its absolute maximum velocity in the presence of a field, which ensures that each acceleration and deceleration phase was treated identically for all the surfaces tested. The motility function was tracked as a function of time. Each frame of capture corresponds to 0.1 seconds and in each frame the velocity of 10 filaments is averaged. The phase post field, in which the filaments are slowly returning to an average velocity seen pre-exposure, was analysed. This

was used in order to correlate the time taken for the filaments to decelerate against the different surface chemistries used and the possible motor orientations causing this behaviour.

6.2.2 Motility on nitrocellulose

As with the previous chapter an initial study was carried out on NC to provide a 'base level' for the motility function in this investigation. This is particularly important for the analysis of the deceleration time due to the need to develop a clear understanding of what defines 'normal motility function' in terms of velocity and directionality. Once the motility is exposed to a field, the values of average velocity and directionality from these controls will be compared with the pre-exposed test samples so as to properly evaluate the deceleration.

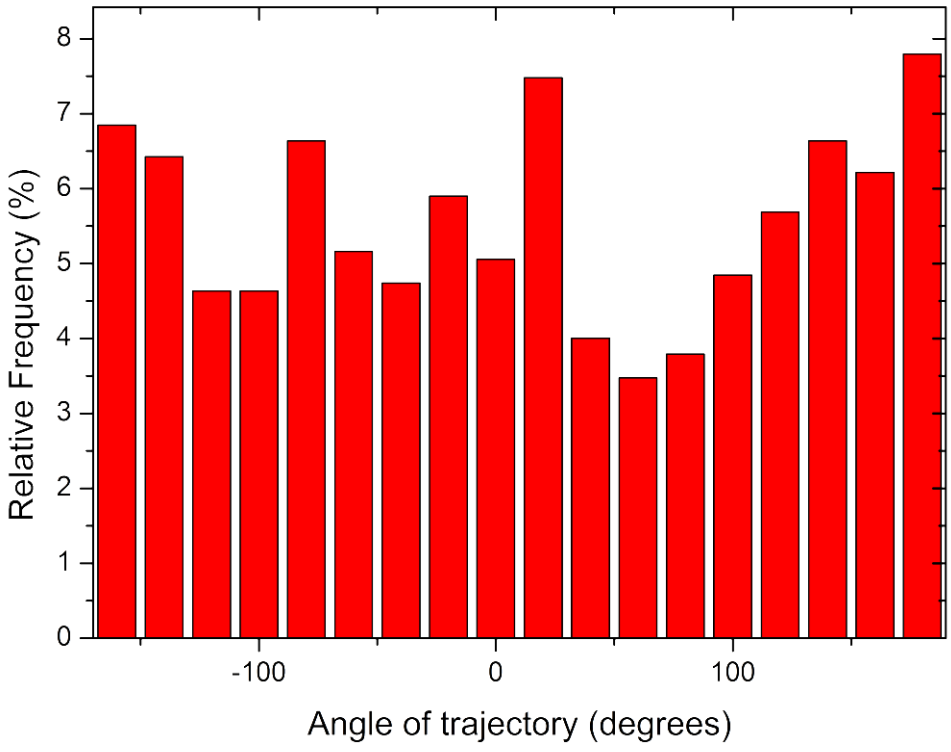

Figure.6.1. The graph shows a frequency count of the angle of trajectory as a percentage of actin filament movements on NC. 0 degrees represents the position of the positive electrode. The data presented represents 20 filaments movement on 2 samples.

As seen in the previous experiments on NC, the motility in the absence of a field proceeds in a random fashion in terms of the angle of trajectory (see Figure 6.1). This is evident on all of the surfaces, until the application of a field there is no preference for filaments to travel in any specific direction. This highlights the random nature of the HMM adsorption on the surface of the gliding assay as there is no alignment of the motors. This shows that the orientation of fully active motors, i.e. tail bound motors, is a dominating factor in directing the movement of the filament along with Brownian motion.

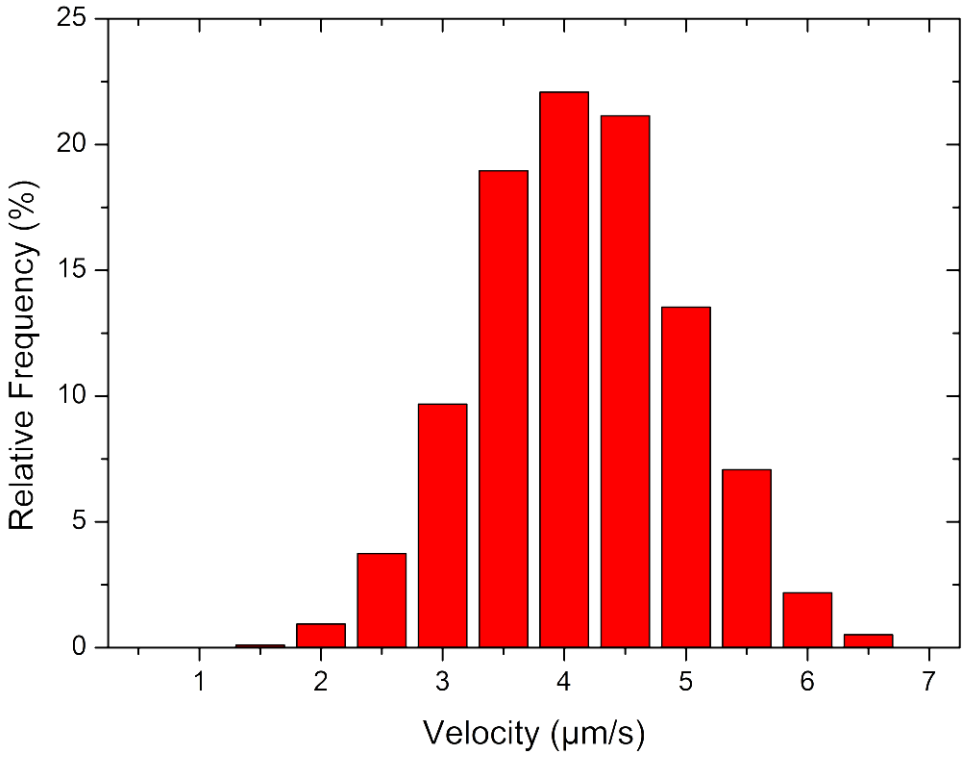

Figure.6.2. The graph shows a frequency count of the velocity of actin filaments movements gliding on NC coated motility assay. The data represents 20 filaments movements over 2 samples.

In addition to the angle of trajectory the average velocity of filaments was within the range of previous experiments and also matched up with previously reported statistics of actin myosin motility when using NC as a surface coating (~2 – 10 μm/s) (see Figure 6.2).[4-7]

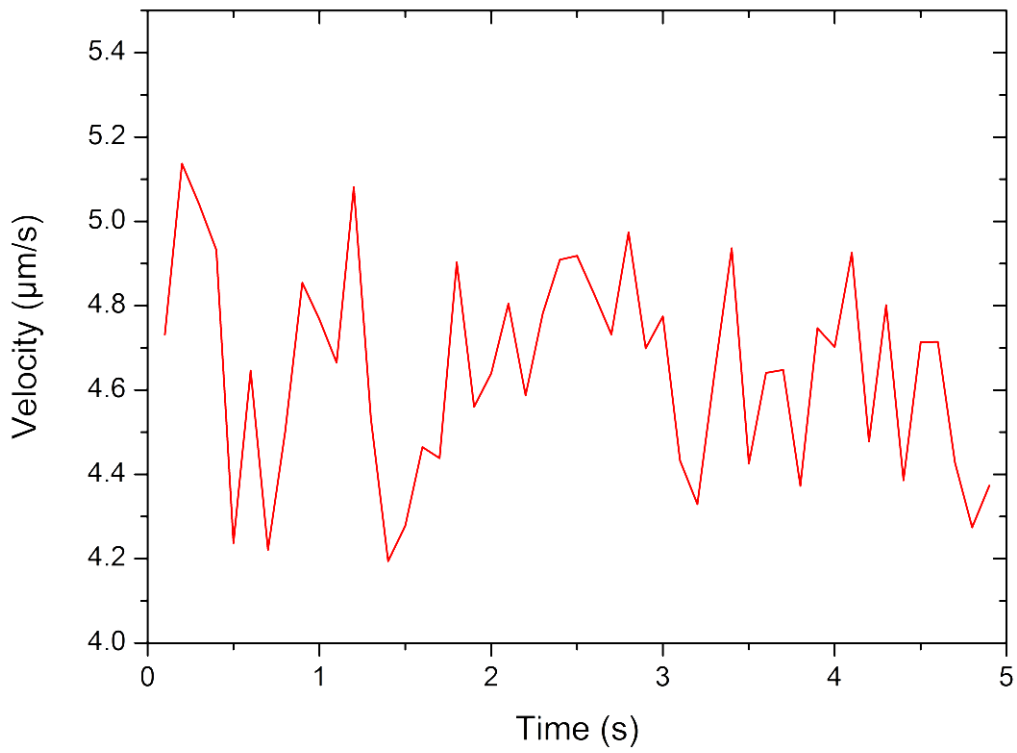

Figure.6.3. The graph shows a frame by frame average of the velocity of actin filament movements when gliding on an NC coated motility assay. The data represents an average of 20 filaments movements over 2 samples.

In this chapter the average filament velocity will be analysed as a function of time, during the course of electrical field application and termination, to evaluate the behaviour of the motility when the field is no longer active after the initial acceleration of the filaments due to the force exerted by the field. It is therefore important to see what the behaviour of the actin filaments is on NC as a function of time in the absence of a field. In Figure 6.3 the velocity of 20 actin filaments per frame (accounting for 0.1 seconds per frame) were analysed for 5 seconds. The average velocity fluctuates around 4.6 µm/s with the average variation being approximately 0.4 µm/s. This gives a good example of how the frame-by-frame analysis will be achieved. During the 'deceleration' study each surface will be recorded for 5 seconds prior to the application of a field. It is the motility function in terms of the velocity in this

period that will be the value used to decide when the motility has returned to 'normal' after the field has been terminated.

6.2.3 Nitrocellulose deceleration study

It also holds similar surface properties with TMCS in terms of hydrophobicity and charge. TMCS, however, is a much more rigid surface with NC allowing more water uptake. The reasoning therefore behind the inclusion of both these surfaces is to evaluate the effect that surface rigidity, and to a small effect surface topography, has on the motility function.

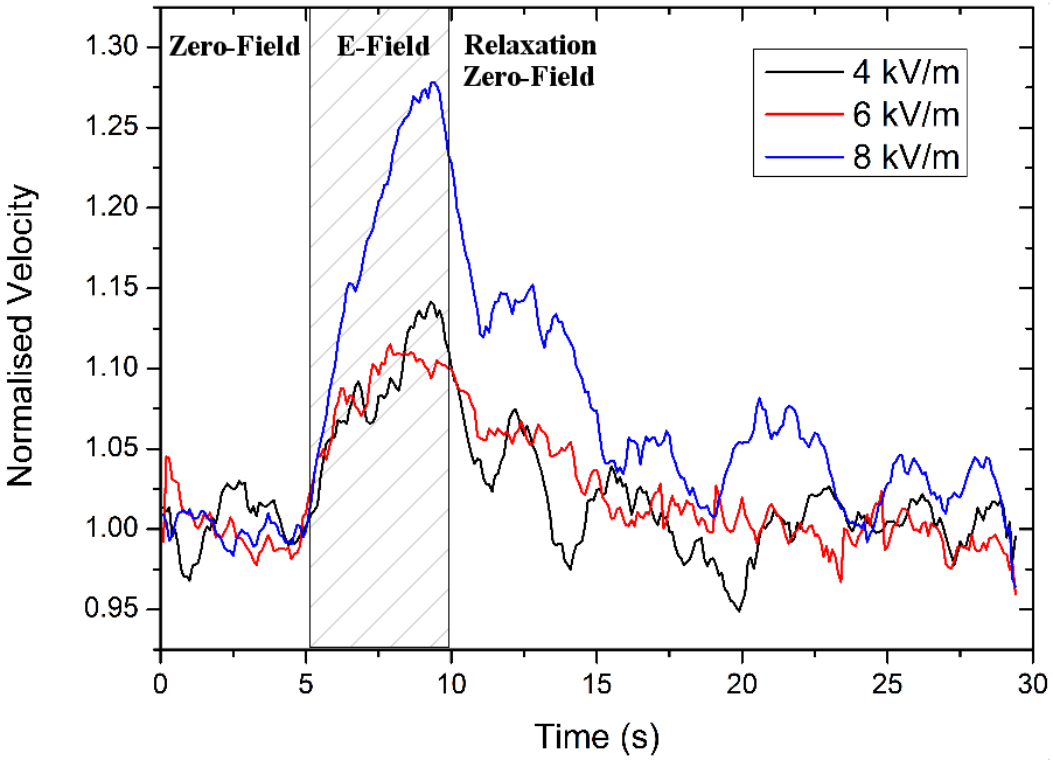

Figure.6.4. The graphs show the average velocity of filament movement during the course of the experiment on nitrocellulose when a field of 4 kV/m, 6 kV/m and 8 kV/m is applied. Labels on graph show when the field is applied and when zero field is present. Each experiment was repeated 3 times with 10 filaments tracked on each sample.

As seen in as seen in Figure 6.4, the results show a rapid acceleration of the actin filaments once the field is applied to the sample. Upon termination of the field the average velocity

decreases to return to that of 'normal' motility function. The time taken for the motility to return to the function seen before the application of a field is of significant interest as this gives further insight as to the motor protein arrangement on a given surface chemistry. As the field increases so does the maximum velocity reached during exposure. This in turn results in an increase in the time taken for accelerated actin filaments to return to their pre-exposed velocities. Different orientation of HMM on the surface will contribute to this decay time, with active HMM facilitating smooth gliding and so extending the period of deceleration. Conversely the obstruction of motility via extended HMM tails or the contribution of ATP insensitive or partially active HMM (the state at which one head is still available for filament interaction) will decrease this decay time.

This is evidenced in Figure 6.4. The area of the peak increases as a higher field is used to accelerate the actin filaments showing the increase in velocity and the greater decay time. Also, as seen in the previous chapter, the maximum velocity reached during the application of the field increase with increasing field strength.

Table.6.1. Table shows significant statistics on the behaviour of the actin filaments during the deceleration study on NC. Standard deviation for the average velocities is presented in brackets.[(1)] Data represents the tracking of 30 filaments over 3 samples.

	4 kV/m	6 kV/m	8 kV/m
Average velocity before exposure to field (μm/s)	6.3 (0.1)	7.5 (0.1)	7.9 (0.1)
Average velocity reached during exposure (μm/s)	6.8 (0.2)	8.1 (0.2)	9.4 (0.7)
Average velocity in final 5 seconds of capture (μm/s)	6.3 (0.3)	7.4 (0.3)	8.1 (0.4)
Time taken to return to pre-exposure range (within standard deviation of initial velocity)(s)	4.0	7.5	9.5

(1) Errors discussed in section 6.2.6

6.2.4 TMCS deceleration study

As detailed above the inclusion of TMCS is useful in this study as a direct parallel to NC as both have similarities in hydrophobicity and charge but differ in their structural composition.

In the previous chapter and indeed in many actin myosin studies, TMCS has shown to perform well as a substrate for HMM immobilisation while retaining motor function.[8] This substrate will therefore be used in this study to highlight how the motility reacts to the experimental conditions when using a high performance surface.

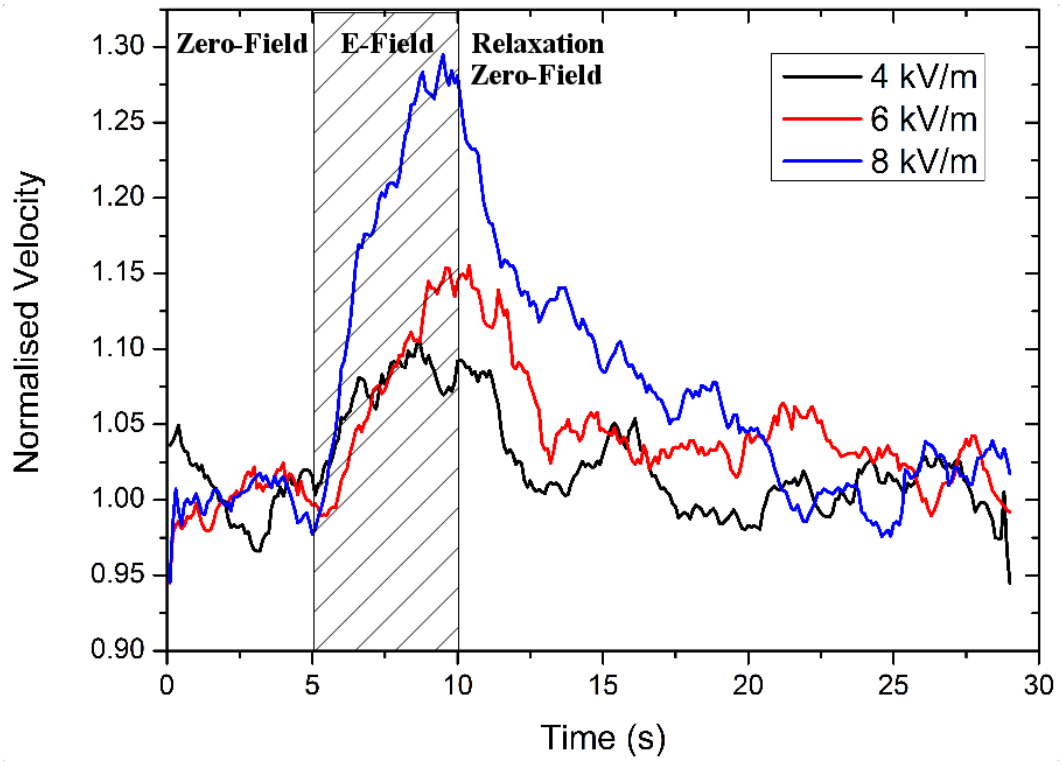

Figure.6.5. The graphs show the average velocity of filament movement during the course of the experiment on TMCS when a field of 4 kV/m, 6 kV/m and 8 kV/m is applied. Labels on graph show when the field is applied and when zero field is present. Each experiment was repeated 3 times with 10 filaments tracked on each sample, data shown is a average of these.

The initial velocity observed on TMCS at 4 kV/m (Figure 6.5) higher (~8 µm/s) than those seen on other samples. This result highlights the wide range of function that can be exhibited on any two samples. Referring back to chapter 5 we can see a relatively high velocity exhibited on PMMA when no field is applied (~8 µm/s), yet the surface clearly exhibits poorer motility characteristics then both NC and TMCS. It is important therefore that the

values of velocity themselves are not taken as the absolute measure of the performance of a given surface chemistry. This is perhaps the best argument in terms of validating the studies in both chapters 5 and 6, where it is the response of the motility function to external forces that is analysed. As seen on NC, the area of the peak signifies the acceleration of the actin filaments as the field is applied and upon termination a gradual return to velocities seen pre-exposure. The widths of the peaks after the point of termination indicate that the deceleration of the filaments is slow on TMCS at 4, 6 and 8 kV/m, see Table 6.2 for values. This type of behaviour implies that the motility of the actin filaments is unhindered on this surface, which further supports the hypothesis that this surface preferentially supports tail immobilised HMM and therefore unhindered smooth gliding motility. The density of active HMM motors on the surface would seem to positively contribute to the movement of the actin even after the external force is no longer applied.

Table.6.2. Table shows significant statistics on the behaviour of the actin filaments during the deceleration study on TMCS. Standard deviation for the average velocities are presented in brackets.(1) Data represents the tracking of 30 filaments over 3 samples.

	4 kV/m	6 kV/m	8 kV/m
Average velocity before exposure to field(μm/s)	8.0 (0.2)	8.2 (0.1)	7.9 (0.1)
Average velocity reached during exposure (μm/s)	8.6 (0.2)	8.8 (0.4)	9.4 (0.8)
Average velocity in final 5 seconds of capture (μm/s)	8.1 (0.4)	8.3 (0.4)	8.1 (0.5)
Time taken to return to pre-exposure range (within standard deviation of initial velocity)(s)	3.6	9.5	11.1

(1) Errors discussed in section 6.2.6

6.2.5 PMMA deceleration study

PMMA is a rigid substrate comparable in these terms to TMCS. Like TMCS the water absorption of PMMA will be minimal and the topography of the surface is expected to be flat and largely featureless. The hydrophobicity and charge characteristics of this surface,

however, are much different to both NC and TMCS. PMMA is relatively hydrophilic in comparison to the two previous surfaces.

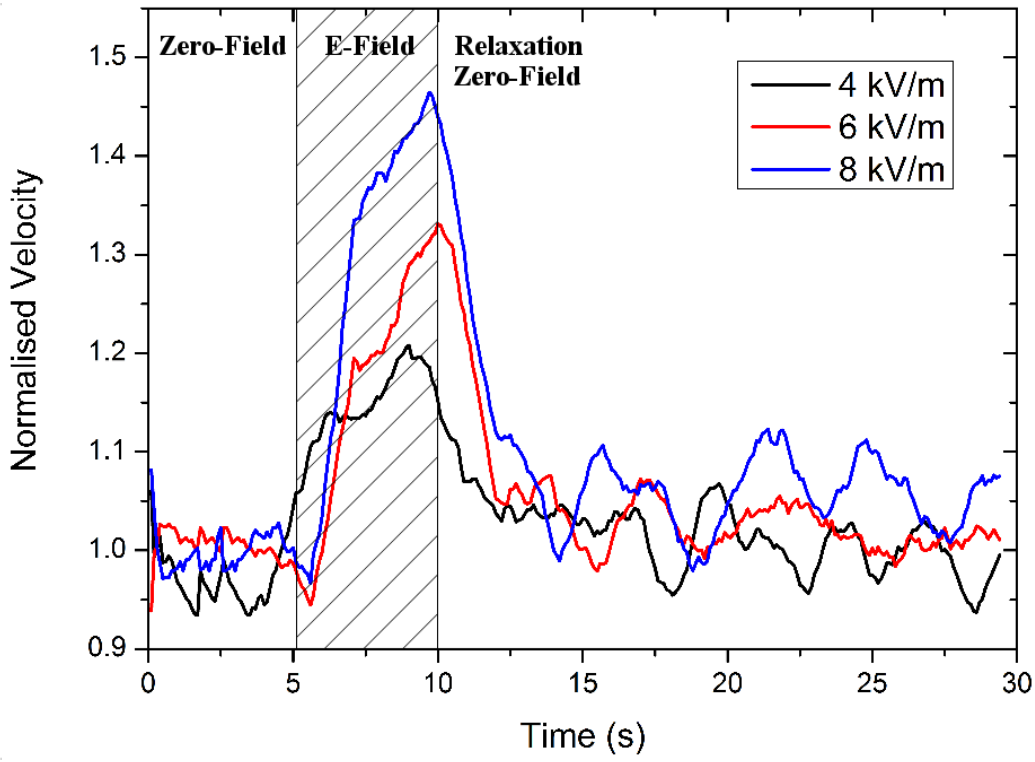

Figure.6.6. The graphs show the average velocity of filament movement during the course of the experiment on PMMA when a field of 4 kV/m, 6 kV/m and 8 kV/m is applied. Labels on graph show when the field is applied and when zero field is present. Each experiment was repeated 3 times with 10 filaments tracked on each sample, data shown is a average of these.

In line with the previous two surfaces the application of a field results in a quick acceleration of the filaments. Once the field is terminated the filaments on the PMMA samples quickly returned to an average velocity of movement seen before the field had been applied. This relationship was present at all three field strengths and indicates that there is a significant amount of hindrance to motility on these samples. The average velocity increase during the acceleration phase was also much less than has been observed in the other two samples. Interestingly, as can be seen in Table 6.3 and later in Figure 6.13, the time taken for the

filaments to return to ‘normal’ velocity does not follow the same relationship as the previous two surfaces. Where the increase in field strength on both NC and TMCS had resulted in an increase in this ‘deceleration’ time, in the case of PMMA at both 6 kV/m and 8 kV/m display similar deceleration phases, with the stronger field taken slightly less time to return to ‘normal’ function. This again would indicate that there is a high level of hindrance to smooth gliding motility on PMMA.

Table.6.3. Table shows significant statistics on the behaviour of the actin filaments during the deceleration study on PMMA. Standard deviation for the average velocities are presented in brackets.(1) Data represents the tracking of 30 filaments over 3 samples.

	4 kV/m	6 kV/m	8 kV/m
Average velocity before exposure to field (μm/s)	5.3 (0.2)	4.6 (0.1)	4.6 (0.1)
Average velocity reached during exposure (μm/s)	6.0 (0.2)	5.8 (0.3)	6.3 (0.4)
Average velocity in final 5 seconds of capture (μm/s)	5.3 (0.3)	4.7(0.3)	4.8 (0.3)
Time taken to return to pre-exposure range (within standard deviation of intial velocity) (s)	3.0	4.5	4.0

(1) Errors discussed in section 6.2.6

6.2.6 Discussion of errors in deceleration study

The data presented in the graphs of the deceleration study (Figures 6.4-6) show a more sporadic motility function after application of a field. This is highlighted by the increase of standard deviation from the initial average velocity, pre exposure to an electrical field, to the standard deviation of average velocity in the final 5 seconds of capture; this is shown in Tables 6.1-3. A possible cause for this behaviour is the use of blocking actin within the deceleration study. The gliding assay procedure includes the use of unlabelled filaments to block off inactive HMM. These unlabelled filaments, however, will still be affected by the field. Once the blocking actin is applied, a solution containing ATP is applied to the cell to allow these filaments to move around the surface with the intention of blocking off any

inactive HMM that the unlabelled filaments come in contact with. Once this assay solution is flushed from the system, labelled actin is applied and these are then less likely to come into contact with inactive HMM as it is presumed that the vast majority of these will be attached to unlabelled filaments. This is true for a conventional gliding assay experiments, however, in the deceleration study all the filaments, both labelled and unlabelled, are influenced by the field. This creates an issue. Prior to the application of the field the system is set up to facilitate smooth gliding motility, hence low standard deviation exhibited. Once a field is applied this system of blocked inactive HMM is essentially broken. Supplied with a sufficient force, filaments attached to inactive HMM may become motile once more leaving the inactive motor head available for binding. This will obviously create barriers to the unhindered gliding of the labelled filaments as the inactive HMM is essentially no longer blocked. The resulting motility function seen after the termination of the electrical field is therefore more sporadic, as not only are there a higher density of free inactive HMM present than there was at the beginning, there is also now a larger number of moving filaments present as the unlabelled filaments that were dislodged by the field which are now motile. If the video capture were to go beyond the 30 seconds used in this study it is thought that there would be a general 'relaxation' of the system were this sporadic motility may return to that seen pre exposure to the field.

6.3 The effect of blocking actin on the motility of actin filaments in the presence of an electrical field

In addition to the deceleration study, the experimental procedure detailed in chapter 5 was repeated for the three surfaces used in this chapter (NC, PMMA, TMCS) at electrical field strengths of 0, 4, 6 and 8 kV/m. At each field the motility assays were performed with and without the use of blocking actin. The use of blocking actin in the motility assay procedure is specifically designed to block inactive myosin heads, specifically motor domains that have

retained the ability to attach to actin but not to propel the filaments. These motor heads would inhibit motility in the gliding assay. Repeating the procedure for these surfaces to investigate the significance of the blocking actin allows the elucidation of several motility properties caused by the different protein adsorption characteristics of the surfaces used. Firstly it will give an insight into the density of inactive heads on a given surface. The effect of crowding, or number of obstacles to motility, can also be investigated by this study. Overcrowding will be exhibited in two forms. The additional filaments present on the surface when blocking actin is used, even when moving, will result in a larger potential of filament collisions. Blocking filament trapped by inactive heads will also create in inhibiting effect particularly when blocking actin is used on a surface that has a high density of inactive motor heads. Finally this study will allow the assessment of whether or not blocking actin is required in gliding assays utilising these surface chemistries and the changes in motility function when it is excluding.

6.3.1 The influence of blocking actin on NC motility function

As seen in Figure 6.7 the same relationship found between velocity and field strength, shown in chapter 5, is present. As the field strength increases, so does the average velocity of filaments in both the motility assays that contain blocking actin and the assay performed in the absence of the unlabelled actin filaments at an average of around 3 μm/s.

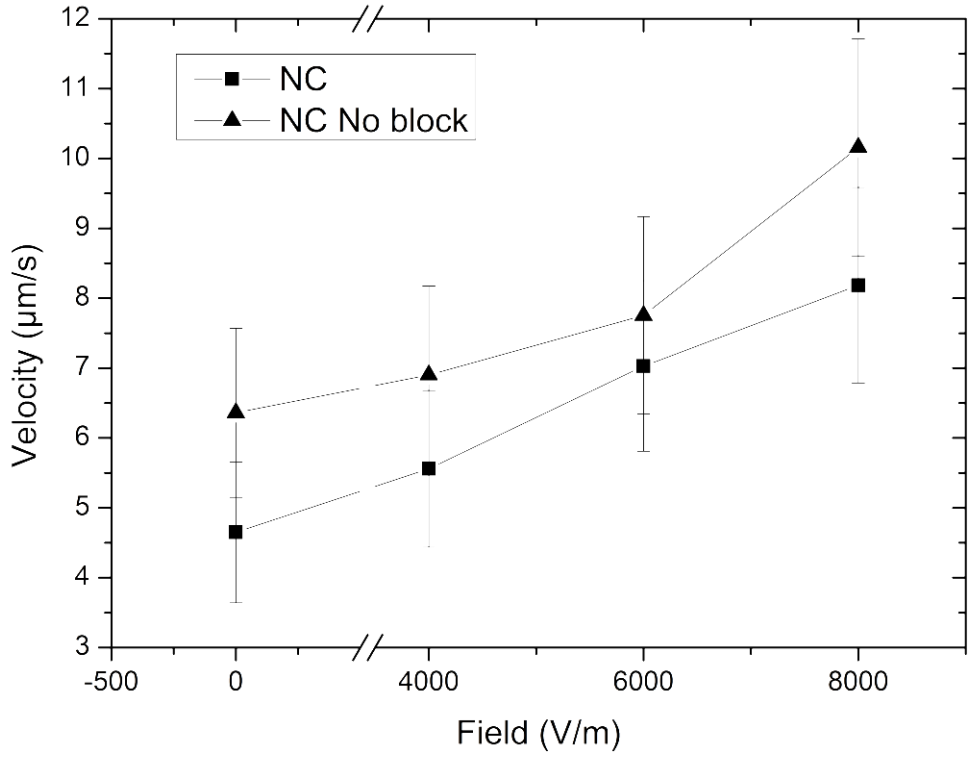

Figure.6.7. The graph shows the velocity of actin filaments when exposed to an electrical field on NC. Each line represents assays done with the inclusion of blocking actin (squares) and when the motility assay was run in the absence of blocking actin (triangles). Each data point is an average of 25 filaments movement over 3 samples.

The motility assays that were performed without the addition of blocking actin resulted in those filaments that were fully motile displaying consistently higher velocity than samples where blocking actin was present. The difference in the velocity of the two samples types remains relatively consistent through all of the fields tested, around 1.5 – 2 µm/s. This supports the hypothesis that the additional filaments present an obstacle to motility (presented in chapter 5 and discussed in section 6.2.8 of this chapter). The inclusion of blocking actin is specifically designed to block any ATP inactive HMM. As can be seen in Table 6.4 the percentage of motile filaments is larger on the samples treated with blocking actin. This clearly shows that, when used, the blocking actin is doing its required job of blocking the sites that are occupied by ATP inactive HMM. Where the samples are without

blocking actin the labelled filaments are exposed to a higher proportion of HMM that will attach to the filaments but are unable to propel them.

Table.6.4. Statistics on the percentage of actin filaments for the samples with and without blocking actin on NC at the tested electrical field strengths. Data represents the tracking of 25 filaments over 3 samples.

	Percentage of motile filaments			
Field (kV/m)	0	4	6	8
NC	87.5	86.5	89	84.9
NC No block	69.6	75.7	79.5	84.4

The relationship between the field strength and the percentage of motile filaments continues here as previously seen in Table 5.7 in chapter 5. Interestingly, upon exposure to the 8 kV/m field the percentage of motile filaments on both samples is comparable. This could be an indication of the upper percentile of motile filaments that one could hope to achieve on NC since both the blocking of ATP inactive HMM (in the blocked sample) and the reduction of crowding (in the non blocked samples) results in very similar ratios of motile and non motile filaments.

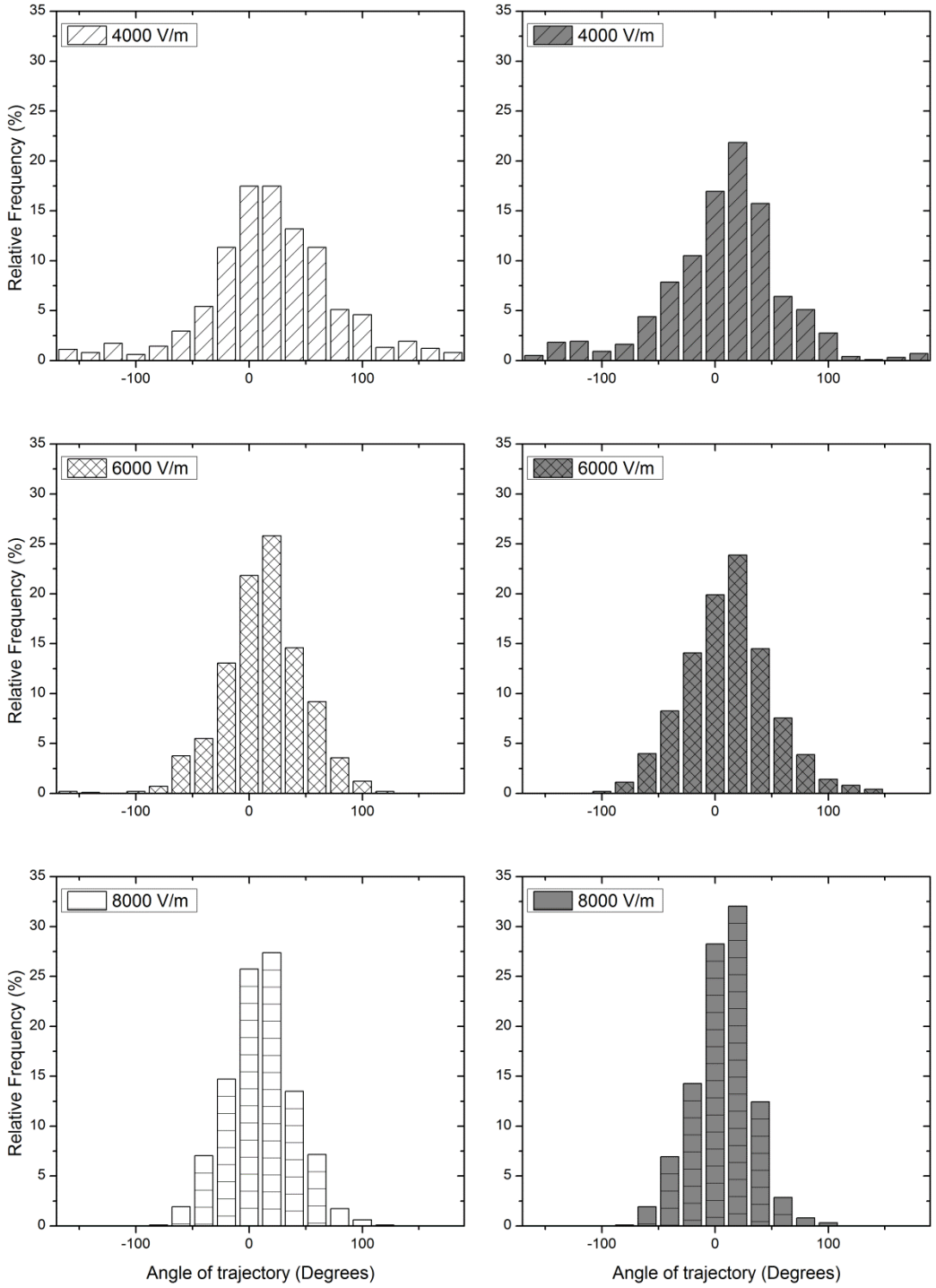

Figure.6.8. The graphs show the angle of trajectory of filaments when an electrical field is applied to an assay made with a NC surface. The white bars show the samples that include blocking actin while the grey bars are samples run without blocking actin. 0 degrees represents the position of the positive electrode. Each graph represents the tracking of 25 filaments over 3 samples.

Figure 6.8 shows the difference in the guidance of the actin filaments across the fields when the samples were tested with and without blocking actin. The general trend is for a slight increase in the proportion of actin filament movements towards the positive electrode on samples that did not have blocking actin applied to them. This is due to the reduction in total filaments present on the surface, both fully motile and non-motile. The result is an overall reduction in possible collisions a motile filament experiences which would divert the filament off its course. The difference between the blocked and unblocked samples is relatively minor indicating that the motile filaments are still being obstructed by obstacles other than unlabelled filaments. As discussed in chapter 5 these could include HMM tails, other filaments, either moving or stationary, and any dual protein layers formed when the motors are adsorbed to the surface. Another factor that will impact upon filament trajectory and potentially move them off course is the planar placement of active HMM. While the reasonably flexible HMM tails will allow room for movement, the direction in which the motor is facing will to some extent dictate the direction of propulsion.

6.3.2 The influence of blocking actin on TMCS motility function

Motility assays run in the absence of blocking actin showed an average velocity that was slightly above that of samples that had blocking actin applied in the assay procedure, consistently around 0.5 μm/s. The TMCS samples displayed very similar characteristics that were seen in previous experiments, albeit with a higher velocity seen in the absence of an electrical field. The difference between the blocked and unblocked samples are, however, very small, indicating that the number of ATP inactive HMM present on the surface is very low. In the case of the unblocked samples, it is evident that there are few inactive motors that hinder the motility and conversely, in the samples where the blocking actin has been added to the assay, crowding is minimal as the initial filaments added are not trapped on inactive motors and thus do not hinder the movement of fully motile filaments.

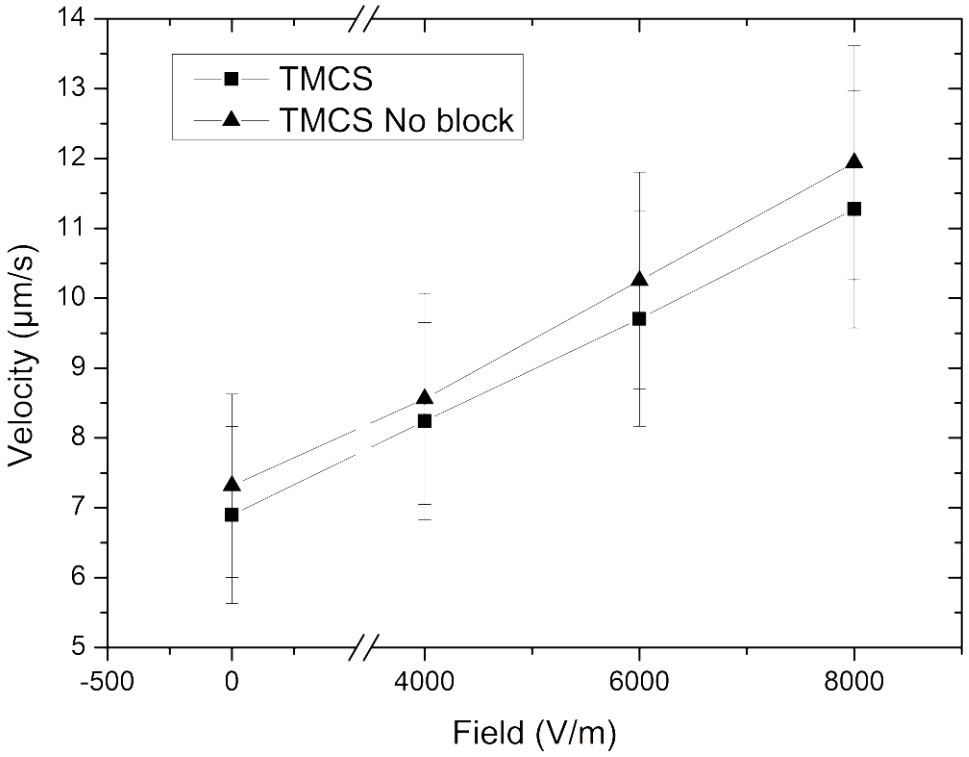

Figure.6.9. The graph shows the velocity of actin filaments when exposed to an electrical field on TMCS. Each line represents assays done with the inclusion of blocking actin (squares) and when the motility assay was run in the absence of blocking actin (triangles). Each data point is an average of 25 filaments movement over 3 samples.

As Table 6.5 shows, the percentage of motile filaments on both sets of samples are comparably high at all fields. This indicates that the density of ATP inactive HMM on TMCS is very low. At 8 kV/m TMCS displays a very high percentage of motile filaments on both sets of samples. As seen in the previous chapter, the percentage of motile filaments increases with the increasing strength of the electrical field.

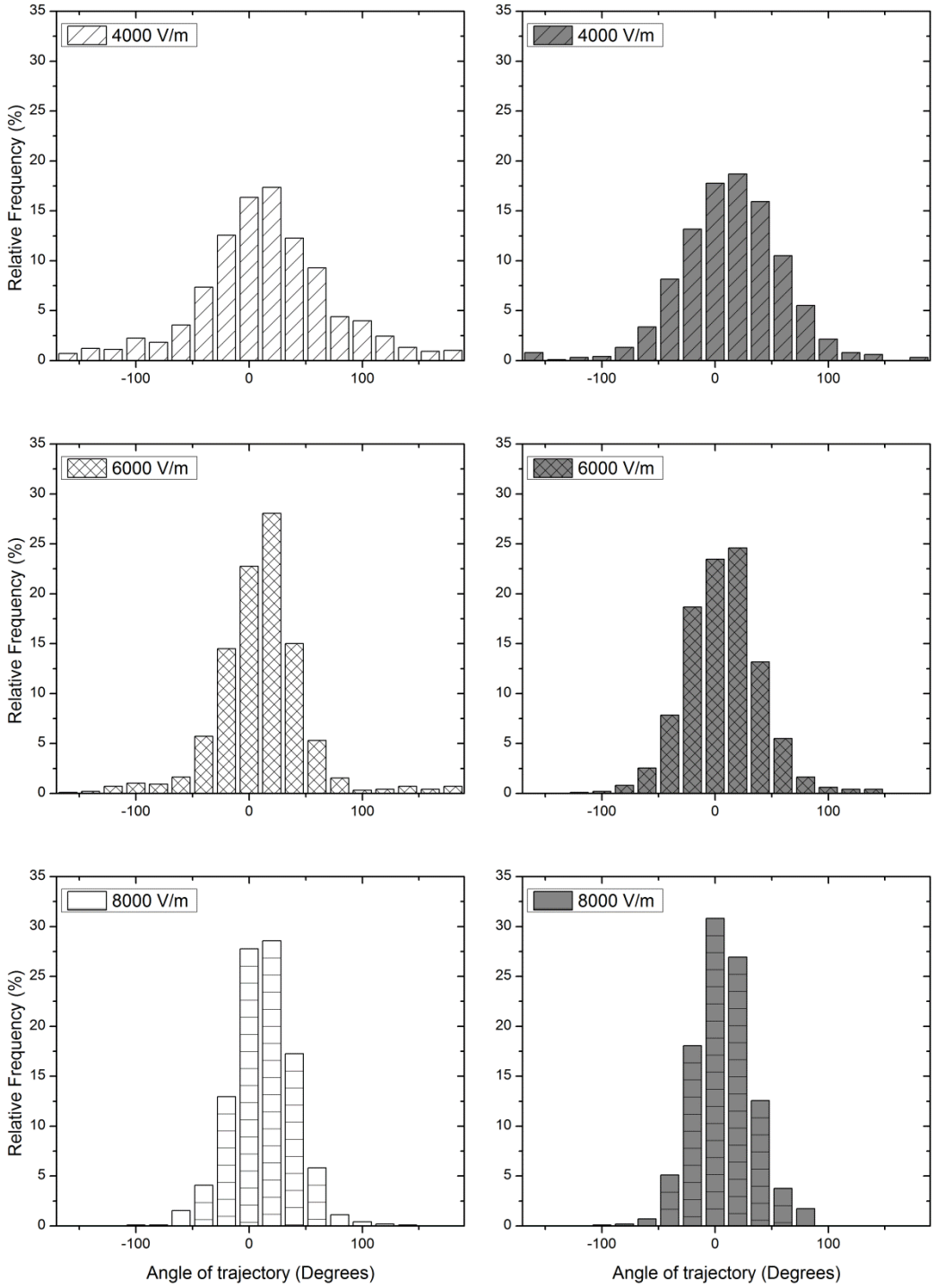

Figure.6.10. The graphs show the angle of trajectory of filaments when an electrical field is applied to an assay made with a TMCS surface. The white bars show the samples that inclusive of blocking actin while the grey bars are samples run without blocking actin. 0 degrees represents the position of the positive electrode. Each graph represents the tracking of 25 filaments over 3 samples.

As show in Figure 6.10 the difference in the angle of trajectory of filaments between samples that had blocking actin present and those that didn't is marginal and no clear relationship can be seen between them on TMCS. This would indicate that in both cases the movement of filaments is comparable and shows a very low density of motors that are required to be blocked. The fact that both sets of samples perform in much the same way points towards a protein layer that has retained much of its function upon adsorption and that there are few obstacles that would divert the filaments off track. Interestingly, the increased number of filaments on the blocked samples does not seem to have had much of an effect in causing crowding and filament – filament collisions that would divert movement away from the direction of the field. This again would point to a high density of fully active HMM, if both sets of filaments, unlabelled and labelled, are fully motile, then the collisions that occur are less likely to take the filament off course as both populations will be moving with the field.

Table.6.5. The percentage of actin filaments for the samples with and without blocking actin on TMCS at the tested electrical field strengths. Data represents the tracking of 25 filaments over 3 samples.

	Percentage of motile filaments			
Field (V/m)	**0**	**4000**	**6000**	**8000**
TMCS	78.8	87.9	93.1	92.6
TMCS No block	80.7	85.5	85.2	90.1

6.3.3 The influence of blocking actin on PMMA motility function

Although the velocity of the filaments on these samples is much higher than that seen in the previous experiment in chapter 5, the proportional increase in velocity from 0 – 8 kV/m is almost identical. This again highlights the value of the electrical motility device in testing the protein binding mechanism on different surface chemistries. Previous studies have

presented statistics to show the motility characteristics observed on a single set of samples on multiple surface chemistries.[9] However, as can be evidenced by the large amount of papers that have studied myosin on various different surfaces, the velocities on any one surface chemistry can be slightly different from sample to sample.[10-13] Imagine for a moment that this study had only taken the characteristics from motility without the effect of a field. In the previous chapter the average velocity of filaments in the absence of a field for PMMA was around 8 μm/s where as TMCS showed an average filament velocity of around 4.5 μm/s at 0 V/m. Taking this statistic alone one might be inclined to think that the PMMA is outperforming the TMCS in terms of protein binding characteristics that favour retaining full motor protein function. However, if we add an external force into the equation, in this instance an electrical field, we can now analyse how the protein layer reacts to this force by studying the effect on filament motion. The statistics then start to give a very different picture to the binding characteristics of the different surface chemistries, one that would not have been possible to come to without significantly increasing the number of samples, experiments and data collected in the absence of this variable.

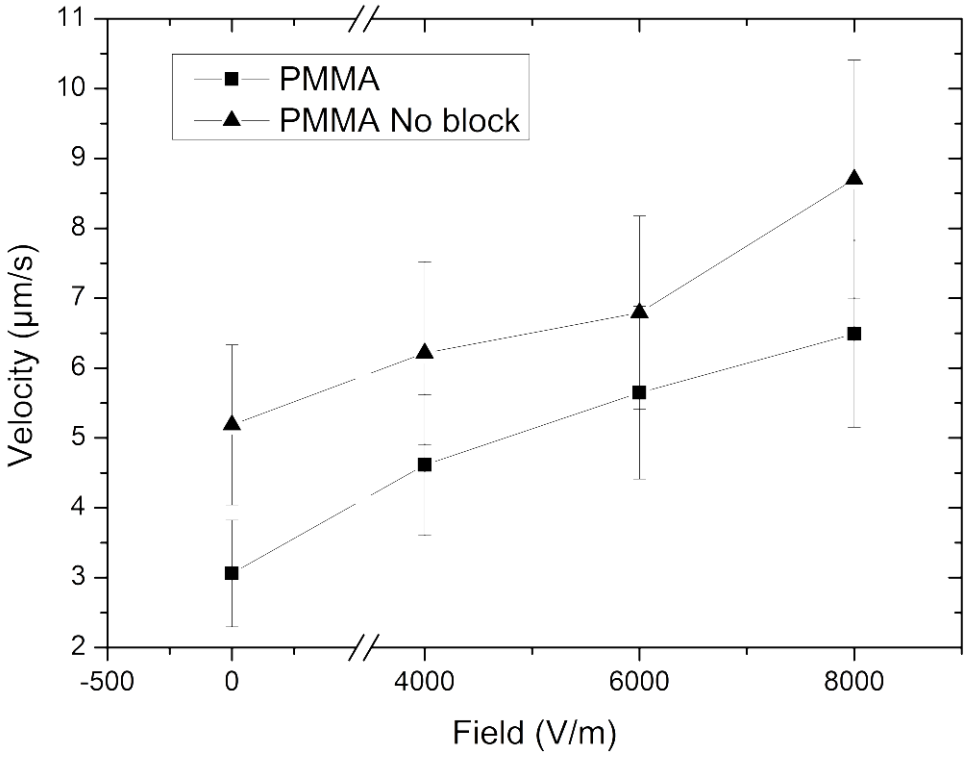

Figure.6.11. The graph shows the velocity of actin filaments when exposed to an electrical field on PMMA. Each line represents assays done with the inclusion of blocking actin (squares) and when the motility assay was run in the absence of blocking actin (triangles). Each data point is an average of 25 filaments movement over 3 samples.

Table 6.6 shows that there is a modest density of ATP inactive HMM bound to the surface. This is shown in the samples that were performed in the absence of blocking actin, as even at 8 kV/m, the percentage of motile filaments is below 80%, which is below that of the other surfaces. The small increase in the percentage of motile filaments, in the case of the assays not treated with blocking actin, would suggest that there is still a significant enough density of inactive motors anchoring the filaments to the surface that even a high field, large force, cannot dislodge them.

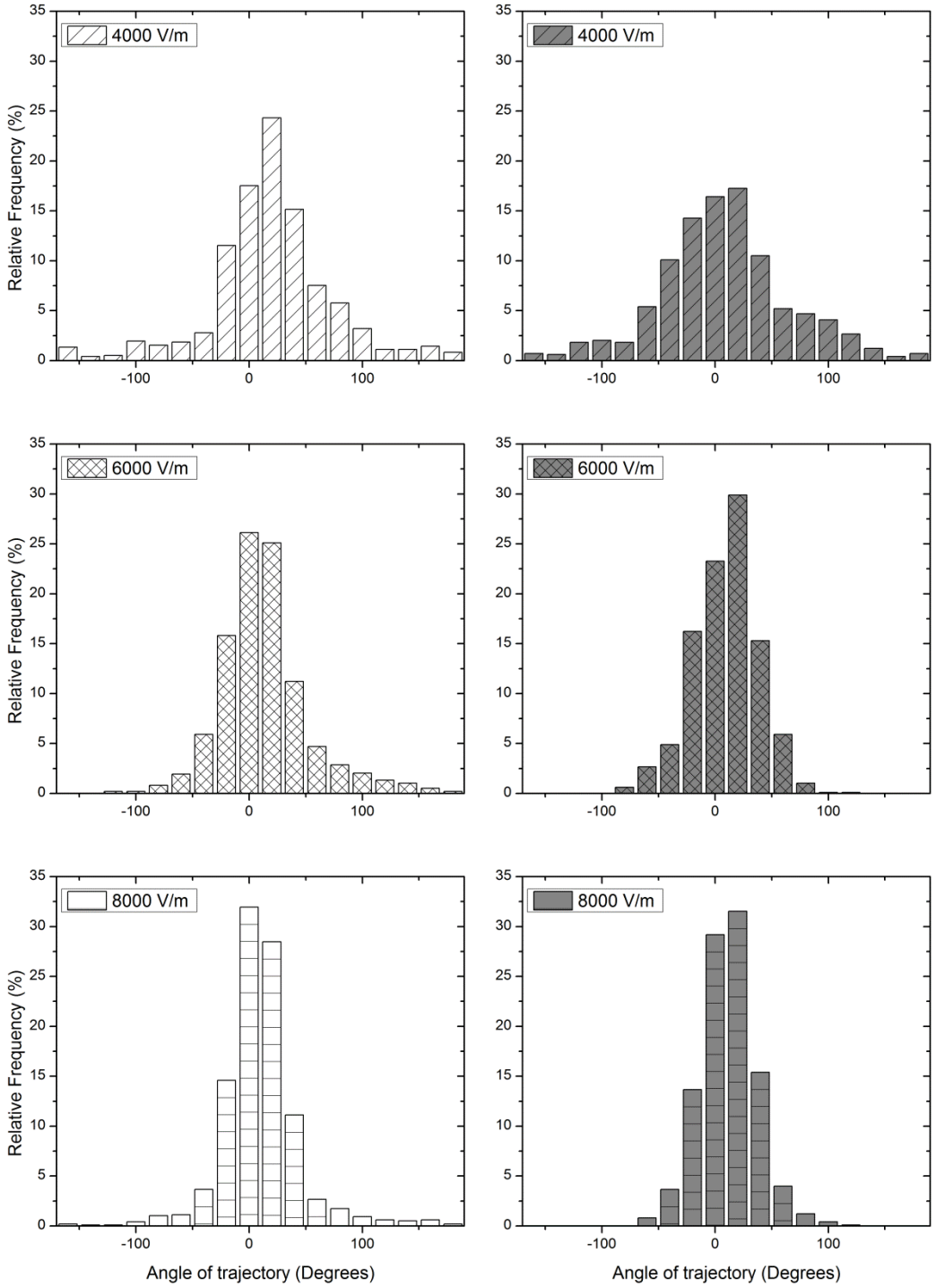

Figure.6.12. The graphs show the angle of trajectory of filaments when an electrical field is applied to an assay made with a PMMA surface. The white bars show the samples that inclusive of blocking actin while the grey bars are samples run without blocking actin. 0 degrees represents the position of the positive electrode. Each graph represents the tracking of 25 filaments over 3 samples.

Both sets of samples, both blocked and unblocked, have similar directionality characteristics presented in Figure 6.12 showing the angle of trajectory of filament movements. A slight difference is seen, with an increase in the percentage of filament movements towards to the positive electrode evident on the non-blocked samples compared with the blocked samples at the same fields. Couple this relationship with the low increase in velocity seen from 0 – 8 kV/m and the speed at which the filaments returned back to their original velocity in the 'deceleration' study, the protein layer on PMMA seems to have a large number of HMM bound to the surface that are unable to propel the filaments. These could be a number of orientations that either trap filaments, as is the case with ATP inactive HMM, or simply block the path of a filament which could result in either diversion or termination of movement.

As the field was increased to 8 kV/m on the samples that had been treated with blocking actin, the percentage of motile filaments is relatively high (not all that far from TMCS). This would indicate that while there is a large portion of ATP inactive HMM bound to the surface, these are being blocked by the unlabelled actin filaments. Once this has been achieved the obstacle of the extra bound non motile filaments hinder the motility function less than the presence of unblocked ATP inactive HMM. In this case the motile filaments only deal with the crowding caused by the extra filaments on the surface, which at 8 kV/m would seem to have been overcome by the force of the field. Therefore it seems that filaments that are trapped or lodged by overcrowding of the protein layer become dislodged much more easily than those trapped at inactive motor sites.

Table.6.6. The percentage of actin filaments for the samples with and without blocking actin on PMMA at the tested electrical field strengths. Data represents the tracking of 25 filaments over 3 samples.

	Percentage of motile filaments			
Field (V/m)	0	4000	6000	8000
PMMA	85.5	88.7	86.8	88.8
PMMA No block	72.9	72.2	78.8	79.6

6.4 Investigation of protein adsorption and resulting motility function

Figure 6.13 shows the relationship between the three surfaces in terms of the time taken for the filaments to decay from the velocity reached during exposure to a field to the velocity exhibited before the field was applied. At 4000 V/m all three surfaces were comparable but as the strength of the field was increased the difference in the deceleration of filaments is dramatic. This is seen as a clear indication of the degree of hindrance there is to motility on each surface and in turn gives an insight into the functionality of the protein layer that is present on each of the surfaces. At both 6 and 8 kV/m the motility on TMCS is slower to return to its original state than the other two surfaces, exhibiting a surface that has HMM motors adsorbed to the surface in an orientation that retains much of the function of the protein. What can also be learned from this data is that TMCS has minimal obstacles to motility. This points to a low density of head bound HMM along with a protein layer which remains relatively clear of trapped filaments, allowing the free movement of the actin filaments across the bound motors.

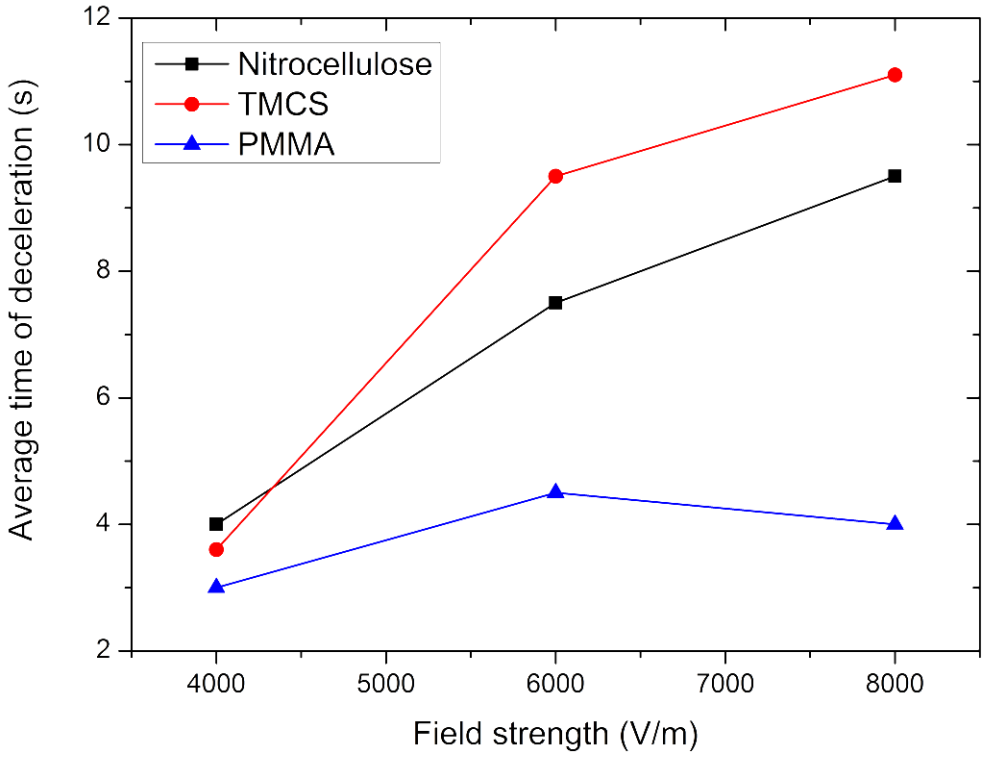

Figure.6.13. The graph shows the average time taken for the velocity of the actin filaments to decrease from the maximum velocity exhibited during exposure to the field, to within the standard deviation of the average velocity of pre-exposed motility on each sample. Each data point is an average of 3 samples representing a total of 30 filaments movement each.

In the case of both NC and PMMA, much less time is required for the filaments to slow down to the initial velocity once the field had been terminated. For NC the difference in this time at 6 and 8 kV/m is around 2 seconds. The variation in these two surfaces has been echoed in all of the assessments made of the protein layer using the electrical motility device. While NC has been used extensively as a viable surface for *in vitro* motility assays there is evidence that the motor protein binding of this surface chemistry is by no means perfect. The results are consistent with a surface that has a number of motors bound to the surface that are unable to facilitate motility. With an increase of the density of non propelling motors also comes an increase in the potential for crowding and in turn hindrance of motility caused by the trapping of filaments and the accumulation of obstacles to the path

of a given filament. However, it must be pointed out that while the difference is significant the surface does produce high quality motility with low density of non-motile filaments in comparison to other surfaces used here and elsewhere. Figure 6.14 shows that while the averaged velocity of filaments during exposure is lower than that seen on TMCS, it still exceeds that of PMMA and shows a smooth increase as the field strength rises.

The motility characteristics exhibited on PMMA indicate a protein layer bound to the surface that while able to support motility also contributes significant hindrance to the translocation of filaments. The rapid decrease in velocity upon termination of the field is a clear indication of not only a lower density of fully active HMM, but also evidence that there are orientations of motor proteins bound that actively hinder motility. This can also be seen in Figure 6.14 where the average velocity reached during application of the field is low when compared to the other two and does not follow the same trend as seen on NC and TMCS. These are thought to be head bound HMM and potentially dual protein layers forming due to further motors interacting with this head bound HMM (see Figure 6.15 C). This may occur due to the different charges held at the head and tail of the HMM along with the amphiphilic nature of the protein. While tail bound HMM would have a positively charged head region available for interaction with actin filaments the head bound HMM would result in tails protruding above this layer. The negatively charged tail region may well interact with other incoming HMM or surrounding HMM in such a fashion that either creates the opportunity to bind further HMM to a position already occupied by a motor protein, i.e. a dual protein layer, or perhaps interfere with the functioning of surrounding tail bound HMM.

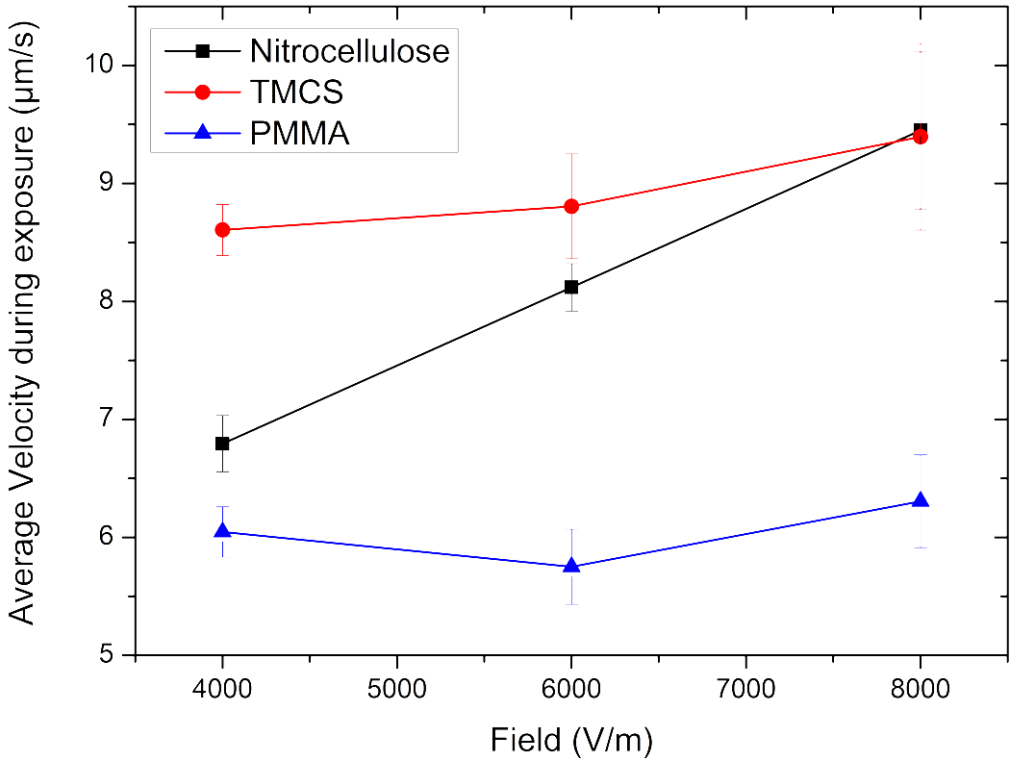

Figure.6.14. The graph shows the mean velocity exhibited while the motility is under the influence of the field. Note here the relatively small increase in velocity on TMCS when compared with the previous results. This is thought to be due to the average velocity at 4000 V/m already being at the upper limits of the maximum velocity that actin-myosin motility will exhibit in an *in vitro* motility assay.[4, 7, 14] Each data point is an average of 3 samples representing a total of 30 filaments movement each.

The angle of trajectory of a filament can be altered in a number of different ways, as highlighted by the results shown in the blocking actin study. Brownian motion will impact to some extent on the path of the head of the filament before the attachment to the next available motor. This becomes a less important factor as the field strength increases and the guidance of the head to the next available motor becomes dominated by the force applied by the field. Any obstacles in the path of the filament will be another important factor in determining its direction. A filament may be propelled against an obstacle such as a trapped

filament and forced to one side or another. As discussed, these can be caused by a variety of reasons, including motor tails (of head bound motors), other filaments and dual protein layers. All of these will cause a filament that comes in contact with them to either, divert its path, dissociate into solution (where attachment to further motors is made impossible), or become trapped, terminating the filament movement altogether. The direction in which the motor is facing will also affect the path taken by a filament. The impact of this particular factor is highlighted when comparing the difference in angular trajectory of filaments on samples that were unblocked to samples inclusive of the unlabelled blocking actin. Even in the unblocked case where there are a dramatically reduced number of filaments present and therefore a significant drop in potential obstacles that a filament could come in contact with, the angular trajectories are comparable even at the highest field strength tested, across all three surfaces. This highlights two things; A, the orientation of active HMM is more important in influencing the motility function than simply the presence of ATP inactive HMM, in terms of velocity and trajectory, and that B, the direction in which the HMM is facing is a highly significant factor when considering the path of a filament even at high field strengths.

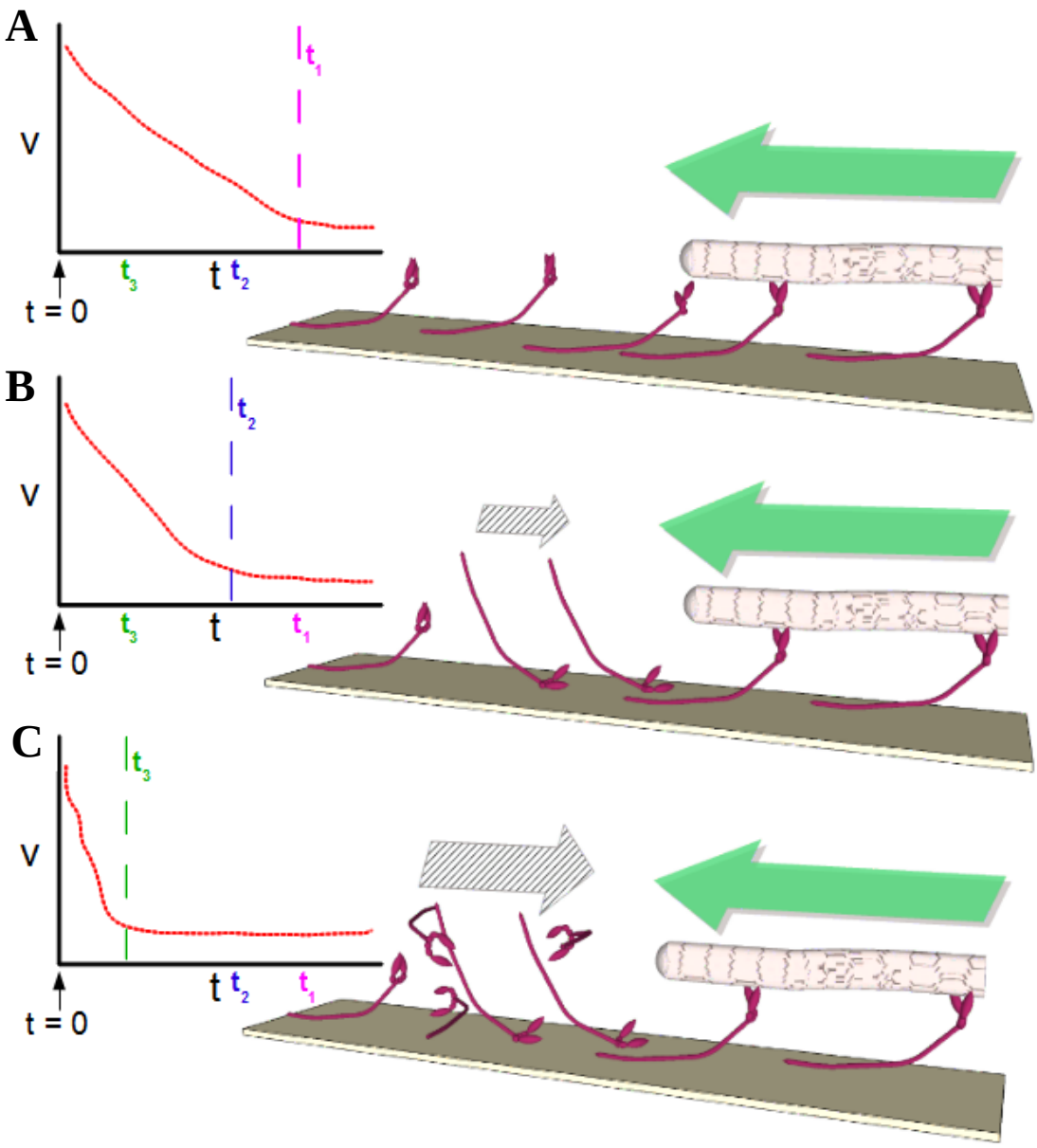

Figure.6.15. The scheme shows examples where different orientations of HMM can influence the rate at which accelerated filaments slow down after the electrical field is terminated. Inset to the right are idealised graphs showing the rate at which the velocity of filaments decreases due to the varying degrees of hindrance to motility. t = 0 represents the point at which the electrical field is terminated. A, This represents a surface with mostly tail bound motors that will facilitate smooth gliding. B, Surface which has some HMM bound in states such a head domain attachment will result in a decrease deceleration period due to the additional hindrances. C, Surfaces that have a preference to binding the motor at the positions that do not facilitate motility will significantly affect smooth gliding. After the termination of the field the filaments are expected to decrease in velocity sharply.

The results from the blocking actin study showed the significance of the blocking actin and the density of inactive HMM present on each surface. Gliding assays that were performed in the absence of blocking actin consistently produce motility with higher velocity than those experiments performed with the inclusion of blocking actin in the assay. This not only gives an indication of the density of ATP inactive HMM that is bound to each surface, but also shows the effect of crowding that occurs due to the additional filaments that are present on the protein layer when blocking actin is present. The number of ATP inactive HMM on the three surfaces in this study is low. This is evidenced by the high percentage of motile filaments (see Table 6.7) and also by the visually observed 'quality' of the motility seen on all the samples. Each sample tested showed varying degrees of fully functioning motility even at low field strengths.

Table.6.7. The percentage of motile filament on both sets of samples for all the surfaces at the fields tested. Data represents the tracking of 25 filaments over 3 samples for each surface.

	Percentage of motile filaments (%)			
field	**0**	**4000**	**6000**	**8000**
NC	87.5	86.5	89	84.9
NC No block	69.6	75.7	79.49	84.4
PMMA	85.5	88.7	86.8	88.8
PMMA No block	72.9	72.2	78.8	79.6
TMCS	78.8	87.9	93.1	92.6
TMCS No block	80.7	85.5	85.2	90.1

There is a clear relationship between the percentage of motile filaments when comparing the samples with blocking actin and the samples without. As can be seen in Table 6.7 a higher number of non-motile filaments was seen on samples where the blocking actin had not been applied to the assay. This is simply due to the fact that the labelled actin, on these samples, is more likely to encounter HMM that would bind to the filaments but is unable to propel the filaments. Interestingly there was a difference in this relationship between the surfaces;

TMCS clearly displays a higher percentage of motile filaments indicating a very low density of ATP inactive HMM. Conversely PMMA samples that were not blocked by unlabelled actin displayed motility characteristics that indicate a higher density of ATP inactive HMM with NC filling the mid range in this study. Important to note is that ATP inactive HMM is perhaps not the only factor in the equation that exacerbates the effect of crowding. That is to say that the blocking actin could also be interacting with other orientations of bound HMM which in turn is producing the motility function seen. For examples, in the previous chapter head bound HMM was hypothesised to be creating a barrier to unhindered motility. There may also be a situations, on surfaces that bind a high density of head bound HMM, where filaments are getting trapped in the areas where the tails of these head bound HMM are extending above the active HMM layer (see Figure 6.15). Therefore the relationship between the three surfaces tested, the inclusion or exclusion of blocking actin and the resulting velocity of motility is most probably a combination of the density of ATP inactive HMM on the surface and the density of head bound HMM on the surface. Both these types of HMM would hinder motility to varying degree. What is clear is that a surface which has a high density of fully functioning protein will display motility characteristics of unhindered motility as there is less chance of a filament experiencing slow down or complete termination of its movement due to either crowding, other filaments or HMM tails, or ATP inactive HMM.

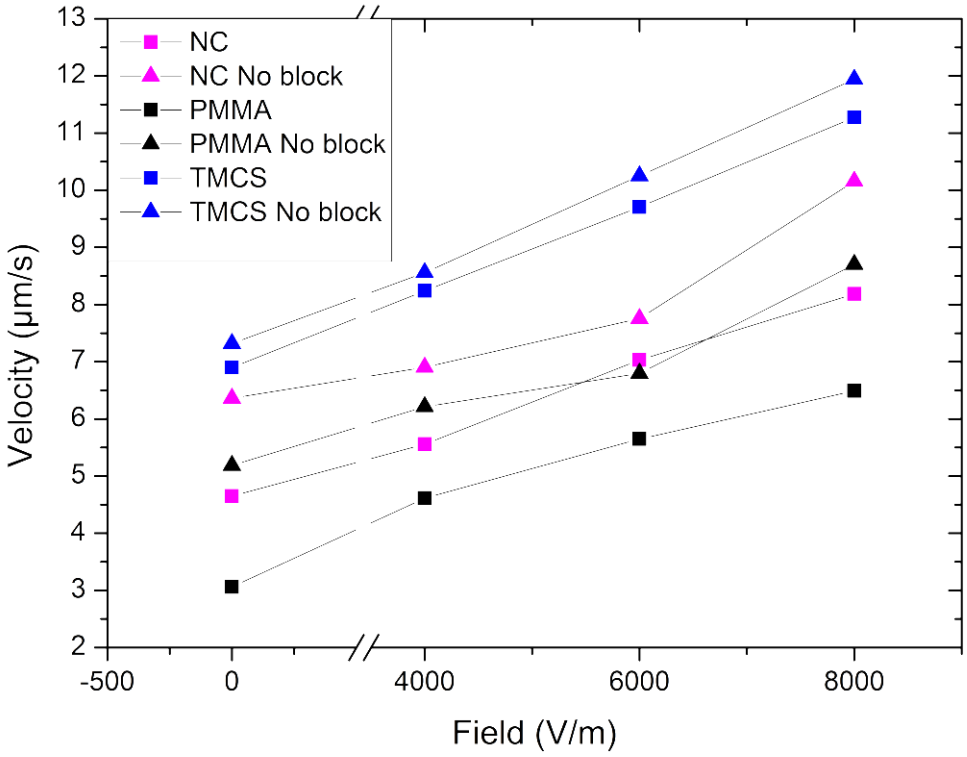

Figure.6.16. The graph shows the velocity of actin filaments on all three surfaces when an electrical field is applied to the motility assays. Each sample was tested with (squares) and without (triangles) the addition of blocking actin in the preliminary steps of the *in vitro* motility assay procedure. On each surface the addition of blocking actin to the procedure resulted in slower motility throughout all of the fields tested. The separation between the velocities on each individual surface is of particular interest as it indicates the number of sites that blocking actin will occupy when in use, and so cause crowding (a hindering of motility), and therefore the binding characteristics of each surface. Each data point is an average of 2 samples representing a total of 20 filaments movement each.

What is particularly interesting is the consistent difference in velocity between the blocked samples and non blocked samples on each of the surfaces. On TMCS the difference in velocity between these samples is very small (~0.5 µm/s), indicating a protein layer that has retained much of its function upon adsorption. PMMA however, has a consistent velocity difference of around 2.5 µm/s, which would suggest an adsorbed protein layer that has a high number of motors bound in states that are unable to facilitate the movement of

filaments. NC exhibits a difference of 1.5 μm/s, which indicates that the surface binds a higher number of fully functioning HMM than exists on PMMA, but that there is still a significant density of motors present that cannot facilitate motility.

Another visually observed phenomenon was the clarity of images produced when the assay was run in the absence of blocking actin. This is thought to be due to crowding of filaments on the protein layer. When blocking actin is included in the assay there is a large percentage of unlabelled filaments that will not encounter a site at which its movement would be terminated, an ATP inactive HMM or an area of high density non functional HMM. This means that on these samples there will be a higher number of moving filaments on the protein layer. With an increase of moving objects there is an increase of obstacles for all filaments present. When filaments collide with each other they can do a number of things. If travelling at the same height they are likely to either 'bounce' off each other and be diverted on to separate roots, or become trapped. Another situation may also occur due to the unevenness in height of the protein layer. A surface made up of entirely fully functional HMM would not be uniform in height due to the slight non uniformity in the height of the surface the protein is bound to, but also due to slight variances in the motor proteins themselves due to the purification procedure of the protein when extracting it from the rabbit muscle (average height of head domain of an active HMM is around 38 nm).[2] This means that moving filaments may be travelling at slightly different heights. Baring in mind that f-actin is only ~10 nm in thickness a filament colliding with another that is perhaps bound to a HMM that is ever so slightly below that of the current track of the incoming filament may have the ability of moving over the lower filament while still retaining motility.[4] Both these types of interactions increase the possibility of filaments moving in and out of the focal plane during the course of an experiment, and the number of these interactions increases when a higher number of filaments, labelled or unlabelled, is present. This would explain why the images taken from samples that did not have blocking actin included in the assay

gave clearer images than those samples that had the unlabelled actin present and therefore a higher number of total filaments moving on the protein layer. This phenomenon is also seen to an extent when comparing images between surfaces. TMCS and PMMA, expected to create the flattest, most rigid surfaces in the study, did show marginally clearer images than NC. This is presumably again down to the slight height difference of the HMM bound to the more gel-like NC and so increasing the potential of filaments dropping out of the focal plane.

The increase in velocity from 0 to 8 kV/m was in agreement with those seen on the same surfaces in the experiments achieved in chapter 5, on both the unblocked and blocked samples. An increase of 4 – 5 μm/s on TMCS, 2.5 – 3 μm/s on NC and 2.5 μm/s on PMMA are very similar to those exhibited on samples in the previous chapter and this evidence highlights the value of the electrical motility study. By using an external tester, in this case a force applied by an electrical field, many of the problems caused by the statistical analysis of standard gliding assays of motility on surfaces can be overcome. When comparing the statistical data obtained from previous studies of myosin behaviour on different surfaces there is a level of discrepancy in the agreed performance of surfaces between papers. For example in some research papers PMMA is shown to produce reasonably high levels of functioning motility, a conclusion that is reached by the observed velocity of filaments moving on the surface.[9] In some cases it is stated that the PMMA surfaces outperforms NC. However, there are papers that show results that contradict these conclusions.[15] Couple this with the evidence shown by other groups using analytical techniques, such as QCM and total internal reflection fluorescence (TIRF), in particular a paper that probes the density and height of myosin layers on electronegative surfaces, and it becomes clear that there is significant value to a highly adaptive study such as the two shown in chapters 5 and 6 of this thesis.[2, 16]

This study is far from exhaustive and leaves room for further study of surface chemistries that allow the immobilisation of myosin. What is also important to point out at this stage is the nature of the discussion in these final two chapters. The analysis of each surface has been based around finding the 'best' possible surface for actin myosin motility i.e. which surface adsorbs a protein layer that retains its function and allows unhindered motility. However, when thinking about the potential uses of molecular motors in lab-on-chip technologies there may be some desire to have a surface that adsorbs a protein layer that slightly or even completely hinders motility. Indeed there may be device designs where varying degrees of motility are required across the chip and therefore there is the possibility to use multiple surface chemistries, each having different motility function.

6.5 Conclusion

The electrical motility device detailed in the last two chapters of this thesis has been used in three distinct ways for the characterisation of the adsorption properties of a number of surface chemistries. In previous papers where groups have outlined the behaviour of myosin motility on surfaces many have concentrated on the ATP inactive motors bound to the surface as being the primary factor in the resulting movement of filaments across the protein layer.[11, 17] Some hypothesise that certain surfaces may result in a higher density of these motor heads that bind to actin but do not facilitate filament motion. One only needs to look at the motility procedure used in this study, with the inclusion of blocking actin, as an indication of how important these motor heads are perceived to be, as this is a standard procedure used in a great many studies that utilise gliding assays. During the course of the last two chapters it has been suggested, and supported by a number of papers, that while certain surface properties may result in varying densities of ATP inactive HMM, this factor alone cannot explain the different motility function seen when using different surfaces in the *in vitro* motility assay.[2, 8, 18-20] The results from this chapter when comparing the motility

function of assays run without the inclusion of blocking actin highlights that while each surface may have slightly different densities of this particular type of bound HMM, the difference in these densities is very small pointing to other factors that are affecting motility function. Results from the 'deceleration' study carried out in this chapter, coupled with the blocking actin experiment backs the hypothesis that the orientation of the motors bound to the surface has the largest impact on the motility function. In particular, the density of head bound HMM seems to be an important factor in the movement of filaments across the protein layer. As detailed in a previous paper the HMM tails when bound to a surface via the head will extend beyond the heads of surrounding fully functional motors.[2] Other orientation of motors, such as motors bound by the tail and head, presumably unable to even interact with the actin, and any potential dual protein layers created by HMM interacting with already bound motors, will also affect the translocation of the filaments. However, what was made evident by the 'deceleration' study was the importance of obstacles and crowding of the protein layer in retaining full and unhindered motility. In chapter 5 TMCS exhibited motility characteristics that point to a protein layer that was retained all of the motors function. This would suggest a high density of HMM bound to the surface that can fully facilitate filament movement i.e. motors bound to the surface by the tail. In the 'deceleration' study this surface showed the slowest decay back to initial velocity of the three surfaces. Couple this with the results from the blocking actin study; TMCS seems to have HMM binding characteristics that favour supporting tail bound HMM producing a protein layer that retains much of its function. In turn we can learn from this that the resistance caused by these motors in response to the electrical field is relatively small. As the field is terminated in these experiments the velocity slowly decays back to its initial velocity, akin to a wooden board slowing down after being pushed over rollers. In the case of the other two surfaces we can see that an increase in bound HMM in orientations that hindered motility, such as extending tails, results in an increase in the resistance to the force applied

by the electrical field and so the decay from the maximum reached velocity back to the initial exhibited velocity is much quicker. Picture the same wooden board being pushed over the same set of rollers, but this time some of the rollers are broken and there are obstacles in the path of the board resulting in a much quicker deceleration.

What has been shown in the last two chapters of this thesis is a novel method of analysing the response of myosin motility to varying strengths of electrical fields. The electrical motility set-up has been used to compare the response of this system when different surface chemistries have been used to immobilise the motor protein. This opens up the potential to use this experimental procedure to not only test a variety of surface chemistries for myosin immobilisation but also the possibility to analyse the response of other motor proteins. As the interest increases for the use of motor proteins in various lab-on-chip devices the detailed analysis of each protein and its adsorption to any particular surface chemistry will be key in creating devices with the high level of reproducibility, efficiency and functionality that is required of lab-on-chip technologies.

6.6 References

1. Ramsey, L. C., Aveyard, J., van Zalinge, H., Persson, M., Månsson, A. and Nicolau, D. V., "Electric field modulation of the motility of actin filaments on myosin-functionalised surfaces," 85940R-85940R-85947 (2013).
2. Persson, M., Albet-Torres, N., Ionov, L., Sundberg, M., Hook, F., Diez, S., Mansson, A. and Balaz, M., "Heavy Meromyosin Molecules Extending More Than 50 nm above Adsorbing Electronegative Surfaces," *Langmuir* 26(12), 9927-9936 (2010)
3. Norde, W., "Adsorption of proteins from solution at the solid-liquid interface," *Advances in Colloid and Interface Science* 25(0), 267-340 (1986)
4. Howard, J., *Mechanics of motor proteins and the cytoskeleton*, Sinauer Associates, Inc., sunderland Massachusetts (2001).
5. Manfred, S., *Molecular Motors*, Wiley-VCH, Weinheim (2003).
6. Spudich, J. A., "How Molecular Motors Work," *Nature* 372(6506), 515-518 (1994)
7. Kron, S. J. and Spudich, J. A., "Fluorescent actin filaments move on myosin fixed to a glass surface," *Proceedings of the National Academy of Sciences* 83(17), 6272-6276 (1986)
8. Sundberg, M., Rosengren, J. P., Bunk, R., Lindahl, J., Nicholls, I. A., Tagerud, S., Omling, P., Montelius, L. and Mansson, A., "Silanized surfaces for in vitro studies of actomyosin function and nanotechnology applications," *Analytical Biochemistry* 323(1), 127-138 (2003)
9. Nicolau, D. V., Solana, G., Kekic, M., Fulga, F., Mahanivong, C., Wright, J. and dos Remedios, C. G., "Surface Hydrophobicity Modulates the Operation of Actomyosin-Based Dynamic Nanodevices," *Langmuir* 23(21), 10846-10854 (2007)
10. Mansson, A., Balaz, M., Albet-Torres, N. and Rosengren, K. J., "In vitro assays of molecular motors - impact of motor-surface interactions," *Front. Biosci.* 13(5732-5754 (2008)
11. Hanson, K. L., Solana, G. and Nicolau, D. V., "Effect of surface chemistry on in vitro actomyosin motility," in *Biomedical Applications of Micro- and Nanoengineering II* D. V. Nicolau, Ed., pp. 13-18, Spie-Int Soc Optical Engineering, Bellingham (2005).
12. Albet-Torres, N., O'Mahony, J., Charlton, C., Balaz, M., Lisboa, P., Aastrup, T., Månsson, A. and Nicholls, I. A., "Mode of heavy meromyosin adsorption and motor function correlated with surface hydrophobicity and charge," *Langmuir* 23(22), 11147-11156 (2007)
13. Sundberg, M., Rosengren, J. P., Bunk, R., Lindahl, J., Nicholls, I. A., Tågerud, S., Omling, P., Montelius, L. and Månsson, A., "Silanized surfaces for in vitro studies of actomyosin function and nanotechnology applications," *Analytical Biochemistry* 323(1), 127-138 (2003)
14. Riveline, D., Ott, A., Julicher, F., Winkelmann, D. A., Cardoso, O., Lacapere, J. J., Magnusdottir, S., Viovy, J. L., Gorre-Talini, L. and Prost, J., "Acting on actin: the electric motility assay," *Eur. Biophys. J. Biophys. Lett.* 27(4), 403-408 (1998)
15. Bunk, R., Klinth, J., Montelius, L., Nicholls, I. A., Omling, P., Tagerud, S. and Mansson, A., "Actomyosin motility on nanostructured surfaces," *Biochemical and Biophysical Research Communications* 301(3), 783-788 (2003)
16. Hanson, K. L., Viidyanathan, V. and Nicolau, D. V., "Actomyosin motility detection using Quartz Crystal Microbalance - art. no. 603602," in *BioMEMS and NanoTechnology II* D. V. Nicolau, Ed., pp. 3602-3602, Spie-Int Soc Optical Engineering, Bellingham (2006).
17. Hanson, K. L., Solana, G. and Nicolau, D. V., "Electrophoretic control of actomyosin motility," in *Microtechnology in Medicine and Biology, 2005. 3rd IEEE/EMBS Special Topic Conference on*, pp. 205-206 (2005).

18. Albet-Torres, N., Gunnarsson, A., Persson, M., Balaz, M., Hook, F. and Mansson, A., "Molecular motors on lipid bilayers and silicon dioxide: different driving forces for adsorption," *Soft Matter* 6(14), 3211-3219 (2010)
19. Albet-Torres, N., O'Mahony, J., Charlton, C., Balaz, M., Lisboa, P., Aastrup, T., Mansson, A. and Nicholls, I. A., "Mode of heavy meromyosin adsorption and motor function correlated with surface hydrophobicity and charge," *Langmuir* 23(22), 11147-11156 (2007)
20. Balaz, M., Sundberg, M., Persson, M., Kvassman, J. and Monsson, A., "Effects of surface adsorption on catalytic activity of heavy meromyosin studied using a fluorescent ATP analogue," *Biochemistry* 46(24), 7233-7251 (2007)

Concluding Thoughts

The studies presented in this thesis have been used to outline several ways in which two protein motor systems could be incorporated in to a lab-on-a-chip device. The main aim of this thesis has been in pointing out many of the practical aspects that require attention when designing a bionanodevice that utilises these proteins. A novel design has been put forward for the control of microtubules and the electrical motility device, used to guide actin filaments, has been used to investigate the protein adsorption of HMM on several surface chemistries in an environment that closely resembles that of a lab-on-a-chip device utilising this method of motility control.

The kinesin study focused almost entirely on the device design, and specifically the design of the gate areas of the chip. In order to create a patterned surface that would effectively control the movement of the microtubules several designs were implemented. In the final design, topographical confinement of the motility was used to guide the microtubules towards the gate areas. The gates were created by leaving small area of gold, coated in a thermoresponsive polymer, between two channels. By passing an electrical current through the surface of the gliding assay these small areas of gold could be locally heated, thus creating specific areas of control. The results showed that the gliding of microtubules was sufficiently confined within the channels and that they provided good guidance of the filaments towards the gate areas. Localised heating of the gates was much improved in the final device. The area where the thermoresponsive polymer was affected by the increase in temperature was approximately 40 μm in diameter. This was evidenced by the unhindered gliding of microtubule motility within this region while the gate was heated. The device showed a reasonable level of control of the motility, however, due to the design of the polymer gate, microtubules that were affected by the gate dissociated into solution. This is an issue if the motility of the affected filament was desired to be reactivated after the turning

off the gate. Alternative designs could be presented whereby the thermoresponsive polymer works within a closed channel, thus preventing the microtubules from dissociated with the motor protein but still inhibiting its movement while the gate is active.

The studies presented in chapters 5 and 6 used the motor protein system myosin II and a separate method of control to those implemented in chapter 4. In chapter 5 electrical fields of various strengths were used to guide the actin filaments across the surface of a gliding assay. The motility function in terms of velocity of filaments and the directing ability of the field when HMM was adsorbed on several surface chemistries was analysed. By studying the effect of the field across all of the surfaces a discussion was put forward as to the protein adsorption properties of the surfaces used. The discussion focused on the orientation of the protein motor on the surface, backed by previous studies, and how this would affect the activity of the HMM.

Chapter 6 implemented the electrical motility device in an alternative experiment procedure to analyse three surface chemistries for their protein adsorption properties. Filaments were exposed to an electrical field for a given time frame and the response of the motility to the termination of the field was analysed. Coupled with this deceleration study, an investigation into the effect of 'blocking actin' to motility function while in the presence of an electrical field was achieved. Together with the results from the deceleration study and chapter 5 a detailed discussion on the orientation of motors on a surface and how these affect motility function was presented. The separate effects of rigidity and hydrophobicity were looked at and conclusions draw as to the protein adsorption properties of the surfaces used.

The result of these two chapters was to find that the rigid, flat, hydrophobic surface of TMCS provided a substrate that exhibited smooth gliding, unhindered motility, seeming to show a preference for protein adsorption at the tail of the motor. Of particular importance seems to be the hydrophobicity of the surface used to immobilise the protein. A window of

relatively high hydrophobicity (contacts angles of between 70-80^{o}) exhibited smooth gliding filament movement. Outside of this window the movement of the actin appeared significantly hindered. Surface rigidity also showed to slightly affect the motility function with, perhaps unsurprisingly, flat rigid surfaces out performing those with a more gel like structure. That is not to say that TMCS provided 'The best' surface. In fact the ability to slightly hinder the motility of actin filaments on a surface may be of some use in some device designs. The studies performed with the electrical motility device showed how the performance of the HMM could be tuned by using different surface chemistries. This could be utilised within a device to create areas of varying degrees of motility function.

Finally the electrical motility device itself showed to be a powerful tool in analysing the motility function of the actin myosin system to different surface chemistries. It has provided a cheap and accessible method of investigating the adsorption of HMM to solid surfaces. The studies achieved with this gliding assay are far from exhaustive and a great many more surface chemistries could easily be analysed in this way.

Further study could easily be achieved with the electrical motility device in several areas. As previously mentioned, additional surfaces could be studied for the adsorption of HMM. In addition to this there are several key areas of the experiment that could be investigated. In chapter 6 the deceleration of filaments was studied, however, one could also look at the acceleration phase of this experiment to try and draw further conclusions as to the effect of HMM orientation on the motility function seen on different surface chemistries. Another line of study for electrically guided motility could be to try and implement this method of control in a lab-on-chip device. This would require investigation into the miniaturisation of the electrode configuration.

The design of the PNIPAM gate in chapter 4 could also be an area of further study. Additional designs could be investigated in which the gate is used in designs closer to that of

the ‘rectifies’ and ‘roundabouts’ discussed in chapter 2 of this thesis. This could allow the creation of selective collection of filaments within a confined area of a device.

Current papers and conference proceedings

1. Electric field modulation of the motility of actin filaments on myosin- functionalized surfaces

L. C. Ramsey, J. Aveyard, H. Van Zalinge, M. Persson, A. Mansson, D. V. Nicolau

SPIE conference proceedings February 2013

2. Control and gating of kinesin-microtubule motility on electrically heated thermo-chips

L.C. Ramsey, V. Schroeder, H. van Zalinge, M. Berndt, T. Korten, S. Diez, D.V. Nicolau

Biomedical Microdevices, DOI: 10.1007/s10544-014-9848-2 (2014)

1.6 Future Papers

1. Investigating the HMM adsorption properties of polymers with DC electrical fields

L. C. Ramsey, J. Aveyard, H. Van Zalinge, M. Persson, A. Mansson, D. V. Nicolau

2. Dynamic study on the effect of electrical fields on actin myosin motility with correlation of surface adsorption properties of polymer surfaces

L. C. Ramsey, J. Aveyard, H. Van Zalinge, M. Persson, A. Mansson, D. V. Nicolau